Plasma Stability in a Dipole Magnetic Field

by

Andrei N. Simakov

M.S. Physics, Moscow Institute of Physics and Technology,
Russia, 1997

Submitted to the Department of Physics
in partial fulfillment of the requirements for the degree of
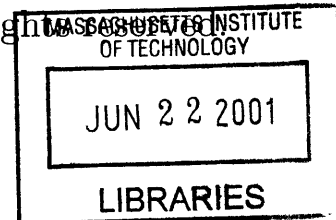
Doctor of Philosophy in Physics

at the   .

MASSACHUSETTS INSTITUTE OF TECHNOLOGY

June 2001

© Massachusetts Institute of Technology 2001. All rights reserved.

Author . . . .
Department of Physics
April 26, 2001

Certified by . . . .
Peter J. Catto
Senior Research Scientist, Plasma Science and Fusion Center
Thesis Supervisor

Certified by .   . . .
Miklos Porkolab
Professor, Department of Physics
Thesis Supervisor

Accepted by . . . .
Thomas J. Greytak
Professor, Associate Department Head for Education

Plasma Stability in a Dipole Magnetic Field

by

Andrei N. Simakov

M.S. Physics, Moscow Institute of Physics and Technology, Russia,

1997

Abstract

The MHD and kinetic stability of an axially symmetric plasma, confined by a poloidal magnetic field with closed lines, is considered. In such a system the stabilizing effects of plasma compression and magnetic field compression counteract the unfavorable field line curvature and can stabilize pressure gradient driven magnetohydrodynamic modes provided the pressure gradient is not too steep.

Isotropic pressure, ideal MHD stability is studied first and a general interchange stability condition and an integro-differential eigenmode equation for ballooning modes are derived, using the MHD energy principle. The existence of plasma equilibria which are both interchange and ballooning stable for arbitrarily large beta = plasma pressure / magnetic pressure, is demonstrated.

The MHD analysis is then generalized to the anisotropic plasma pressure case. Using the Kruskal-Oberman form of the energy principle, and a Schwarz inequality, to bound the complicated kinetic compression term from below by a simpler fluid expression, a general anisotropic pressure interchange stability condition, and a ballooning equation, are derived. These reduce to the usual ideal MHD forms in the isotropic limit. It is typically found that the beta limit for ballooning modes is at or just below that for either the mirror mode or the firehose.

Finally, kinetic theory is used to describe drift frequency modes and finite Larmor radius corrections to MHD modes. An intermediate collisionality ordering in which the collision frequency is smaller than the transit or bounce frequency, but larger than the mode, magnetic drift, and diamagnetic frequencies, is used for solving the full electromagnetic problem. An integro-differential eigenmode equation with the finite Larmor radius corrections is derived for ballooning modes. It reduces to the ideal MHD ballooning equation when the mode frequency exceeds the drift frequencies. In addition to the MHD mode, this ballooning equation permits an entropy mode solution whose frequency is of the order of the ion magnetic drift frequency. The entropy mode is an electrostatic flute mode, even in equilibrium of arbitrary beta.

3

Stability boundaries for both modes, and the influence of collisional effects on these boundaries has also been investigated.

Thesis Supervisor: Peter J. Catto
Title: Senior Research Scientist, Plasma Science and Fusion Center

Thesis Supervisor: Miklos Porkolab
Title: Professor, Department of Physics

Acknowledgments

Contents

List of Figures

Chapter 1

Introduction

1.1 Dipole Magnetic Fields in the Universe

Plasmas confined by dipolar magnetic fields are extremely common in the Universe. Typical examples are stellar and planetary magnetospheres [2].

The observation that the terrestrial magnetic field is similar to that of a simple bar magnet was first recognized at the end of the sixteenth century by Gilbert who described this fact in his book published in 1600 on the Earth's magnetism [3]. This field is about $0.3\,G$ at the surface of the Earth at the equator, decreasing as the cube of the radial distance from the center of the planet, and is of internal origin. The dipolar magnetic moment of this field is approximately $8.2 \times 10^{25}\,G\,cm^3$. The realization that the terrestrial magnetic field was connected with the phenomenon of the polar aurora occurred in the early seventeenth century when Halley suggested that the aurora results from the motion of "magnetic particles" along the magnetic field lines [3]. Now we know that these particles are mostly electrons and protons brought to the Earth by the solar wind or coming from the Earth's ionosphere and confined by its magnetic field.

Magnetospheres somewhat like that of the Earth have been discovered around Jupiter, Mercury, and Saturn; although considerable differences exist. For example, the magnetosphere of Jupiter is much larger than that of the Earth, with the magnetopause at approximately 100 Jovian radii or $7,000,000\,km$ from the planetary

surface in the sunward direction [3] (for the Earth this distance is approximately 10 Earth radii or $63,000\,km$). Jupiter's moon Io is the primary source of the high $\beta =$ (plasma pressure / magnetic pressure) ~ 1 plasma, consisting mainly of sulphur and oxygen ions and electrons, confined by the Jovian dipolar magnetic field.

Geometric properties of dipolar confinement systems, with the possible exception of neutron stars, are relatively simple. If the magnetic and rotation axes are aligned then such systems are axially symmetric, with purely toroidal equilibrium currents and purely poloidal equilibrium magnetic fields, so that there are no parallel currents. Magnetic field lines are closed so that equilibrium "flux" surfaces are defined by their surfaces of rotation about the symmetry axis of the system. The presence of closed field lines (or a large trapped particle population, if we consider a kinetic theory point of view) provides such systems with favorable stability properties due to plasma and magnetic field compression which we discuss in more detail in the Sec. 1.3.

1.2 Laboratory Plasma Confinement by Dipole Magnetic Fields

The favorable confinement properties of magnetic dipolar systems due to the stabilizing influence of plasma and magnetic compression have been known for a long time (recall that $\beta \sim 1$ for plasma confined by the Jovian magnetic field). It is, therefore, not surprising that several attempts were made to study these properties in the laboratory. Here, we mention two attempts; the Large Axisymmetric Mirror Experiment [4] (LAMEX) at UCLA and the Collisionless Terrella Experiment [5] (CTX) at Columbia University. Both studied axisymmetric magnetic configurations. In the CTX case there is a central current carrying coil suspended mechanically in the vacuum vessel to produce the dipolar magnetic field. In both cases stabilization of MHD interchange modes by populations of collisionless charged particles is observed. In the case of the LAMEX experiment the Rosenbluth-Longmire interchange stability criterion [6] was used to explain the results obtained.

14

Apart from good confinement, natural dipolar systems, such as planetary magnetospheres, possess rather unusual transport properties [7]. For such systems large scale electric and magnetic perturbations, with frequencies of the order of particle precession frequency, can be introduced into the planetary magnetosphere by the solar wind, breaking the third (flux) adiabatic invariant. This results in particle diffusion from the magnetosphere boundary into the central regions, even when the plasma density in the central regions greatly exceeds the density at the boundary. Simultaneously, adiabatic heating of the diffusing particles takes place. This aspect of dipolar confinement systems was also studied in the CTX experiment where electron cyclotron resonance heating (ECRH) was employed to break the flux invariant and produce radial electron transport.

Hasegawa was aware of the favorable stability properties of dipolar magnetic fields and in 1987 proposed a concept for a $D - {}^{3}He$ fusion reactor based on a dipole magnetic trap with the magnetic field produced by a one turn superconducting coil levitated in an external magnetic field [8]. Levitation is essential for preventing losses to supporting structures. The Levitated Dipole Experiment [9] (LDX), whose construction began at the Massachusetts Institute of Technology in 1998, will be a detailed test of the dipole confinement concept.

The main element of the LDX, the $450\,kg$ superconducting coil, will carry a current of $I = 1.36\,MA$ and be levitated inside a $5\,m$ diameter vacuum chamber by the magnetic field of an external coil. It will create a purely poloidal magnetic field close to that of a pure dipole (see Fig. 1-1). Steady state levitation of the coil is expected. ECRH will be employed to produce and heat the plasma inside the vacuum vessel. Since the magnetic field is purely poloidal there are no particle drifts off the flux surfaces and, therefore, in the absence of turbulent transport, confinement may be "classical".

The major goals of the LDX experimental program as listed on the LDX web site include investigations of the following: (i) high beta plasma stabilization by plasma and magnetic compressibility; (ii) the relationship between profiles having absolute interchange stability and the elimination of drift-wave turbulence; (iii) the

15
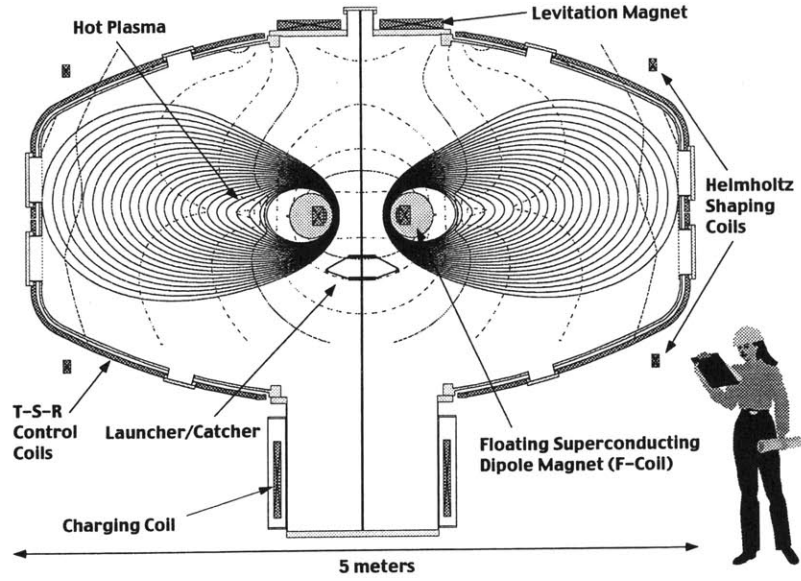
Figure 1-1: High β plasma equilibrium in LDX.

coupling between the scrape-off-layer and the confinement and stability of a high-temperature core plasma; (iv) the stability and dynamics of high-beta, energetic particles in dipolar magnetic fields; and (v) the long-time (near steady-state) evolution of high-temperature magnetically-confined plasma.

1.3 Qualitative Estimates of Plasma Stability in a Dipole Magnetic Field

Unlike most toroidal magnetic confinement devices with both poloidal and toroidal magnetic fields (such as tokamaks), which provide plasma stability by means of magnetic shear and favorable "average" field line curvature, a dipolar magnetic field is purely poloidal, the field line curvature is unfavorable everywhere and magnetic shear is absent. In this respect plasma confinement by dipolar magnetic fields differs from that in quadrupoles or octopoles where regions of favorable average curvature were

an important feature. Stability of systems with favorable average curvature was studied, especially in the collisionless limit, by Coppi *et al.* [10, 11]. Due to the closed magnetic field lines, plasma perturbations in dipolar fields (or other configurations with closed lines) compress plasma and magnetic field. This requires energy and is, therefore, a stabilizing influence.

It is well known that perturbations which do not bend magnetic field lines (the so-called "interchange" or "flute" perturbations) are likely to be the most unstable since they do not require the energy needed for field line bending. As a result, we first consider perturbations which do not bend the field but instead simply interchange, adiabatically, two close flux tubes inside the plasma. In the simple case of a low β equilibrium, which we consider here following Rosenbluth and Longmire [6], such an interchange does not produce a change in the magnetic energy of the system. However, a change in plasma thermal energy does occur and is given by the expression

$$\delta W = \frac{1}{\gamma - 1} \left[p_1 \frac{V_1^\gamma}{V_2^\gamma} V_2 + p_2 \frac{V_2^\gamma}{V_1^\gamma} V_1 - p_1 V_1 - p_2 V_2 \right], \qquad (1.1)$$

where $\gamma = 5/3$ is the ratio of specific heats, and p_1 (p_2) and $V_1 = \phi \oint_1 [\mathrm{d}\theta / (\boldsymbol{B} \cdot \boldsymbol{\nabla}\theta)]$ ($V_2 = \phi \oint_2 [\mathrm{d}\theta / (\boldsymbol{B} \cdot \boldsymbol{\nabla}\theta)]$) denote the pressure and the volume of the first (second) flux tube before the interchange takes place, respectively. After the interchange, the first (second) flux tube occupies the volume V_2 (V_1) and possesses the pressure $p_1 V_1^\gamma / V_2^\gamma$ ($p_2 V_2^\gamma / V_1^\gamma$). Here, ϕ is the magnetic flux inside the tube which is assumed to be the same for both tubes in order for the magnetic energy of the system to stay constant. Assuming

$$p_2 = p_1 + \delta p, \qquad V_2 = V_1 + \delta V, \qquad (1.2)$$

the energy δW in Eq. (1.1) is of second order in the small quantities δp and δV, and can be expressed as

$$\delta W = \delta p \, \delta V + \gamma \, p \, \frac{\delta V^2}{V}. \qquad (1.3)$$

The condition $\delta W > 0$ means that the perturbation has to spend energy to exchange

the two flux tubes and so is stable, while the condition $\delta W < 0$ indicates instability since a lower energy state exists. In Eq. (1.3) the first term describes the work of the plasma pressure force and is usually destabilizing (< 0), while the second term describes plasma compression and is manifestly stabilizing [12] (> 0). Closed field lines (or large populations of collisionless trapped particles) are the essential ingredients in this compressional stabilization. Otherwise plasma can slip along the field lines and the stabilizing compression term is equal to zero or reduced [13].

Next, we consider, for simplicity, the so-called hard core Z-pinch, where an infinitely long cylindrical plasma is confined by a purely poloidal magnetic field produced by a current carrying wire along the axis of the cylinder. In such a system all equilibrium parameters depend only on the cylindrical radial coordinate R and $V \propto R^2 > 0$. Assume now that we adiabatically interchange two flux tubes at a differentially small distance δR. Recalling that the gradient of the potential energy gives the force, we treat the derivative $-\delta W/\delta R$ as a force $F = M \, \mathrm{d}^2 \left(\delta R \right) / \mathrm{d}^2 t = -\rho V \omega^2 \delta R$ acting on the interchanged flux tubes. Then, Eq. (1.3) gives the expression for the frequency of stable oscillations ($\delta W > 0$) or the instability growth rate ($\delta W < 0$):

$$\omega^2 = \frac{2}{\rho R} \left(\frac{\mathrm{d}p}{\mathrm{d}R} + \frac{2\gamma p}{R} \right). \tag{1.4}$$

Notice that the stabilizing influence of plasma compressibility is from the term containing γ, while the pressure gradient in a curved magnetic field provides the destabilizing drive.

The hydrodynamic Rayleigh-Taylor instability, occurring when a heavier fluid is supported by a lighter one in a gravitational field, is an analog to the plasma instability just described. In this case the destabilizing pressure gradient term is replaced by the gravitational drive term $g \, d\ln N/dR$ with g the gravitational acceleration and N the plasma density.

Expression (1.4) can be generalized for the case of perturbations which bend magnetic field lines by adding to the right hand side of Eq. (1.4) the term $k_\parallel^2 V_A^2$ with $k_\parallel$ the parallel wave vector of the perturbation and $V_A^2 \equiv B^2/4\pi\rho$ the Alfvén speed (see,

for example, Ref. [14], where the problem of MHD plasma stability in a gravitational field is studied). The field line bending term is, of course, always stabilizing, giving

$$\omega^2 = k_\parallel^2 V_A^2 + \frac{2}{\rho R}\left(\frac{dp}{dR} + \frac{2\gamma p}{R}\right).$$ (1.5)

An analog to this expression is obtained from the ideal MHD energy principle, for arbitrary axially symmetric plasmas confined by a magnetic field with closed field lines, in Chapter 2.

1.4   Magnetic Point Dipole Equilibrium at Finite Pressure

We cannot make explicit predictions concerning plasma stability without discussing specific equilibria. Chapters 2 and 3 of this thesis develop the MHD theory of plasma stability in arbitrary axisymmetric poloidal magnetic fields with closed field lines for both isotropic and anisotropic plasma pressure. The theory is then applied to isotropic [1] and anisotropic [15] equilibria. It is therefore appropriate to give a short summary of the equilibrium results of Refs. [1, 15].

1.4.1   Isotropic Pressure Point Dipole Equilibrium

At sufficiently high densities and/or low temperatures laboratory plasma confined in a levitated dipole device is expected to be isotropic. Reference [1] presents a self-consistent semi-analytical solution of the Grad-Shafranov equation for a point dipole model which is valid for distances much larger than the radius of the levitated ring in LDX.

The Grad-Shafranov equation for a magnetic dipole is particularly simple and can be written as

$$\nabla \cdot \left(\frac{\nabla\psi}{R^2}\right) = -4\pi\frac{dp}{d\psi},$$ (1.6)
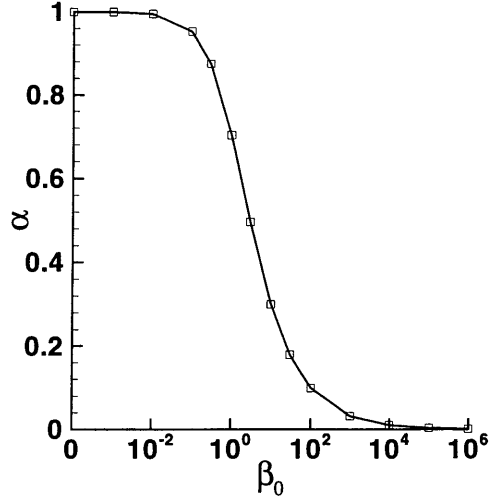
Figure 1-2:   Eigenvalue α for point dipole equilibrium vs. β_0
(Eq. (1.7)).

where ψ is the poloidal flux function, $\boldsymbol{B} = \nabla\psi \times \nabla\zeta$ is the equilibrium magnetic field, and R, Z and ζ are cylindrical coordinates. From force balance the plasma pressure must be a flux function, i.e. $p = p(\psi)$. The local beta is defined as $\beta = 8\pi p/B^2$ and its value at the equatorial plane ($Z = 0$) is denoted by β_0.

For a point dipole we look for a separable solution of Eq. (1.6) of the form $\psi = \psi_0 (R_0/r)^\alpha h(\mu)$, where r is the spherical radial coordinate, $\mu = \cos\theta$, θ is the poloidal angle, h is an unknown function of μ only, α is an unknown eigenvalue ($0 < \alpha < 1$), and R_0 is the cylindrical radius at which the reference surface ψ_0 intersects the symmetry plane $\mu = 0$. In order for h to be a function of μ only one must assume $p = p_0 (\psi/\psi_0)^{2+4/\alpha}$. Then $\beta = \beta(\mu)$ and $\beta_0 = \beta(\mu = 0)$. In this case Eq. (1.6) can be transformed into a nonlinear ordinary second order differential equation for h

$$\frac{\mathrm{d}}{\mathrm{d}\mu}\left[\left(1-\mu^2\right)^2 \frac{\mathrm{d}}{\mathrm{d}\mu}\left(\frac{h}{1-\mu^2}\right)\right] - (1-\alpha)(2+\alpha)h = -\beta_0\alpha(2+\alpha)\left(1-\mu^2\right)h^{1+4/\alpha}$$

(1.7)

with boundary conditions $h(|\mu| \to 1) \to (1 - |\mu|)$ and $\mathrm{d}h/\mathrm{d}\mu|_{\mu=0} = 0$.

In general, equation (1.7) must be solved numerically, but for the limiting cases

20

of large and small β_0 analytic solutions can be found and give $1 - \alpha = (512/1001)\,\beta_0$ for $\beta_0 \ll 1$ and $\alpha = 1/\beta_0^{1/2}$ for $\beta_0 \gg 1$. This separable solution of the Grad-Shafranov equation exists for arbitrarily large β_0. The dependence of $\alpha\,(\beta_0)$ can be found numerically and is shown in Fig. 1-2. As β_0 increases the constant ψ surfaces become more and more extended and localized about the symmetry plane, resembling an accretion disk, as shown in Fig. 1-3, where the magnetic field lines are shown for $\beta_0 = 0$ (the vacuum case) and $\beta_0 = 20$.
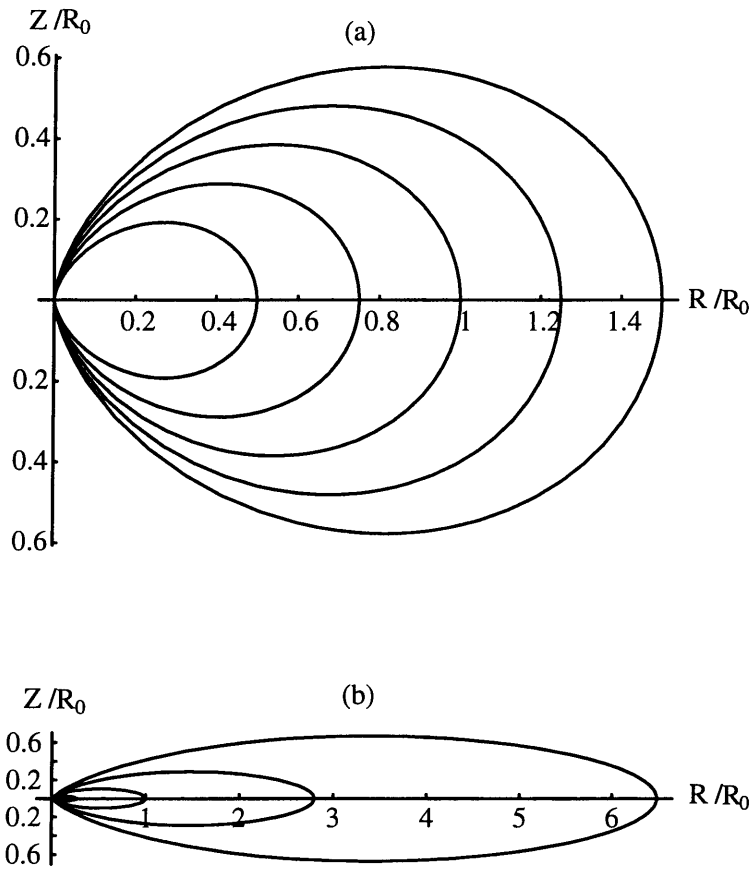
Figure 1-3: Flux surfaces for point dipole with (a) $\beta_0 = 0$ and (b) $\beta_0 = 20$.

1.4.2 Anisotropic Pressure Point Dipole Equilibrium

Astrophysical plasmas, and laboratory plasmas heated with ECRH, have anisotropic pressure so the treatment of the previous section must be generalized to account for anisotropic pressure [15]. We briefly summarize the results in this section.

In the presence of pressure anisotropy the Grad-Shafranov equation can be written as [16]

$$\nabla \cdot \left[\frac{\nabla \psi}{R^2} \left(1 + \frac{p_\perp - p_\parallel}{B^2/4\pi} \right) \right] = -4\pi \frac{\partial p_\parallel}{\partial \psi}, \tag{1.8}$$

where $p_\parallel$ and $p_\perp$ are functions of ψ and B, and the ψ derivative in Eq. (1.8) is performed at fixed B. In Ref. [15] a separable solution of Eq. (1.8) is found for $p_\perp = (1 + 2a)p_\parallel$, where $a > -1/2$ is an adjustable constant anisotropy parameter. Then for $p_\parallel = \hat{p}(\psi)(B_0/B)^{2a}$, where $B_0 = \alpha\psi_0/R_0^2$ is a constant, and $\hat{p}(\psi) = p_0(\psi/\psi_0)^{2(1+a)(2+\alpha)/\alpha}$, Eq. (1.8) can be rewritten as a nonlinear ordinary second order differential equation for $h(\mu)$ with eigenvalue α. As in the isotropic pressure case, the equation for h must be solved numerically, but it can be shown analytically that for $\beta_0 = 8\pi(1+a)p_0/B_0^2 \gg 1$, $\alpha \approx 1/\beta_0^{1/2}$ as before.

It is well known (see for example Ref. [17]) that anisotropic pressure equilibria may be unstable at high β_0 due to either firehose instability for $p_\parallel > p_\perp$ $(a < 0)$ or the mirror mode instability for $p_\perp > p_\parallel$ $(a > 0)$. In particular, these instabilities limit the β_0 achievable for the equilibrium of Ref. [15] as follows: $\beta_0 < \beta_{\mathrm{mm}} \equiv (1 + a)/[a(1 + 2a)]$ for $a > 0$, and $\beta_0 < \beta_{\mathrm{fh}} \equiv -(1 + a)/a$ for $a < 0$.

1.5 Stability of Dipole Equilibria with Isotropic Pressure

After a plasma equilibrium is found, it is necessary to determine if it is stable or unstable. The problem of isotropic pressure plasma stability in an axisymmetric magnetic field with closed field lines was studied in several works, for example in Refs. [1, 14, 18, 19, 20, 21, 22, 23]. The variational MHD energy principle, which

allows stability boundaries to be determined and can be used to give an estimate for mode growth rates in unstable situations is formulated in Ref. [18]. Reference [14] proposed a theory, based on instability of MHD ballooning modes, to explain the localized depletions of thermal plasma around Jupiter, observed by the Voyager 2 spacecraft in 1979. In References [22] and [23] the authors studied the MHD stability of solar arcades and solar loops (somewhat similar in nature to the planetary dipole problem). The MHD stability of the point dipole equilibrium of Ref. [1] is investigated in Refs. [1, 20], while Refs. [19, 21] study the stability of LDX equilibria, obtained by 2D numerical solution of the Grad-Shafranov equation (1.6).

Chapter 2 of this thesis, which is published as Ref. [20], presents an ideal MHD formulation of the isotropic plasma pressure stability case in an axisymmetric magnetic field with closed field lines and then applies this formulation to the point dipole equilibrium of Ref. [1].

As has already been mentioned, parallel currents are absent for the systems under consideration and so there is no drive for kink modes. However, field line curvature is always unfavorable so pressure driven interchange and ballooning modes may be unstable. For interchange modes the perpendicular plasma displacement is constant along a field line, and the general arbitrary β interchange stability condition is found to be [1, 18, 19, 20]

$$\frac{1}{p}\frac{\mathrm{d}p}{\mathrm{d}\psi} + \frac{\gamma}{V}\frac{\mathrm{d}V}{\mathrm{d}\psi} < 0. \tag{1.9}$$

Equation (1.9) is identical to that derived by Rosenbluth and Longmire [6] for a low β plasma (recall Eq. (1.3)). Using Eq. (1.9) it is possible to show [24] that, in the zero β limit, a dipole equilibrium is interchange stable whenever the pressure profile is more gentle than $r^{-20/3}$.

Next, we consider ballooning stability and observe that the shortest wavelengths are the most unstable [18]. We therefore concentrate on $\ell \gg 1$, where ℓ is the toroidal mode number. Taking this into account we derive the integro-differential ballooning equation (Eq. (2.10) of Chapter 2)

$$R^2 B^2 \boldsymbol{B} \cdot \boldsymbol{\nabla} \left(\frac{\boldsymbol{B} \cdot \boldsymbol{\nabla} \xi}{R^2 B^2} \right) + 4\pi \left(2\,\boldsymbol{\kappa} \cdot \boldsymbol{\nabla} p + \rho\,\omega^2 \right) \xi = 16\pi\gamma p \left(\boldsymbol{\kappa} \cdot \boldsymbol{\nabla} \psi \right) \frac{\langle \xi\,\boldsymbol{\kappa} \cdot \boldsymbol{\nabla}\,\psi / R^2 B^2 \rangle}{1 + 4\pi\gamma p \,\langle B^{-2} \rangle},$$

$$(1.10)$$

where ξ defines the radial plasma displacement $\boldsymbol{\xi}_\psi = (\xi / R^2 B^2)\,\boldsymbol{\nabla}\psi$, and $\boldsymbol{\kappa} \equiv \hat{\boldsymbol{n}} \cdot \boldsymbol{\nabla}\hat{\boldsymbol{n}}$ is the magnetic field line curvature ($\hat{\boldsymbol{n}} \equiv \boldsymbol{B}/|\boldsymbol{B}|$). In this equation, the first term on the left hand side and the term on the right hand side describe field line bending and plasma plus magnetic field compression, respectively. Both of these effects are stabilizing. The $\rho\,\omega^2$ term represents the plasma inertia, while the $\boldsymbol{\kappa} \cdot \boldsymbol{\nabla} p$ term is the destabilizing pressure drive (compare with Eq. (1.5)).

Following Ref. [18], in Chapter 2 the eigenvalues of Eq. (1.10) are related to the eigenvalues of a simpler homogeneous ordinary differential equation (Eq. (1.10) with the right hand side set to zero). In particular, it is shown that a necessary and sufficient condition for the stability of any equilibrium (arbitrary β) is that (i) the equilibrium is interchange stable (the lowest even eigenmode becomes an interchange, $\xi = $ constant, for a marginally stable equilibrium), (ii) the second even mode of the homogeneous equation is stable, and (iii) the first odd mode of the homogeneous equation is also stable. This powerful result means that solutions of the full integro-differential equation (1.10) are never required unless one is interested in growth rates or frequencies of the modes.

It turns out that the point dipole equilibrium of Ref. [1] is interchange stable for arbitrary β (i.e. the pressure fall off is always slower than $r^{-20/3}$). Moreover, the first odd and the second even modes of the homogeneous version of Eq. (1.10) are also always stable. Thus this equilibrium is MHD stable for arbitrary β.

1.6 Stability of Dipole Equilibrium with Anisotropic Pressure

When radio frequency heating is used to increase the plasma temperature in LDX a mild pressure anisotropy may result. Stronger anisotropy is of interest for space

and astrophysical dipole configurations, where the plasma is more collisionless. Consequently, the interchange and ballooning stability of an anisotropic pressure plasma confined by a dipole magnetic field is also of interest.

Anisotropic pressure stability in a dipole magnetic field was investigated in Refs. [25, 26, 27]. However, Refs. [25, 26] neglected plasma compressibility effects on ballooning stability by conjecturing that the most unstable mode would be antisymmetric with respect to the equatorial plane. In Chapter 3 we show that this conjecture does not hold in general and that the lowest symmetric mode can be more unstable than the antisymmetric mode.

Chapter 3 of this thesis, which is published as Ref. [27], presents a hybrid fluid-kinetic stability formulation for anisotropic pressure equilibria in an axisymmetric magnetic field with closed lines and then applies it to the anisotropic pressure point dipole equilibrium of Ref. [15].

We employ the Kruskal-Oberman [17, 28] formulation of the energy principle, in which the plasma is treated kinetically along the magnetic field. Again, the parallel current density term is zero. The stabilizing plasma compressibility term of Ref. [28] was derived using a kinetic theory approach and is given in terms of integrals along particle trajectories. These can be bounded by a fluid form using the Schwarz inequality [17]. Both upper and lower bounds for the Kruskal-Oberman energy δW_{KO} can be obtained, with the the upper bound being related to the Chew-Goldberger-Low [29] form of the energy:

$$\delta W_{\mathrm{MHD}}\left(p_\parallel, p_\perp\right) \leq \delta W_{\mathrm{KO}} \leq \delta W_{\mathrm{CGL}}. \tag{1.11}$$

In Chapter 3 we use the lower bound, which reduces to the isotropic MHD limit as $p_\parallel \rightarrow p_\perp \rightarrow p$. Thus the stability criteria we develop in Chapter 3 are sufficient conditions for stability of a collisionless anisotropic plasma in a dipole, but may not be necessary conditions for stability.

The resulting "fluid" form of the energy principle is minimized with respect to the component of plasma displacement in the toroidal direction to give a finite β inter-

change stability condition and the general anisotropic pressure ballooning equation in the most unstable limit of large toroidal mode numbers, $\ell \gg 1$.

Next, we apply the general stability analysis to the family of anisotropic pressure point dipole equilibria of Ref. [15], where the mirror instability or fire hose instability set limits on the achievable plasma beta, β_0, when the perpendicular pressure $p_\perp$ is greater (mirror) or less than (fire hose) the parallel pressure $p_\parallel$. We find that the point dipole equilibria are interchange stable for all plasma betas up to the mirror mode (β_{mm}) or firehose (β_{fh}) limits, whichever is appropriate. In addition, ballooning modes are stable for all betas up to some critical value. This β limit lies below β_{mm} for $1 < p_\perp/p_\parallel < 8$ and is equal to β_{mm} for $p_\perp/p_\parallel > 8$. At modest anisotropy the beta threshold may be observable in the high beta plasmas expected in LDX (for $p_\perp/p_\parallel = 1.2$ the beta limit becomes $\beta_{limit} \approx 6$). We also find that for some cases the lowest symmetric ballooning mode is more unstable than the lowest antisymmetric ballooning mode, demonstrating that the conjecture of Refs. [25, 26] is not always valid.

Finally, we have also investigated the case of tied field line boundary conditions [30]. These are more appropriate for solar and planetary applications. Ballooning modes are more stable than with periodic boundary conditions because of the additional line bending stabilization of the symmetric modes introduced by line tying.

1.7 Why Is It Not Always Sufficient to Use MHD Theory?

Ideal MHD assumes a short mean free path and large wave frequency ordering which can not, strictly speaking, be applied to many problems, and in particular to the Levitated Dipole Experiment. More quantitatively, ideal MHD normally assumes that

$$\Omega \gg \nu_c \gg \omega_b \sim \omega \gg \omega_d, \omega_*,$$ (1.12)

where Ω is the cyclotron frequency, $\omega_b \sim \boldsymbol{v} \cdot \boldsymbol{\nabla}$ is the transit (bounce) frequency, ν_c is the collision frequency, ω_d is the magnetic drift frequency, ω_* is the diamagnetic drift frequency, and ω is the mode frequency. For this ordering the collision frequency dominates all the other frequencies (except for the gyro-frequency), and the mode frequency is much larger than the drift frequencies so that the lower frequency drift modes do not appear in ideal MHD.

After initial operation at low density, LDX is expected to operate at high plasma density ($N_e \approx N_i \sim 10^{13}\,cm^{-3}$) and low temperature ($T_i \sim T_e \sim 100\,eV$). Noting that the characteristic magnetic field at the expected point of maximum pressure is $B \sim 2\,kG$ and the characteristic machine dimension is $R \sim 1\,m$, we estimate for the ions, for example, that $\omega_{bi}/\nu_{ii} \sim 10$ while $\omega_{*i}/\nu_{ii} \sim 0.1$. Accordingly, the orderings (1.12) can not be used. Instead, we must use the orderings

$$\Omega_j \gg \omega_{bj} \gg \nu_{cj} \gg \omega \gtrsim \omega_{dj} \sim \omega_{*j}, \qquad (1.13)$$

where $j = i,\, e$ and we assume $\omega \gtrsim \omega_d,\, \omega_*$ in order to be able to study drift modes. The initial low density discharges and later discharges, which are expected to operate at much higher temperatures, will have lower collisionality ions. Of course, these lower collisionality regimes are of considerable interest for LDX, as well as for space, plasmas. After the MHD treatment of Chapter 2, high frequency modes ($\omega \gg \omega_d \sim \omega_*$) in collisionless plasmas are considered in detail in Chapter 3 for anisotropic pressures such as those that might be encountered during electron cyclotron heating of LDX, or for planetary and astrophysical dipolar fields. Chapters 4 and 5 present kinetic treatments appropriate for the orderings (1.13).

For low frequency modes (or drift modes) density and temperature gradients play a key role in the stability, whereas MHD analysis is only sensitive to pressure gradients. In Chapters 4 and 5 we demonstrate that the MHD modes, which are still present in the system despite the different orderings, can couple to drift modes near the MHD marginal stability boundary, and that the so-called Finite Larmor Radius (FLR) effects due to diamagnetic and magnetic drifts must be taken into account in order

to describe this phenomenon correctly - effects not accounted for by ideal MHD.

1.8 Kinetic Plasma Stability in Dipole Magnetic Field

Although MHD is a useful description, it has a number of limitations and so must be replaced in many cases by kinetic theory. Kinetic approaches to stability of plasma confined by magnetic fields with closed field lines, in particular, magnetic dipoles and multipoles, were developed, for example, in Refs. [10, 21, 31, 32, 33, 34]. Reference [10] considers collisionless electrostatic modes in closed field line multipole devices with regions of favorable average curvature when the mode frequency is between the magnetic and diamagnetic drift frequencies. Magnetic and diamagnetic drift frequencies of the same order are studied in Ref. [31] for collisionless electrostatic drift frequency modes for plasmas confined in dipolar fields. In Ref. [32] the authors consider an electromagnetic treatment of collisionless plasmas in the Earth's magnetosphere. Of more concern here is the intermediate collisionality ordering (1.13) considered in Refs. [21, 33] for electrostatic modes. These intermediate collisionality studies will be extended in Chapters 4 and 5 of this thesis to obtain kinetic treatments of plasma stability in dipole magnetic fields for electrostatic and electromagnetic modes, respectively.

Before describing the content of Chapters 4 and 5, we look more closely at the applicability of the the orderings (1.13) and, hence, the kinetic theory we are going to present. To do so it is useful to write the orderings in terms of the plasma (density and temperature) and machine (magnetic field and dimensions) parameters. Noticing that the inequalities (1.13) are more difficult to satisfy for ions than electrons, we rewrite the ion inequalities as

$$2.78 \times 10^{11} \frac{\ell \, (T_i \, [eV])^{5/2}}{B \, [kG] \, (R \, [cm])^2} \ll N_i \, [cm^{-3}] \ll 1.9 \times 10^{12} \frac{(T_i \, [eV])^2}{R \, [cm]}, \qquad (1.14)$$

where, as usual, $\ell \gg 1$ is the toroidal mode number. Substituting the LDX machine parameters and taking $\ell \sim 5$, we see that there is a range of two orders of magnitude permitted by the orderings for the ion density at $T_i = 10\,eV$, $2.2 \times 10^{10}\,cm^{-3} \ll N_i \ll 1.9 \times 10^{12}\,cm^{-3}$, and that this range gradually shrinks, and simultaneously requires the density to increase, with increasing ion temperature. In particular, for anticipated LDX temperatures $T_i \sim 100\,eV$, the plasma density must satisfy the inequalities $6.9 \times 10^{12}\,cm^{-3} \ll N_i \ll 1.9 \times 10^{14}\,cm^{-3}$.

The kinetic stability analysis is rather complex. We therefore consider the simpler case of electrostatic perturbations first, in Chapter 4. This is appropriate for zero β equilibria and also serves to develop much of the necessary algebraic techniques. Next, the more complicated electromagnetic problem is treated in Chapter 5, accounting for the stability of arbitrary β equilibria.

1.9 Kinetic Stability: Electrostatic Treatment

In this section we describe the analysis of electrostatic modes, presented in Chapter 4. The contents of the chapter is based on Ref. [35] where we extend the treatment of Refs. [21, 33] to the case of arbitrary ratio of the electron and ion equilibrium temperatures and retain ion collisional effects.

We begin by solving the gyro-kinetic equation with the full Fokker-Planck collision operators retained for both electrons and ions using the orderings (1.13). The equilibrium distribution function is given by a Maxwellian, f_{Mj}, $(j = i,\, e)$ with its diamagnetic correction

$$f_{0j} = f_{Mj} + \frac{1}{\Omega_j}\, \boldsymbol{v} \times \hat{\boldsymbol{n}} \cdot \boldsymbol{\nabla} f_{Mj}. \tag{1.15}$$

For the ordering (1.13) the perturbed distribution function is shown to be a perturbed Maxwellian of the form

$$f_{1j} = \left[-\frac{Z_j e \hat{\Phi}}{T_j} + \left(\alpha_j\left(\psi\right) + \beta_j\left(\psi\right) \frac{M_j v^2}{2T_j} \right) e^{iL_j} \right] f_{Mj}\, e^{iS - i\omega t}, \tag{1.16}$$

with S the eikonal, $\boldsymbol{k}_\perp = \boldsymbol{\nabla} S$, $L_j = (\boldsymbol{v} \cdot \hat{n} \times \boldsymbol{k}_\perp)/\Omega_j$, $\Phi = \hat{\Phi}e^{iS-i\omega t}$ the perturbed electrostatic potential, $Z_j e$, M_j and T_j the species charge, mass and temperature, α_j and β_j some functions of the poloidal flux, and the toroidal mode number $\ell \gg 1$.

The important feature of Eq. (1.16) is that, although collisions are assumed to be less frequent than in the short-mean-free path MHD ordering, they nevertheless constrain the perturbed distribution function to be in the form of a perturbed Maxwellian because $\nu_c \gg \omega$. In addition, the assumption of large transit (or bounce) frequency ($\omega_b \gg \omega$) constrains the perturbed distribution to satisfy $\hat{n} \cdot \boldsymbol{\nabla} f_1 \equiv 0$ so that no perturbed longitudinal flow is permitted. The perturbed "number" and "pressure" (represented by the α_j and β_j of Eq. (1.16)) are then determined in higher order by the gyro-kinetic equation from solubility conditions and are functions of ω, ω_{*j}, $\langle \omega_{dj} \rangle_\theta$ and $\hat{\Phi}$ as shown in detail in Chapter 4 ($\langle \ldots \rangle_\theta$ denotes a field line average).

In Ref. [36] it is shown that ion collisional "dissipative" effects, in particular the so-called gyro-relaxation effects, are important in determining stability for the collisionality regime under consideration and can destabilize otherwise stable modes. Gyro-relaxation effects describe the collisional relaxation of a perturbed distribution function which is anisotropic, or isotropic but non-Maxwellian in energy, towards a Maxwellian, and are the most important collisional effects for orderings (1.13). In order to account for these effects we have to obtain a solution of the gyro-kinetic equation to the second order in the small expansion parameter for orderings (1.13). It can be shown, that gyro-relaxation effects (responsible for an instability with a growth rate $\gamma_{gr} \sim \omega_{di}^2/\nu_{ii}$) dominate over resistive effects [37, 38] ($\gamma_r \sim \eta_\parallel k_\perp^2 c^2/4\pi$) for plasmas obeying the intermediate collisionality orderings (1.13), since $\gamma_{gr}/\gamma_r \sim \beta \left(\omega_{bi}/\nu_{ii}\right)^2 \left(M_i/M_e\right)^{1/2} \gg 1$. Here $\eta_\parallel$ is the parallel resistivity.

Using the perturbed distribution function (1.16), with the gyro-relaxation corrections retained as well, quasineutrality results in an integral equation for $\hat{\Phi}(l)$, where l is length along the field. It is shown in Chapter 4 that all the solutions of this equation are flute-like to the leading order in a small expansion parameter. Using this fact, we are able to obtain the following *electrostatic dispersion relation*

$$\left(d - \frac{5}{3} \right) \lambda^2 + \frac{5}{9} \left(d \frac{3\eta - 7}{1 + \eta} + 5 \right) + \frac{\langle b_i \rangle_\theta}{2} \lambda^4 + O \left(\mathrm{i} \frac{\langle \omega_{di} \rangle_\theta}{\nu_{ii}} \lambda^3 \right) = 0, \qquad (1.17)$$

where $\lambda \equiv \omega / \langle \omega_{di} \rangle_\theta$, $d \equiv \omega_{*i} (1 + \eta) / \langle \omega_{di} \rangle_\theta = -\mathrm{d} \ln p / \mathrm{d} \ln V$, $\eta \equiv \eta_i = \eta_e = \mathrm{d} \ln T_{i,e} / \mathrm{d} \ln N_{i,e}$ and we assume $\tau \equiv Z_i T_e / T_i = 1$, and $b_i \equiv (k_\perp^2 T_i / M_i \Omega_i^2) \ll 1$. The full expression is presented in Chapter 4.

The dispersion relation (1.17) permits two classes of modes: a low frequency ($\lambda \sim 1$) entropy mode, obtained by dropping all the small terms of order $b_i \ll 1$ and $\langle \omega_{di} \rangle_\theta / \nu_{ii} \ll 1$, and a high frequency MHD mode (which is just the zero β limit of the MHD modes described in Chapter 2) obtained by balancing the $b_i \lambda^4$ and $(d - 5/3) \lambda^2$ terms.

The entropy mode was given its name by Kadomtsev [39] in 1960 because, unlike the usual MHD mode, it perturbs the plasma entropy. It has analogs in collisionless plasma [10, 34]. The entropy mode is represented by two toroidal waves, with phase velocity of the order of $\langle \omega_{di} \rangle_\theta / k_\perp$ when it is stable, or by a convective instability with growth rate of the order of $\langle \omega_{di} \rangle_\theta$ when it is unstable. Its stability depends on $d = -\mathrm{d} \ln p / \mathrm{d} \ln V$ and $\eta = \mathrm{d} \ln T / \mathrm{d} \ln N$ only. The MHD mode is stable (unstable) whenever $d < 5/3$ ($d > 5/3$), which is consistent with the interchange stability condition (1.9). The two modes couple together for $|d - 5/3| \leq \langle b_i \rangle_\theta^{1/2}$.

The gyro-relaxation effects (due to the terms of order $\langle \omega_{di} \rangle_\theta / \nu_{ii}$ in Eq. (1.17)) can either generate or dissipate energy, depending on d and η. This property, together with the fact that the stable entropy modes can be either positive or negative energy waves, depending on the values of d and η, drives otherwise stable modes unstable in certain regions of the d, η parametric space. Instability occurs when energy dissipation coincides with a negative energy mode, or when energy generation coincides with a positive energy mode. However, significant portions of the d, η parametric space with $d < 5/3$ are left stable even in the presence of these collisional gyro-relaxation effects. These are shown in Figs. 1a and 1c of Chapter 4 for equal temperatures, $T_e = T_i$, and a hot electron plasma with $T_e = 10\,T_i$, respectively.

1.10   Kinetic Stability: Electromagnetic Treatment

After considering the electrostatic stability problem for zero β equilibria we finally consider the full electromagnetic stability problem of arbitrary β equilibria. A solution to this problem is presented in Chapter 5.

Unlike the electrostatic problem, where only the electric field is perturbed, in the electromagnetic problem both electric and magnetic fields are perturbed. To describe this situation we use the perturbed electrostatic potential Φ, the parallel component of the perturbed electromagnetic potential $A_\parallel$, and the parallel component of the perturbed magnetic field $\delta B_\parallel$. In order to simplify the algebra it is convenient to replace $A_\parallel$ by an auxiliary potential Ψ defined by the expression

$$A_\parallel = \frac{c}{i\,\omega}\hat{n}\cdot\boldsymbol{\nabla}\Psi, \tag{1.18}$$

where c is the speed of light. Then, by solving the electromagnetic gyro-kinetic equations for electrons and ions to the leading order in a small expansion parameter, similarly to the electrostatic case, the perturbed distribution functions can be evaluated.

In order to obtain a dispersion relation for the electromagnetic modes we need three equations relating the unknown Fourier amplitudes $\hat{\Phi}$, $\delta\hat{B}_\parallel$ and $\hat{\Psi}$, namely quasineutrality and two components of Ampere's equation. The quasineutrality condition and the radial component of the Ampere's equation can be solved to give expressions for $\hat{\Phi}$ and $\delta\hat{B}_\parallel$ in terms of $\hat{\Psi}$. On substituting these expressions into the parallel component of Ampere's equation we obtain a second order integro-differential ballooning equation for the electromagnetic modes.

The resulting *electromagnetic ballooning equation* takes the form (see Chapter 5)

$$R^2B^2\boldsymbol{B}\cdot\boldsymbol{\nabla}\left(\frac{\boldsymbol{B}\cdot\boldsymbol{\nabla}\tilde{\Psi}_i}{R^2B^2}\right) + 4\pi\left(2\boldsymbol{\kappa}\cdot\boldsymbol{\nabla}p + \rho\,\Lambda^2\right)\tilde{\Psi}_i = 16\pi p\Gamma\left(\boldsymbol{\kappa}\cdot\boldsymbol{\nabla}\psi\right)\frac{\left\langle\frac{\boldsymbol{\kappa}\cdot\boldsymbol{\nabla}\psi}{R^2B^2}\tilde{\Psi}_i\right\rangle_\theta}{1+\frac{\Gamma}{2}\left\langle\beta_{pl}\right\rangle_\theta}, \tag{1.19}$$

where $\tilde{\Psi}_i \equiv Z_ie\hat{\Psi}/T_i$. This equation differs from the MHD ballooning equation (1.10)

in two important aspects. First, ω^2 in the inertia term is changed to

$$\Lambda^2 \equiv \omega^2 - \omega \left[\omega_{*i} \left(1 + \eta \right) - \left(\frac{5}{2} \omega_{\kappa i} - \omega_{\nabla B i} \right) \right] - \omega_{*i} \left(1 + 2\eta \right) \left(\frac{5}{2} \omega_{\kappa i} - \omega_{\nabla B i} \right), \quad (1.20)$$

where $\omega_{\kappa i}$ and $\omega_{\nabla B i}$ are the curvature and ∇B pieces of the ion magnetic drift frequency $\omega_{di} = \omega_{\kappa i} + \omega_{\nabla B i}$. Second, $\gamma = 5/3$ in the compression term is replaced by $\Gamma = \Gamma \left(\omega, \omega_{*i}, \langle \omega_{di} \rangle_\theta \right)$, a rather complicated function of the eigenvalue ω.

As in our discussion of MHD ballooning eigenmodes, Eq. (1.19) permits both even and odd parity modes. For the antisymmetric modes the term on the right hand side is equal to zero. Moreover, $\Lambda^2 \to \omega^2$ in the limit of $\omega \gg \omega_{*i}, \langle \omega_{di} \rangle_\theta$, so that, despite the differences in the orderings employed, the kinetic electromagnetic ballooning equation for the odd modes is the ideal MHD ballooning equation with FLR corrections. The FLR corrections (i.e. the drift terms within Λ^2) are more complicated than those which are usually discussed in tokamak stability [40, 41, 42] because in a dipole we must allow $\omega_d \sim \omega_*$. Furthermore, they are not necessarily a stabilizing correction to the MHD eigenmode.

In the case of symmetric modes the limit $\omega \gg \omega_{*i}, \langle \omega_{di} \rangle_\theta$ gives $\Gamma \to \gamma$ so that the MHD limit for the even modes is recovered as well. However, in addition to the high frequency MHD symmetric mode, Eq. (1.19) also permits a low frequency symmetric mode. After thorough analysis this is shown to be the electrostatic entropy mode discussed in Sec. 1.9. The symmetric MHD mode also becomes flute-like when it couples to the entropy mode.

Chapter 2

Isotropic Pressure MHD Stability in a Dipole Magnetic Field

2.1 Introduction

In dipole confinement devices the poloidal dipole magnetic field is created by an axisymmetric current ring [8, 9]. All other equilibrium currents are plasma currents in the toroidal direction so that there is no parallel current flow along the magnetic field. All magnetic field lines are closed so that "flux" or pressure surfaces are defined by their surfaces of rotation about the symmetry axis of the current ring.

In this chapter, the ideal MHD stability of plasma confined by a dipolar magnetic field is investigated. Kink modes are of no concern for such plasma as there is no parallel electric current. However, the curvature of the magnetic dipole field is always unfavorable so that pressure gradient driven instabilities, such as ballooning modes, may exist.

The chapter is structured in the following way. First, the ideal MHD energy principle is used to derive the general interchange stability condition and ballooning integro-differential equation. Next, this theory is applied to the family of separable point dipole equilibria of Ref. [1] to show that these equilibria are both interchange and ballooning stable for arbitrarily large plasma beta = (plasma pressure / magnetic pressure).

2.2 Stability

When the energy principle is employed to investigate the stability of a dipole equilibrium the parallel current density term may be set to zero. Minimizing the potential energy $W \propto \omega^2$ for a dipole field with respect to parallel displacements gives rise to a stabilizing plasma compressibility term ($\propto \gamma = 5/3$) due to the closed field lines [18, 43]:

$$
W = \int \mathrm{d}^3 r \left[\frac{Q_\perp^2}{8\pi} + \frac{B^2}{8\pi} \left(\boldsymbol{\nabla} \cdot \boldsymbol{\xi}_\perp + 2\boldsymbol{\kappa} \cdot \boldsymbol{\xi}_\perp \right)^2 + \frac{\gamma p}{2} \langle \boldsymbol{\nabla} \cdot \boldsymbol{\xi}_\perp \rangle_\theta^2 - \left(\boldsymbol{\xi}_\perp \cdot \boldsymbol{\nabla} p \right) \left(\boldsymbol{\kappa} \cdot \boldsymbol{\xi}_\perp \right) \right],
\tag{2.1}
$$

where $\boldsymbol{\xi}_\perp$ is the perpendicular displacement, p and B are the plasma pressure and magnetic field strength, $\boldsymbol{\kappa}$ is the curvature, $\langle \cdots \rangle_\theta = V^{-1} \oint [(\cdots) \, \mathrm{d}\theta / \boldsymbol{B} \cdot \boldsymbol{\nabla}\theta]$ with $V = \oint [\mathrm{d}\theta / \boldsymbol{B} \cdot \boldsymbol{\nabla}\theta]$ the volume per unit flux at fixed ψ, θ is the poloidal angle, $\boldsymbol{Q} = \boldsymbol{\nabla} \times (\boldsymbol{\xi}_\perp \times \boldsymbol{B})$, $\boldsymbol{B} = \boldsymbol{\nabla}\psi \times \boldsymbol{\nabla}\zeta$ is the dipole magnetic field, and ω is the mode frequency.

Writing the displacement as

$$
\boldsymbol{\xi}_\perp = \left(\xi / R^2 B^2 \right) \boldsymbol{\nabla}\psi - \eta R^2 \boldsymbol{\nabla}\zeta
$$

with ψ the poloidal flux function, ζ the toroidal angle variable, and R the distance to the axis of symmetry, we may minimize Eq. (2.1) with respect to η. Since the integrand in Eq. (2.1) depends on ζ only via the functions ζ and η, Fourier analyzing with respect to ζ can be employed to show that the higher toroidal mode number ℓ is the more unstable the mode (see Ref. [18] for details). Therefore, we need only consider the $\ell \to \infty$ limit. Then, minimization of W with respect to η gives

$$
B^2 \left(\boldsymbol{\nabla} \cdot \boldsymbol{\xi}_\perp + 2\boldsymbol{\kappa} \cdot \boldsymbol{\xi}_\perp \right) + 4\pi\gamma p \langle \boldsymbol{\nabla} \cdot \boldsymbol{\xi}_\perp \rangle_\theta = 0,
\tag{2.2}
$$

which also implies that $\eta = 0$ for $\ell \to \infty$ since $\partial/\partial\zeta \propto \ell$. Using the preceding equation to eliminate $\boldsymbol{\nabla} \cdot \boldsymbol{\xi}_\perp$ and $\langle \boldsymbol{\nabla} \cdot \boldsymbol{\xi}_\perp \rangle_\theta$ from Eq. (2.1) we obtain the reduced energy principle

$$W = \int \mathrm{d}^3r \left[\frac{Q_\perp^2}{8\pi} + \frac{2\gamma p \left\langle \boldsymbol{\kappa} \cdot \boldsymbol{\xi}_\perp \right\rangle_\theta^2}{1 + 4\pi\gamma p \left\langle B^{-2} \right\rangle_\theta} - \left(\boldsymbol{\xi}_\perp \cdot \boldsymbol{\nabla} p \right) \left(\boldsymbol{\kappa} \cdot \boldsymbol{\xi}_\perp \right) \right], \qquad (2.3)$$

where now $\boldsymbol{\xi}_\perp = (\xi/R^2 B^2) \boldsymbol{\nabla}\psi$ and $Q_\perp^2 = R^{-2} B^{-2} (\boldsymbol{B} \cdot \boldsymbol{\nabla}\xi)^2$.

To investigate the stability of the equilibrium and obtain an *estimate* for the mode frequency ω we introduce the perpendicular kinetic energy H,

$$H = \frac{1}{2} \int \mathrm{d}^3r \, \rho \, \xi_\perp^2, \qquad (2.4)$$

and perform the minimization with respect to ξ by varying the functional

$$\Lambda = \frac{W}{H} \propto \omega^2, \qquad (2.5)$$

where ρ is the mass density. Equation (2.5) only provides an estimate of $\Lambda \propto \omega^2$ because the minimization with respect to parallel displacements does not retain the parallel kinetic energy (the retention of the full perpendicular kinetic energy does not alter the minimization of Λ with respect to η since the infinite ℓ modes remain the least stable).

2.2.1 Interchange Stability

We begin by briefly considering interchange modes for which $\boldsymbol{B} \cdot \boldsymbol{\nabla}\xi = 0$. Then variation of Eq. (2.3) with respect to ξ gives the general finite beta interchange stability condition:

$$2\gamma p \left\langle \boldsymbol{\kappa} \cdot \boldsymbol{\nabla}\psi / R^2 B^2 \right\rangle_\theta > \left(1 + 4\pi\gamma p \left\langle B^{-2} \right\rangle_\theta \right) \left(\mathrm{d}p/\mathrm{d}\psi \right). \qquad (2.6)$$

Notice that closed field lines result in plasma compressibility acting to make curvature a stabilizing influence for interchange modes. To rewrite the curvature term in Eq. (2.6) we use the equilibrium force balance to obtain the convenient result

$$2\boldsymbol{\kappa} \cdot \boldsymbol{\nabla}\psi / R^2 B^2 = 4\pi B^{-2} \mathrm{d}p/\mathrm{d}\psi - \boldsymbol{\nabla} \cdot \left(R^{-2} B^{-2} \boldsymbol{\nabla}\psi \right), \qquad (2.7)$$

which gives

$$2 \left\langle \boldsymbol{\kappa} \cdot \boldsymbol{\nabla} \, \psi / R^2 B^2 \right\rangle_\theta = 4\pi \left\langle B^{-2} \right\rangle_\theta \mathrm{d}\, p / \mathrm{d}\, \psi - V^{-1} dV/d\psi. \tag{2.8}$$

As a result, Eq. (2.6) becomes [1, 18]

$$\frac{1}{p} \frac{\mathrm{d}\, p}{\mathrm{d}\, \psi} + \frac{\gamma}{V} \frac{\mathrm{d}\, V}{\mathrm{d}\, \psi} < 0. \tag{2.9}$$

For the point dipole equilibrium of Ref. [1], $p \propto \psi^{2+4/\alpha}$ and $V \propto \psi^{-1-3/\alpha}$, where α decreases from unity towards zero as the reference plasma beta $= \beta_0$ increases from zero toward infinity. As a result, the arbitrary beta interchange stability condition for the point dipole solution of Ref. [1] becomes $\gamma > 2\,(2 + \alpha) \, / \, (3 + \alpha) > 4/3$ so that interchange stability is maintained at all plasma pressures as noted there.

2.2.2 Ballooning Stability

We next consider the ballooning stability of the equilibrium. For short wavelength ballooning modes the stabilizing influence of plasma compressibility can be enhanced by the stabilizing influence of line bending ($Q_\perp^2 \neq 0$). To consider ballooning modes we minimize Eq. (2.5) with respect to ξ to find the infinite ℓ ballooning mode equation:

$$R^2 B^2 \boldsymbol{B} \cdot \boldsymbol{\nabla} \left(\frac{\boldsymbol{B} \cdot \boldsymbol{\nabla} \xi}{R^2 B^2} \right) + 4\pi \left(2\, \boldsymbol{\kappa} \cdot \boldsymbol{\nabla}\, p + \rho \Lambda \right) \xi$$
$$= 16\pi \gamma p \left(\boldsymbol{\kappa} \cdot \boldsymbol{\nabla}\, \psi \right) \frac{\left\langle \xi\, \boldsymbol{\kappa} \cdot \boldsymbol{\nabla}\, \psi / R^2 B^2 \right\rangle_\theta}{1 + 4\pi \gamma p \left\langle B^{-2} \right\rangle_\theta}. \tag{2.10}$$

Equation (2.10) is somewhat awkward to solve because of its integro-differential nature. Fortunately, Bernstein *et al.* [18] have shown that key properties of the eigenvalues Λ_j of Eq. (2.10) can be determined by considering the eigenvalues λ_j of the corresponding homogeneous differential equation:

$$R^2 B^2 \boldsymbol{B} \cdot \boldsymbol{\nabla} \left(\frac{\boldsymbol{B} \cdot \boldsymbol{\nabla} \xi}{R^2 B^2} \right) + 4\pi \left(2\, \boldsymbol{\kappa} \cdot \boldsymbol{\nabla}\, p + \rho \lambda \right) \xi = 0, \tag{2.11}$$

where $j = 0, 1, 2, \ldots$. Equation (2.11) is a Sturm-Liouville differential equation which for specified boundary conditions has a complete set of eigenfunctions ξ_j with corresponding distinct eigenvalues λ_j. Reference [18] demonstrates that the Λ_j have the important property that they are greater than or equal to the corresponding λ_j. For our up-down symmetric equilibrium we assign even (odd) indices to the up-down symmetric (asymmetric) eigenfunctions. Therefore, $\lambda_{2j+1} = \Lambda_{2j+1} < \lambda_{2j+3} = \Lambda_{2j+3}$ for the up-down asymmetric eigenfunctions since $\langle \xi \, \boldsymbol{\kappa} \cdot \boldsymbol{\nabla} \psi / R^2 B^2 \rangle_\theta = 0$. Then, according to Ref. [18] the ordering of the up-down symmetric eigenvalues becomes $\lambda_{2j} \leq \Lambda_{2j} \leq \lambda_{2j+2} \leq \Lambda_{2j+2}$. Consequently, if $\lambda_0 \geq 0$ and $\lambda_1 \geq 0$ then $\Lambda_j \geq 0$ and the equilibrium is stable, while if $\Lambda_{2j} \leq \lambda_{2j+2} < 0$ or if $\lambda_{2j+1} = \Lambda_{2j+1} < 0$, then the lower ballooning eigenmodes are unstable. In the more subtle case where $\lambda_0 < 0 < \lambda_2$ and $\lambda_1 > 0$, Ref. [18] gives a simple proof that the lowest even ballooning mode is stable (unstable) if the equilibrium is interchange stable (unstable). (Notice that this result implies the lowest even ballooning mode and the interchange mode are indistinguishable at marginal stability.) The point dipole equilibrium of Ref. [1] is interchange stable so its ballooning stability is simply determined by the signs of λ_1 and λ_2 with $\lambda_1 > 0$ and $\lambda_2 > 0$ ($\lambda_1 < 0$ or $\lambda_2 < 0$) enough to insure stability (instability)! However, since we will find that $\lambda_1 < \lambda_2$ we need only consider the case $\lambda_0 < 0 < \lambda_1$.

For the point dipole equilibrium of Ref. [1], it is convenient to rewrite Eqs. (2.11) in ψ, μ, ζ variables. Introducing the spherical coordinates r, θ and ζ with $\mu = \cos\theta$ and $R = r\sin\theta$ and using

$$\psi = \psi_0 \left(R_0/r\right)^\alpha h\left(\mu\right), \qquad p = p_0 \left(\psi/\psi_0\right)^{2+4/\alpha},$$
$$B = B_0 \left(\psi/\psi_0 h\right)^{1+2/\alpha} G, \qquad G \equiv \left[h^2/\left(1-\mu^2\right) + \left(\alpha^{-1}\mathrm{d}\,h/\mathrm{d}\,\mu\right)^2\right]^{1/2} \qquad (2.12)$$

and $\beta_0 = 8\pi p_0/B_0^2$, where p_0, ψ_0, and $B_0 = \alpha\psi_0/R_0^2$ are the values of the plasma pressure, poloidal flux function, and magnetic field at a reference flux surface located at $R = R_0$, we may perform the stability evaluation conveniently by using the Grad-Shafranov equation to rewrite Eq. (2.7) as

$$\boldsymbol{\kappa} \cdot \boldsymbol{\xi}_\perp = -\frac{\xi}{B} \boldsymbol{\nabla} \cdot \left(\frac{\boldsymbol{\nabla} \, \psi}{R^2 B} \right). \qquad (2.13)$$

After a bit of tedious, but straightforward, algebra we find that Eq. (2.11) can be cast into the form

$$\frac{\mathrm{d}}{\mathrm{d}\,\mu} \left[A\left(\mu\right) \frac{\mathrm{d}\,\xi}{\mathrm{d}\,\mu} \right] - [D\left(\mu\right) - \lambda^* C\left(\mu\right)]\,\xi = 0, \qquad (2.14)$$

where

$$A\left(\mu\right) = \frac{h^{2-1/\alpha}}{\left(1 - \mu^2\right) G^2}, \quad C\left(\mu\right) = \frac{h^{2+5/\alpha}}{\left(1 - \mu^2\right) G^2},$$

$$\lambda^* = \frac{\lambda R_0^2}{V_A^2} \left(\frac{\psi}{\psi_0} \right)^q,$$

$$D\left(\mu\right) = \frac{4\beta_0 \left(1 + \alpha/2\right) h^{2+3/\alpha}}{\alpha G^2} \left[\frac{G}{h} \frac{\mathrm{d}}{\mathrm{d}\,\mu} \left(\frac{1}{G} \frac{\mathrm{d}\,h}{\mathrm{d}\,\mu} \right) - \frac{\alpha}{1 - \mu^2} \right],$$

$q = \left(2 + 4/\alpha\right)/\gamma - 2 - 6/\alpha$, and $V_A^2 = B^2/4\pi\rho$ is the Alfvén speed.

The point dipole equilibrium under consideration is up-down symmetric about the equatorial plane so we need only seek solutions of Eq. (2.14) that are up-down symmetric or anti-symmetric. The symmetric solutions are even in μ, have $0, 2, 4, ...2k, ...$ nodes in the interval $-1 < \mu < 1$, and determined by the boundary conditions $\mathrm{d}\,\xi/\mathrm{d}\,\mu|_{\mu=0} = \mathrm{d}\,\xi/\mathrm{d}\,\mu|_{\mu=1} = 0$. The odd in μ, or anti-symmetric, solutions have $1, 3, 5, ...2k + 1, ...$ nodes in the interval $-1 < \mu < 1$ and are determined by the boundary conditions $\xi\left(\mu = 0\right) = \xi\left(\mu = 1\right) = 0$. The more nodes an eigenfunction has the larger its eigenvalue for a Sturm-Liouville differential equation for given boundary conditions. Therefore, λ_j is the eigenvalue of the eigenfunction with j nodes for $-1 < \mu < 1$, and we need only consider the lowest odd and second even eigenfunctions by evaluating λ_1 and λ_2 to determine the ballooning stability of the point dipole model of Ref. [1].

We first consider ballooning stability in the $\beta_0 \gg 1$ limit by employing the lowest order solution found in Ref. [1], namely

$$\alpha \beta_0^{1/2} = 1, \quad \frac{\mathrm{d}\,h}{\mathrm{d}\,\mu} = -\left(1 - h^{2+4/\alpha}\right)^{1/2}.$$ (2.15)

Letting $t = h^{2+4/\alpha}$, replacing $1 - \mu^2$ by unity in terms retained, and ignoring small corrections except for an α^2 correction that must be kept to prevent B from vanishing as $\mu \to 0$, Eq. (2.14) becomes

$$\frac{\mathrm{d}}{\mathrm{d}\,t} \left[\frac{t^{3/4}\left(1 - t\right)^{1/2}}{1 + \alpha^2 - t} \frac{\mathrm{d}\,\xi}{\mathrm{d}\,t} \right] + \left[\frac{4\left(1 + t\right) + \lambda^* \alpha^2 t^{1/2} \left(1 + \alpha^2 - t\right)}{16 t^{1/4}\left(1 - t\right)^{1/2}\left(1 + \alpha^2 - t\right)^2} \right] \xi = 0.$$ (2.16)

From Eq. (2.16) we obtain a variational expression for λ^*

$$\lambda^* \alpha^2 = \frac{\int_0^1 \mathrm{d}t \left[\frac{16 t^{3/4}(1-t)^{1/2}}{1+\alpha^2-t} \left(\frac{\mathrm{d}\xi}{\mathrm{d}t}\right)^2 - \frac{4(1+t)\xi^2}{t^{1/4}(1-t)^{1/2}(1+\alpha^2-t)^2} \right]}{\int_0^1 \frac{\mathrm{d}t\,\xi^2 t^{1/4}}{(1-t)^{1/2}(1+\alpha^2-t)}},$$ (2.17)

which can be used to determine $\lambda^* = \lambda^*\left(\beta_0\right)$ for $\beta_0 \gg 1$. To do so we need a trial function that is a good approximation to the first odd eigenfunction of Eq. (2.16). A reasonable trial function $\tilde{\xi}_1$ can be constructed by examining the solutions to Eq. (2.16) for $\alpha^2 = 0$ in the vicinity of $t = 0$ and $t = 1$ (where the λ^* term is unimportant). This procedure suggests

$$\tilde{\xi}_1 = t^{1/4}\left(1 - t\right)^{1/2}.$$ (2.18)

Notice that if $\lambda^* \alpha^2 t^{1/2} \to \lambda^* \alpha^2$ in Eq. (2.16) then (2.18) is an exact solution for $\alpha^2 = 0$ if $\lambda^* \alpha^2 = 4$. Using Eq. (2.18) as the trial function in Eq. (2.17) and evaluating the integrals analytically (by integrating the second term in the numerator by parts) gives $\lambda_1^* \approx 4.86\beta_0$, indicating ballooning stability for $\beta_0 \gg 1$. Since we also expect $\beta_0 \ll 1$ to be stable, we anticipate that the first odd eigenfunction will be ballooning stable for arbitrary beta.

The case of arbitrary β_0 must be investigated numerically to obtain confirmation of stability. To do so we solve Eq. (2.14) for different values of β_0 to obtain the eigenvalue λ_1^*. The dependence of $\lambda_1^*\left(\beta_0\right)$ for $10^{-4} \le \beta_0 \le 10^4$ is shown in Fig. 2-
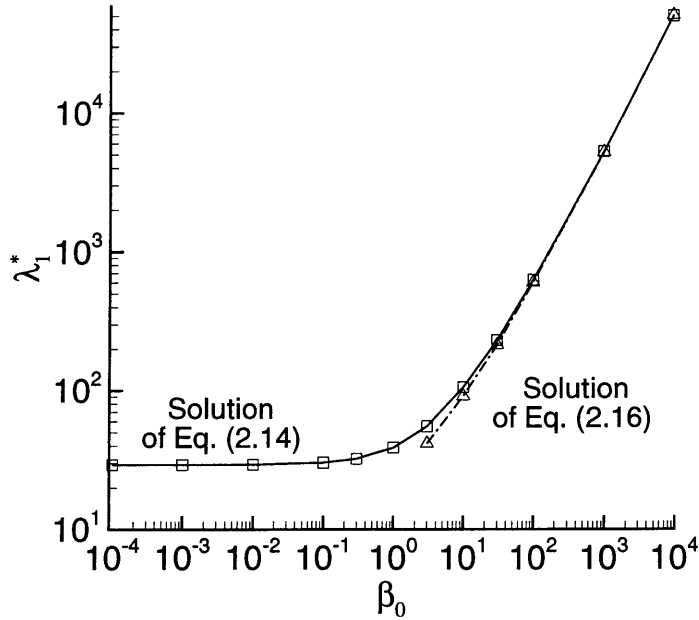
Figure 2-1:   The eigenvalue λ_1^* as a function of β_0 as obtained by numerically solving Eqs. (2.14) and (2.16) for the first odd eigenvalue.

1 along with the numerical solution of Eqs. (2.16). We see that λ_1^* is positive for all β_0 and increases linearly with β_0, giving $\lambda_1^* \approx 4.83\beta_0$ for $\beta_0 \gg 1$. The $\beta_0 \gg 1$ limit coincides with the numerical solution of Eq. (2.16) as expected and is very well approximated by the result obtained using the trial function (2.18). The eigenvalue $\lambda_2^* (\beta_0)$ corresponding to the second even eigenfunction of Eq. (2.14) (two nodes) is positive for all β_0 with $\lambda_2^* (\beta_0) > \lambda_1^* (\beta_0)$ and shows the same qualitative behavior as $\lambda_1^* (\beta_0)$ as shown in Fig. 2-2.

Because the point dipole equilibrium is interchange stable and $\lambda_2^* > \lambda_1^* > 0$ for all β_0 we conclude that $\Lambda_0 > 0$ based on the proofs of Ref. [18]. Consequently, the separable point dipole equilibrium found in Ref. [1] is ballooning stable. Interestingly, the lowest eigenvalue $\lambda_0^* (\beta_0)$ of the auxiliary differential equation (2.14) corresponding to its first even eigenfunction (no nodes) is negative for all β_0 and goes to zero in the limit of small β_0 as shown in Fig. 2-2. The numerical solution of Eq. (2.14) gives $\lambda_0^* \approx -5.6\beta_0^2$ for $\beta_0 \gg 1$. A variational treatment at $\beta_0 \gg 1$ using the trial function $\tilde{\xi}_0 = (1 + \alpha^2 - t)^{-1}$ in Eq. (2.17) gives $\lambda_0^* \approx -5\beta_0^2$. This result means that for the first

42
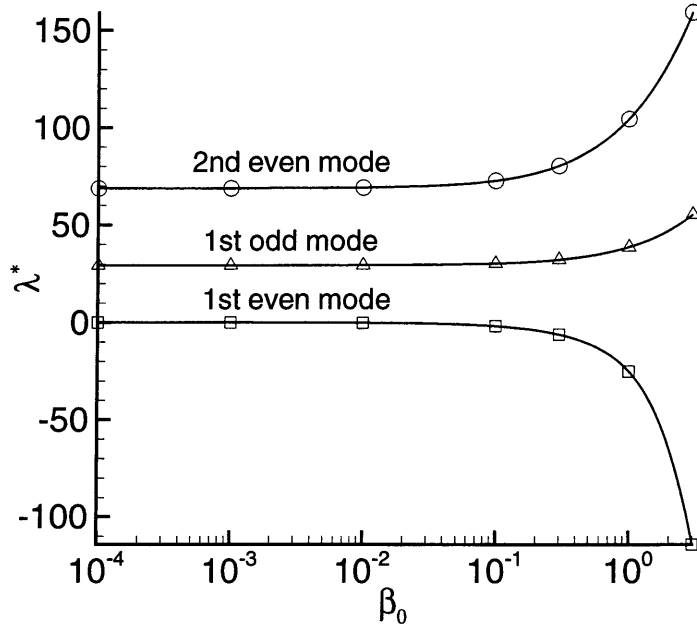
Figure 2-2: The first three eigenvalues as functions of β_0 from a numerical solution of the auxiliary differential equation (2.14).

even auxiliary eigenfunction $8\pi B^{-2}\boldsymbol{\kappa}\cdot\boldsymbol{\nabla}p\sim\beta_0^2/R_0^2$ (indicating that $\kappa\sim\beta_0/R_0$ and $\boldsymbol{\nabla}\ln p\sim 1/R_0$ for $\beta_0\gg 1$) since line bending is weak, while for the actual physical first even eigenmode stability is provided by plasma compressibility. Moreover, our results for the first odd eigenfunction at $\beta_0\gg 1$ imply that the line bending term and the pressure times curvature drive term cancel to lowest order so we may roughly say that $\xi^{-1}R^2\boldsymbol{B}\cdot\boldsymbol{\nabla}\left(R^{-2}B^{-2}\boldsymbol{B}\cdot\boldsymbol{\nabla}\xi\right)\sim\beta_0^2/R_0^2\sim 8\pi B^{-2}\boldsymbol{\kappa}\cdot\boldsymbol{\nabla}p$, but with the $1/\beta_0$ corrections determining stability in this case.

2.2.3   Previous Work

The numerical results of Ref. [19] for the Levitated Dipole Experiment (LDX) [9] are obtained by solving the $\lambda=0$ version of Eq. (2.11) appropriate for their finite ring dipole configuration. To determine ballooning stability the authors replace κ by $\sigma\kappa$ in Eq. (2.11) and find solutions satisfying the boundary conditions by adjusting σ, with $\sigma>1$ ($\sigma<1$) corresponding to a stable (unstable) equilibrium. Such a procedure only recovers solutions with at least one node since with σ inserted and

43

$\lambda = 0$ the solutions of Eq. (2.11) must satisfy the constraint $\langle \xi R^{-2} B^{-2} \boldsymbol{\kappa} \cdot \boldsymbol{\nabla} p \rangle_\theta = 0$. However, because of the proof given in Ref. [18] only the first odd eigenfunction and its associated eigenvalue need be evaluated so the procedure of Ref. [19] is adequate for determining the ballooning stability of interchange stable dipole configurations.

The original point dipole work of Ref. [1] considered only interchange stability at arbitrary β_0 and obtained the result of Eqs. (2.6) and (2.9). Equation (2.6) was also obtained in Ref. [19]. In addition to interchange instability, Ref. [44] contains a preliminary investigation of the ballooning stability of a the point dipole equilibrium at $\beta_0 \gg 1$. It uses a matched asymptotic analysis to investigate marginal stability that is inadequate because as we show here the point dipole is always ballooning stable.

2.3   Discussion

The preceding results along with the proofs from Ref. [18] demonstrate that the point dipole equilibrium of Ref. [1] is interchange and ballooning stable for arbitrary plasma pressure. As the destabilizing bad curvature becomes stronger about the equatorial plane at high beta, ballooning stability is obtained because the plasma compression associated with the closed field line geometry stabilizes any displacement whose radial component does not change sign along the field line, provided compressibility stabilizes the interchange mode. Of course, line bending provides additional stabilization. Incompressible displacements must have nodes along the magnetic field and are stabilized by the increased line bending.

Chapter 3

Anisotropic Pressure MHD Stability in a Dipole Magnetic Field

3.1 Introduction

Plasma stability of dipolar magnetic field equilibria are of interest for both cyclotron heated plasma laboratory experiments, such as the Levitated Dipole Experiment (LDX) [9], and space and astrophysical plasma applications [2], where the effects of anisotropic pressure should be considered.

A model point dipole plasma equilibrium with isotropic and anisotropic pressure was studied in Refs. [1] and [15] respectively, and the resulting Grad-Shafranov equation was shown to permit a relatively simple separable solution. While in the isotropic plasma pressure case the equilibrium exists for arbitrarily large plasma beta = (plasma pressure/magnetic pressure) [1], in the case of anisotropic plasma pressure a stable equilibrium is possible only for plasma betas below some critical value [15]. At high beta the equilibrium is destroyed either by the fire hose instability or the mirror mode instability, depending on whether the parallel or perpendicular pressure is larger, respectively.

This chapter studies interchange and ballooning mode stability for a general anisotropic pressure plasma equilibrium in an axisymmetric magnetic field with closed field lines and then applies these results to the case of the model point dipole plasma equilibrium of Ref. [15]. Prior work [26] on the ballooning stability of anisotropic pressure plasma equilibria in dipole magnetic fields neglected plasma compressibility effects on ballooning by conjecturing that the most unstable mode was up-down asymmetric with respect to the equatorial plane, and did not employ a self consistent equilibrium to obtain the critical beta. The validity of this conjecture is discussed here based on a consideration of the full ballooning integro-differential equation and its numerical solution for a self-consistent anisotropic pressure point dipole equilibrium.

The chapter is structured in the following way. In Sec. 3.2 the Kruskal-Oberman form of the Energy Principle [28] is used with a Schwarz inequality to derive a criterion for interchange stability and the Euler form of the integro-differential equation for the eigenvalues and eigenfunctions of the ballooning modes for general anisotropic pressure plasma equilibrium. In Sec. 3.3 these results are applied to the case of anisotropic plasma pressure when perpendicular pressure is proportional to parallel pressure with a constant proportionality factor. It is shown that, for the case of laboratory plasma experiments (for example LDX, with periodic boundary conditions for the ballooning mode equation), ballooning stability of the equilibrium can be derived from the "simplified" Sturm-Liouville differential ballooning equation - the ballooning equation without the integral part. Section 3.4 then applies these results to the particular model point dipole equilibrium of Ref. [15] to show that the equilibrium is interchange stable for all plasma betas and ballooning stable for all betas up to some critical value. The solar and planetary case, with "tied" field line boundary conditions [30], is considered in Sec. 3.5. Ballooning mode beta limits can be found in this case only by solving the full Euler integro-differential ballooning equation. The equilibrium is found to be more ballooning stable than in the periodic boundary condition case because of the additional magnetic field line bending. The results are summarized in Section 3.6.

3.2   General Stability Properties of Anisotropic Plasma Pressure Equilibrium

For an axisymmetric dipolar magnetic configuration with only a poloidal magnetic field all equilibrium plasma currents are in the toroidal direction so that there is no parallel current flow along the magnetic field. All magnetic field lines are closed so that "flux" or pressure surfaces are defined by their surfaces of rotation about the symmetry axis of the system.

To investigate the stability of an anisotropic pressure plasma equilibrium in a dipolar magnetic field the Kruskal-Oberman form of the Energy Principle [28, 17] can be used with the parallel current density term set to zero. Unlike the case of isotropic pressure [20] the expression for the stabilizing plasma compressibility term is derived using a kinetic theory approach and is more complicated. After some algebra the expression for the potential energy $W \propto \omega^2$ (where ω is the mode frequency) from Ref. [17] can be rewritten in a form

$$W = W_{\text{fluid}} + W_{\text{kinetic}}, \tag{3.1}$$

with

$$W_{\text{fluid}} \equiv \int \mathrm{d}^3 r \left\{ \frac{Q_\perp^2 \left(1 - \sigma_- \right)}{8\pi} + \frac{B^2 \left(1 + \sigma_\perp \right)}{8\pi} \left[\nabla \cdot \boldsymbol{\xi}_\perp + \left(\boldsymbol{\kappa} \cdot \boldsymbol{\xi}_\perp \right) \Sigma_- \right]^2 \right.$$
$$\left. + \frac{B \left(1 - \sigma_- \right)}{8\pi} \Sigma_+ \left(\boldsymbol{\kappa} \cdot \boldsymbol{\xi}_\perp \right)^2 - \frac{1}{2} \left(\boldsymbol{\kappa} \cdot \boldsymbol{\xi}_\perp \right) \left(\nabla \left(p_\parallel + p_\perp \right) \cdot \boldsymbol{\xi}_\perp \right) \right\}, \tag{3.2}$$

$$W_{\text{kinetic}} \equiv \frac{1}{2} \int \mathrm{d}^3 r \int \mathrm{d}^3 v \left\{ \left(-\frac{\partial F}{\partial \epsilon} \right) \right.$$
$$\left. \times \frac{\left[\oint \left\{ \mathrm{d}l / \left| v_\parallel \right| \left[\mu B \left(\nabla \cdot \boldsymbol{\xi}_\perp + \boldsymbol{\kappa} \cdot \boldsymbol{\xi}_\perp \right) - v_\parallel^2 \left(\boldsymbol{\kappa} \cdot \boldsymbol{\xi}_\perp \right) \right] \right\} \right]^2}{\left[\oint \mathrm{d}l / \left| v_\parallel \right| \right]^2} \right\}, \tag{3.3}$$

where $W_{kinetic}$ corresponds to the plasma compressibility term; $F = M_i f_i + M_e f_e$ with $f_{i,e} = f_{i,e}(\mu, \epsilon, \psi)$ the ion and electron distribution functions expressed in terms of the magnetic moment $\mu = v_\perp^2/2B$, kinetic energy $\epsilon = v^2/2$, and the poloidal flux function ψ; M_e and M_i are electron and ion masses. The parallel velocity $v_\parallel$ is given by $v_\parallel^2/2 = \epsilon - \mu B$, $d^3 v = \left(4\pi B/\left|v_\parallel\right| d\epsilon d\mu\right)$, and dl is an incremental distance along the dipole magnetic field $\boldsymbol{B} = \boldsymbol{\nabla}\psi \times \boldsymbol{\nabla}\zeta$, with ζ the toroidal angle variable. In Eqs. (3.2) and (3.3) $\boldsymbol{Q} = \boldsymbol{\nabla} \times (\boldsymbol{\xi}_\perp \times \boldsymbol{B})$ with $\boldsymbol{\xi}_\perp$ the perpendicular plasma displacement; $p_\parallel$, $p_\perp$, and B are the parallel and perpendicular plasma pressure and magnetic field magnitude; $\boldsymbol{\kappa}$ is the magnetic field line curvature; $\Sigma_+ = (\sigma_- + \sigma_\perp)/(1 + \sigma_\perp)$ and $\Sigma_- = 1 + (1 - \sigma_-)/(1 + \sigma_\perp)$ with $\sigma_- = 4\pi\left(p_\parallel - p_\perp\right)/B^2$, $\sigma_\perp = 4\pi\left(C + 2p_\perp\right)/B^2$ and $C = \int d^3 v \left\{(\mu B)^2 (\partial F/\partial\epsilon)\right\}$.

The orbit integrals in the expression for $W_{kinetic}$ are difficult to work with. To make the expression for W suitable for minimization we can use the Schwarz inequality [17]

$$\int\int d\mu d\epsilon \left\{\left(-\frac{\partial F}{\partial\epsilon}\right)\frac{J^2}{K}\right\} \geq \frac{\left[\int\int d\mu d\epsilon \left(-\partial F/\partial\epsilon\right) g\left(\mu, \epsilon\right) J\right]^2}{\int\int d\mu d\epsilon \left(-\partial F/\partial\epsilon\right) g^2\left(\mu, \epsilon\right) K}, \qquad (3.4)$$

where $g\left(\mu, \epsilon\right)$ is an arbitrary well-behaved weighting function. Using the fact that $\int d^3 r = \int d\zeta \int d\psi \oint (dl/B)$, the expression for $W_{kinetic}$ can easily be bounded using Eq. (3.4) with $J = \oint \left(dl/\left|v_\parallel\right|\right)\left[\mu B\left(\boldsymbol{\nabla}\cdot\boldsymbol{\xi}_\perp + \boldsymbol{\kappa}\cdot\boldsymbol{\xi}_\perp\right) - v_\parallel^2\left(\boldsymbol{\kappa}\cdot\boldsymbol{\xi}_\perp\right)\right]$ and $K = \oint \left(dl/\left|v_\parallel\right|\right)$. Taking the weighting function $g\left(\mu, \epsilon\right) = \epsilon$, using the expressions for the parallel and perpendicular pressure $p_\parallel = \int d^3 v \, v_\parallel^2 F$, $p_\perp = \int d^3 v \, \mu B F$ and the Schwarz inequality (3.4), we find

$$W_{kinetic} \geq \frac{1}{2}\int d\zeta \int d\psi \times \left\{\frac{\left[\oint \left\{dl/\left|v_\parallel\right|\left[(\boldsymbol{\nabla}\cdot\boldsymbol{\xi}_\perp)\Gamma_1 - (\boldsymbol{\kappa}\cdot\boldsymbol{\xi}_\perp)\Gamma_2\right]\right\}\right]^2}{\oint (dl/B)\Gamma_3}\right\}, \qquad (3.5)$$

where $\Gamma_1 = p_\perp/2 - C$, $\Gamma_2 = p_\perp/2 + 3p_\parallel/2 + C$ and $\Gamma_3 = p_\perp + 3p_\parallel/4 - C$.

Notice that in general we can consider a family of weighting functions $g_\alpha\left(\mu, \epsilon\right) = \epsilon^\alpha$, which will generate a family of corresponding Schwarz inequalities. It can be shown that the most "restrictive" inequality is given by $\alpha = 1$. It is interesting to note that in this case the inequality (3.5) for the isotropic pressure case ($p_\perp = p_\parallel = -C/2 = p$)

48

reduces to $W_{\text{kinetic}} \geq \left(\frac{1}{2}\right) \int d^3r \,(5/3) p \,\langle \boldsymbol{\nabla} \cdot \boldsymbol{\xi}_\perp \rangle_\theta^2$, which is the usual expression for plasma compressibility (see Ref. [20]).

Writing the displacement as

$$\boldsymbol{\xi}_\perp = \left(\xi/R^2B^2\right) \boldsymbol{\nabla}\psi - \eta R^2\boldsymbol{\nabla}\zeta,$$

with R the cylindrical distance to the axis of symmetry and replacing W_{kinetic} by Eq. (3.5), we may minimize the expression for the potential energy W with respect to η. Since the integrands in the expression for W depend on ζ only via the functions ξ and η, Fourier analysis with respect to ζ can be employed to show that the higher the toroidal mode number ℓ the more unstable the mode (see Ref. [18] for details). Therefore, we need only consider the $\ell \to \infty$ limit. Then, minimization of W with respect to η gives

$$B^2\left(1+\sigma_\perp\right)\left(\boldsymbol{\nabla}\cdot\boldsymbol{\xi}_\perp + \left(\boldsymbol{\kappa}\cdot\boldsymbol{\xi}_\perp\right)\Sigma_-\right)$$

$$+4\pi\Gamma_1\frac{\oint\left(dl/B\right)\left[\left(\boldsymbol{\nabla}\cdot\boldsymbol{\xi}_\perp\right)\Gamma_1 - \left(\boldsymbol{\kappa}\cdot\boldsymbol{\xi}_\perp\right)\Gamma_2\right]}{\oint\left(dl/B\right)\Gamma_3} = 0, \qquad (3.6)$$

and also implies that $\eta = 0$ for $\ell \to \infty$ since $\partial/\partial\zeta \propto \ell$. Using the preceding observations to eliminate $\boldsymbol{\nabla}\cdot\boldsymbol{\xi}_\perp$ from the expression for W we obtain the reduced energy principle

$$W = \int d^3r \left\{ \frac{Q_\perp^2\left(1-\sigma_-\right)}{8\pi} + \frac{B^2\left(1-\sigma_-\right)}{8\pi}\Sigma_+\left(\boldsymbol{\kappa}\cdot\boldsymbol{\xi}_\perp\right)^2 \right.$$

$$\left. -\frac{1}{2}\left(\boldsymbol{\kappa}\cdot\boldsymbol{\xi}_\perp\right)\left(\boldsymbol{\nabla}\left(p_\parallel+p_\perp\right)\cdot\boldsymbol{\xi}_\perp\right)\right\} \qquad (3.7)$$

$$+\frac{1}{2}\int d\psi \left\{ \frac{\left\{\int\left(dl/B\right)\left(\boldsymbol{\kappa}\cdot\boldsymbol{\xi}_\perp\right)\left[\Sigma_-\Gamma_1+\Gamma_2\right]\right\}^2}{\oint\left(dl/B\right)\left\{\Gamma_3+4\pi\Gamma_1^2/B^2\left(1+\sigma_\perp\right)\right\}} \right\},$$

where now

$$\boldsymbol{\xi}_\perp = \left(\xi/R^2B^2\right)\boldsymbol{\nabla}\psi, \quad Q_\perp^2 = R^{-2}B^{-2}\left(\boldsymbol{B}\cdot\boldsymbol{\nabla}\xi\right)^2.$$

To investigate the stability of the equilibrium and obtain an *estimate* for the mode

49

frequency ω we introduce the perpendicular kinetic energy H

$$H = \frac{1}{2} \int \mathrm{d}^3 r \rho \xi_\perp^2,$$

and perform the minimization with respect to ξ by varying the functional

$$\Lambda = \frac{W}{H} \propto \omega^2, \qquad (3.8)$$

where ρ is the mass density.

We begin by considering interchange modes for which $\boldsymbol{B} \cdot \boldsymbol{\nabla} \xi = 0$. Then variation of Eq. (3.7) with respect to ξ and using the expression from Ref. [17]

$$\frac{\boldsymbol{\nabla} \psi \cdot \boldsymbol{\kappa}}{R^2 B^2} = \frac{4\pi}{B^2 (1 - \sigma_-)} \boldsymbol{\nabla} \left(p_\perp + \frac{B^2}{8\pi} \right) \cdot \frac{\boldsymbol{\nabla} \psi}{R^2 B^2}$$

gives the general finite beta interchange stability condition:

$$\oint \frac{\mathrm{d}l}{B} \left\{ \frac{1}{R^2 B^2} \left[\Sigma_+ \boldsymbol{\kappa} \cdot \boldsymbol{\nabla} \left(p_\perp + \frac{B^2}{8\pi} \right) - \boldsymbol{\kappa} \cdot \boldsymbol{\nabla} \left(p_\parallel + p_\perp \right) \right] \right\}$$

$$+ \frac{\left\{ \oint (\mathrm{d}l/B) \left(\boldsymbol{\kappa} \cdot \boldsymbol{\nabla}\psi / B^2 R^2 \right) [\Sigma_- \Gamma_1 + \Gamma_2] \right\}^2}{\oint (\mathrm{d}l/B) \left\{ \Gamma_3 + 4\pi \Gamma_1^2 / B^2 (1 + \sigma_\perp) \right\}} \geq 0. \qquad (3.9)$$

We next consider the ballooning stability of the equilibrium. For short wavelength ballooning modes the stabilizing influence of plasma compressibility can be enhanced by the stabilizing influence of line bending $(Q_\perp^2 \neq 0)$. We minimize Eq. (3.8) with respect to ξ to find the infinite ℓ Euler integro-differential ballooning mode equation:

$$R^2 B^2 \boldsymbol{B} \cdot \boldsymbol{\nabla} \left(\frac{1 - \sigma_-}{R^2 B^2} \boldsymbol{B} \cdot \boldsymbol{\nabla} \xi \right) + 4\pi \left[\boldsymbol{\kappa} \cdot \boldsymbol{\nabla} \left(p_\parallel + p_\perp \right) \right.$$

$$\left. - \Sigma_+ \boldsymbol{\kappa} \cdot \boldsymbol{\nabla} \left(p_\perp + \frac{B^2}{8\pi} \right) + \rho \Lambda \right] \xi = 4\pi \left(\boldsymbol{\kappa} \cdot \boldsymbol{\nabla}\psi \right) [\Sigma_- \Gamma_1 + \Gamma_2] \qquad (3.10)$$

$$\times \frac{\oint (\mathrm{d}l/B) \left\{ \left(\boldsymbol{\kappa} \cdot \boldsymbol{\nabla}\psi / B^2 R^2 \right) \xi [\Sigma_- \Gamma_1 + \Gamma_2] \right\}}{\oint (\mathrm{d}l/B) \left\{ \Gamma_3 + 4\pi \Gamma_1^2 / B^2 (1 + \sigma_\perp) \right\}}.$$

Note that if we operate on Eq. (3.10) with $\oint \mathrm{d}l / \left(4\pi B^3 R^2 \right)$ the result is consistent

with Eq. (3.9) for $\Lambda > 0$.

As the physical system is symmetric with respect to the equatorial plane, Eq. (3.10) has two families of solutions: (1) up-down antisymmetric or "odd" with $\xi = 0$ at the equatorial plane; and (2) up-down symmetric or "even" with $\boldsymbol{B} \cdot \boldsymbol{\nabla} \xi = 0$ at the equatorial plane. For the odd solutions the integral in the numerator of the right-hand side of Eq. (3.10) is obviously equal to zero, so we need to only solve the homogeneous differential equation. For the even solutions the full integro-differential equation (3.10) must be solved.

As in Ref. [18], some important properties of the eigenvalues Λ_j of Eq. (3.10) can be determined by considering the eigenvalues λ_j of the corresponding homogeneous differential equation:

$$R^2 B^2 \boldsymbol{B} \cdot \boldsymbol{\nabla} \left(\frac{1 - \sigma_-}{R^2 B^2} \boldsymbol{B} \cdot \boldsymbol{\nabla} \xi \right) + 4\pi \left[\boldsymbol{\kappa} \cdot \boldsymbol{\nabla} \left(p_\parallel + p_\perp \right) \right.$$

$$\left. - \Sigma_+ \boldsymbol{\kappa} \cdot \boldsymbol{\nabla} \left(p_\perp + \frac{B^2}{8\pi} \right) + \rho \lambda \right] \xi = 0, \tag{3.11}$$

where $j = 0, 1, 2, \dots$. It can be shown that Eq. (3.11) coincides with the anisotropic pressure homogeneous ballooning equation (48) of Ref. [26].

Equation (3.11) is a Sturm-Liouville differential equation and for given boundary conditions it has a complete set of eigenfunctions ξ_j with corresponding distinct eigenvalues λ_j. We assume that odd j's correspond to the odd eigenfunctions and even j's to the even ones (note that odd and even cases have different boundary conditions). Moreover, we choose j in such a way that it gives the number of zeros of the corresponding eigenfunction. Then, as follows from the general theory of Sturm-Liouville differential equations, $\lambda_0 < \lambda_2 < \dots < \lambda_{2j} < \dots$ and $\lambda_1 < \lambda_3 < \dots < \lambda_{2j+1} < \dots$. It can be shown (see Appendix A) that the Λ_j 's are greater than or equal to the corresponding λ_j's, namely $\Lambda_{2j+1} = \lambda_{2j+1}$ and $\lambda_{2j} \leq \Lambda_{2j} \leq \lambda_{2j+2} \leq \Lambda_{2j+2}$. Consequently, if $\lambda_0 \geq 0$ and $\lambda_1 \geq 0$, then $\Lambda_j \geq 0$ and the equilibrium is stable, while if $\lambda_{2j+2} < 0$ then $\Lambda_{2j} < 0$ and if $\lambda_{2j+1} < 0$ then $\Lambda_{2j+1} = \lambda_{2j+1} < 0$, so that the low ballooning eigenmodes are unstable. In the more subtle case when $\lambda_0 < 0 < \lambda_2$ it is not clear

if Λ_0 is positive (stable), negative (unstable) or can change sign. For the particular case when the parallel and perpendicular pressures are proportional to each other the resolution of this last issue is given in the next section.

3.3 Stability of Anisotropic Plasma Pressure Equilibrium When $p_\perp = (1 + 2a) \, p_\parallel$

In the case of general anisotropic plasma pressure equilibrium the momentum balance equation gives

$$\frac{\partial p_\parallel}{\partial B} = \frac{p_\parallel - p_\perp}{B} \quad \text{and} \quad \frac{\partial p_\perp}{\partial B} = \frac{C + 2p_\perp}{B}, \tag{3.12}$$

where $p_\perp = p_\perp(\psi, B)$ and $p_\parallel = p_\parallel(\psi, B)$. We then simplify to the less general, but more analytically tractable, case where $p_\perp = (1 + 2a) \, p_\parallel$, with a a constant anisotropy parameter. This special case occurs, for example, when the particle distribution function has the form $F = h(\epsilon, \psi)(\mu/\epsilon)^{2a}$, where h is an arbitrary function of ϵ and ψ [45]. We can show using (3.12) that

$$\left\{ \begin{array}{c} p_\parallel \\ p_\perp \\ C \end{array} \right\} = \left\{ \begin{array}{c} 1 \\ 1 + 2a \\ -2(1+a)(1+2a) \end{array} \right\} \times \hat{p}(\psi) \, w(B), \tag{3.13}$$

where $\hat{p}(\psi)$ is an arbitrary function of the poloidal magnetic flux and $w(B) = (B_0/B)^{2a}$ with B_0 = constant reference magnetic field. It follows that $\Gamma_1 = (4a + 5)(a + 1/2)\hat{p}w$, $\Gamma_2 = -a(4a + 5)\hat{p}w$ and $\Gamma_3 = (4a + 5)(a + 3/4)\hat{p}w$.

Using Eq. (3.13) the interchange stability condition (3.9) can be rewritten as

$$-\frac{\mathrm{d}\hat{p}}{\mathrm{d}\psi} \oint \frac{\mathrm{d}l}{B} \left\{ \frac{\boldsymbol{\kappa} \cdot \boldsymbol{\nabla}\psi}{B^2 R^2} w \left[(1 + 2a)\Sigma_- - 2a\right] \right\}$$

$$+ \frac{\hat{\gamma}\hat{p}(\psi) \left\{ \oint (\mathrm{d}l/B)(\boldsymbol{\kappa} \cdot \boldsymbol{\nabla}\psi/B^2 R^2) w \left[(1 + 2a)\Sigma_- - 2a\right] \right\}^2}{\oint (\mathrm{d}l/B)\{w\} + 4\pi \hat{\gamma}(1 + 2a)^2 \hat{p}(\psi) \oint (\mathrm{d}l/B)\{w^2/B^2(1 + \sigma_\perp)\}} \geq 0, \tag{3.14}$$

52

with $\hat{\gamma} = \frac{5}{3} \left[1 + (4/5)\,a\right] / \left[1 + (4/3)\,a\right]$. In the isotropic pressure limit $a \to 0$, Eq. (3.14) reduces to the corresponding formula for the interchange stability from Refs. [1] and [20], namely

$$\frac{1}{p}\frac{\mathrm{d}p}{\mathrm{d}\psi} + \frac{5}{3}\frac{1}{V}\frac{\mathrm{d}V}{\mathrm{d}\psi} \leq 0.$$

with $V = \oint \mathrm{d}l/B$.

Similarly, upon using Eq. (3.13) the ballooning equation (3.10) becomes

$$R^2 B^2 \boldsymbol{B} \cdot \boldsymbol{\nabla} \left(\frac{1 - \sigma_-}{R^2 B^2} \boldsymbol{B} \cdot \boldsymbol{\nabla}\xi\right) + 4\pi \left[\boldsymbol{\kappa} \cdot \boldsymbol{\nabla}\,\hat{p}\,(\psi)\,w\left[(1 + 2a)\,\Sigma_- - 2a\right]\right.$$

$$\left.+\rho\Lambda\right]\xi = 4\pi\,\hat{\gamma}\,\hat{p}\,(\psi)\,w\left[(1 + 2a)\,\Sigma_- - 2a\right] \tag{3.15}$$

$$\times \frac{(\boldsymbol{\kappa} \cdot \boldsymbol{\nabla}\psi)\,\oint (\mathrm{d}l/B)\,\{\xi w\,(\boldsymbol{\kappa} \cdot \boldsymbol{\nabla}\psi/B^2 R^2)\,[(1 + 2a)\,\Sigma_- - 2a]\}}{\oint (\mathrm{d}l/B)\,\{w\} + 4\pi\,\hat{\gamma}\,(1 + 2a)^2\,\hat{p}\,(\psi)\,\oint (\mathrm{d}l/B)\,\{w^2/B^2\,(1 + \sigma_\perp)\}}.$$

which also coincides with the corresponding ballooning equation from Ref. [20] in the isotropic pressure limit.

As in the general case, Eq. (3.15) has two families of eigenfunctions: even and odd with respect to the equatorial plane with the corresponding boundary conditions $\boldsymbol{B} \cdot \boldsymbol{\nabla}\xi = 0$ and $\xi = 0$. Odd eigenfunctions cause the right hand side of Eq. (3.15) to vanish, so again $\Lambda_{2j+1} = \lambda_{2j+1}$, with λ_j denoting the eigenvalues of the Eq. (3.15) with right hand side equal to zero. The even eigenfunctions must be found by solving the full Eq. (3.15), but the ordering $\lambda_{2j} \leq \Lambda_{2j} \leq \lambda_{2j+2} \leq \Lambda_{2j+2}$ obviously still holds, so that the conditions $\lambda_0 > 0$ and $\lambda_1 > 0$ imply ballooning stability of the equilibrium and the condition $\lambda_j < 0$, $j = 1, 2, \ldots$, means that the low j ballooning modes are unstable.

The subtlety of the important case $\lambda_0 < 0 < \lambda_2$ can be resolved for the particular equilibrium $p_\perp = (1 + 2a)\,p_\parallel$ by generalizing the procedure of Ref. [18]. Indeed, as is shown in the Appendix A the eigenvalues of Eq. (3.15) are given by the equation

$$F\left(\Lambda\right) \equiv \sum_j \frac{a_j^2}{\Lambda - \lambda_j} = \frac{4\pi}{\hat{\gamma}\hat{p}\left(\psi\right)} \oint \frac{\mathrm{d}l}{B} \left\{ w + \frac{4\pi\hat{\gamma}\left(1 + 2a\right)^2 \hat{p}\left(\psi\right) w^2}{B^2\left(1 + \sigma_\perp\right)} \right\} \geq 0 \qquad (3.16)$$

where the coefficients a_j are determined by the expansion

$$D \equiv \left(\boldsymbol{\kappa} \cdot \boldsymbol{\nabla}\psi\right) \left[\left(1 + 2a\right)\Sigma_- - 2a\right] \hat{p}\left(\psi\right) w/\rho = \hat{p}\left(\psi\right) \sum_j a_j \xi_j.$$

The function $F\left(\Lambda\right)$ decreases monotonically in each of the intervals $\lambda_{2j} < \Lambda_{2j} < \lambda_{2j+2}$ and, as is shown in the Appendix A,

$$F\left(0\right) - F\left(\Lambda\right) = -\frac{4\pi V}{\hat{\gamma}\hat{p}'} \left\{ \frac{\hat{\gamma}V'}{V} + \frac{\hat{p}'}{\hat{p}} \right\}, \qquad (3.17)$$

where $V\left(\psi\right) = \oint \mathrm{d}l\left(w/B\right)$, $V' = \mathrm{d}V\left(\psi\right)/\mathrm{d}\psi$ and $\hat{p}' = \mathrm{d}\hat{p}\left(\psi\right)/\mathrm{d}\psi$. Due to the monotonic behavior of $F\left(\Lambda\right)$, the $F\left(0\right) - F\left(\Lambda\right) > 0 \ (< 0)$ means that $\Lambda > 0 \ (< 0)$ so that the corresponding eigenmode is stable (unstable).

Introducing the functions $L\left(\psi\right) = 4\pi\left(1 + 2a\right)^2 \oint \left(\mathrm{d}l/B\right) \left\{w^2/B^2\left(1 + \sigma_\perp\right)\right\}$ and $U\left(\psi\right) = \oint \left(\mathrm{d}l/B\right) \left\{\left(\boldsymbol{\kappa} \cdot \boldsymbol{\nabla}\psi/B^2 R^2\right) w\left[\left(1 + 2a\right)\Sigma_- - 2a\right]\right\}$ and using the relation $U\left(\psi\right) = L\left(\psi\right)\hat{p}'\left(\psi\right) - V'\left(\psi\right)$ proven in the Appendix B, it can easily be shown that the interchange stability condition (3.14) can be rewritten in the form

$$\frac{\left(V' - \hat{p}'L\right)\hat{p}V}{V + \hat{\gamma}\hat{p}L} \left\{ \frac{\hat{\gamma}V'}{V} + \frac{\hat{p}'}{\hat{p}} \right\} \geq 0 \qquad (3.18)$$

For confined plasma both plasma pressure and poloidal magnetic flux decrease with distance from the point dipole so $\hat{p}'\left(\psi\right) > 0$, while $V'\left(\psi\right) < 0$ since $V\left(\psi\right) \propto \oint \mathrm{d}l/B^{2a+1}$ increases with the distance from the point dipole for $a > -\frac{1}{2}$. As a result, since $L\left(\psi\right) > 0 \ (1 + \sigma_\perp > 0$ for mirror mode stability), the negative (positive) sign of the expression in the curly brackets in Eqs. (3.17) and (3.18) determines both interchange stability (instability) and ballooning stability (instability) of the lowest even mode, that is,

$$\frac{\hat{\gamma} V'}{V} + \frac{\hat{p}'}{\hat{p}} < 0 \qquad (3.19)$$

for interchange and lowest even ballooning mode stability. Indeed, we can conclude, that the equilibrium with $p_\perp = (1 + 2a) p_\parallel$ is ballooning stable if $\Lambda_1 = \lambda_1 > 0$, $\lambda_2 > 0$ and the equilibrium is interchange stable as well.

We also notice here that when the equilibrium is interchange stable it follows from Eq. (3.17) that $\Lambda > 0$. Consequently, if $\lambda_2 > 0$ and $\lambda_0 < 0$, then both λ_2 and Λ_0 must pass through zero at *exactly* the same value of beta since $\Lambda_0 \leq \lambda_2$. Therefore, marginal beta points can be found form Eq. (3.15) with right hand side equal to zero.

3.4 Stability of Anisotropic Plasma Pressure Equilibrium for a Point Dipole

In this section we apply the formulas derived in Section 3.3 to the case of the point dipole equilibrium of Ref. [15] which is a specific example of an equilibrium with $p_\perp = (1 + 2a) p_\parallel$. As is well known, stable anisotropic pressure plasma equilibria do not exist for all plasma betas. For $p_\parallel > p_\perp$ there is the, so-called, firehose beta limit $\beta_{\rm fh}$ (given by $1 - \sigma_- = 0$), and for $p_\perp > p_\parallel$ there is a mirror mode stability beta limit $\beta_{\rm mm}$ (given by $1 + \sigma_\perp = 0$). As is shown in Ref. [15] for the case of the plasma equilibrium under consideration these two conditions can be written as constraints on the equilibrium plasma beta $\beta_0 = 8\pi (1 + a) p_0 / B_0^2$ and anisotropy parameter a $(a > -\frac{1}{2})$ as

$$\beta_{\rm mm} \equiv \frac{1 + a}{a (1 + 2a)} > \beta_0 \quad \text{and} \quad \beta_{\rm fh} \equiv -\frac{1 + a}{a} > \beta_0. \qquad (3.20)$$

At this point it is convenient to rewrite Eqs. (3.15) and (3.18) by introducing the spherical coordinates spherical coordinates r, θ and ζ with $\mu = \cos \theta$ and $R = r \sin \theta$ and using the separable point dipole forms from Ref. [15] that satisfy the anisotropic pressure form of the Grad-Shafranov equation:

$$\psi\left(\boldsymbol{r}\right) = \psi_0 \left(r_0/r\right)^\alpha h\left(\mu\right), \quad \hat{p}\left(\psi\right) = p_0 \left(\psi/\psi_0\right)^{2(1+a)(2+\alpha)/\alpha}$$

$$B = B_0 \left(\psi/\psi_0 h\right)^{1+2/\alpha} G, \tag{3.21}$$

$$G^2 \equiv h^2/\left(1-\mu^2\right) + \left(\alpha^{-1}\mathrm{d}\,h/\mathrm{d}\,\mu\right)^2$$

where p_0, ψ_0, and $B_0 = \alpha\psi_0/r_0^2$ are the values of the plasma pressure, poloidal flux function, and magnetic field at the equatorial plane of a reference flux surface with $r = r_0$, and $\alpha = \alpha\left(p, \beta_0\right)$ is an eigenvalue of the equilibrium equation lying in the range $0 < \alpha \le 1$.

We first consider the interchange stability condition given by Eq. (3.19). For the point dipole equilibrium under consideration $\hat{p}'\left(\psi\right) = \left(1+a\right)\left(2+4/\alpha\right)\hat{p}\left(\psi\right)/\psi$, $V'\left(\psi\right) = -\left[1 + 3/\alpha + 2a\left(1+2/\alpha\right)\right]V\left(\psi\right)/\psi$, so that the stability condition can be rewritten as

$$\alpha < 3 + 4a \tag{3.22}$$

where $a > -1/2$. As a result, it follows that this equilibrium is interchange stable for all β_0.

Next we consider the ballooning stability of the anisotropic pressure point dipole equilibrium. After some tedious, but straightforward, algebra the ballooning Eq. (3.15) can be cast into the form

$$\frac{\mathrm{d}}{\mathrm{d}\,\mu}\left[A\left(\mu\right)\frac{\mathrm{d}\,\xi}{\mathrm{d}\,\mu}\right] + \left[\Lambda^* C\left(\mu\right) + D\left(\mu\right)\right]\xi = \frac{1}{2\beta_0\left(1+a\right)\left(2+\alpha\right)^2}$$
$$\times \frac{\hat{\gamma}D\left(\mu\right)\int_0^1 \mathrm{d}\,\mu\left\{D\left(\mu\right)\xi\right\}}{\int_0^1 \mathrm{d}\,\mu\left\{h^{3/\alpha}Y^a\left(\mu\right)\left[1 + \hat{\gamma}\beta_0\left(1+2a\right)^2 Y^{1+a}\left(\mu\right)/2\left(1+a\right)\left(1+\sigma_\perp\right)\right]\right\}}, \tag{3.23}$$

where

56

$$A(\mu) = \frac{(1 - \sigma_-) \, h^{2-1/\alpha}}{(1 - \mu^2) \, G^2}, \quad C(\mu) = \frac{h^{2+5/\alpha}}{(1 - \mu^2) \, G^2},$$

$$\Lambda^* = \frac{\Lambda r_0^2}{V_A^2} \left(\frac{\psi}{\psi_0} \right)^q,$$

$$D(\mu) = \frac{2\beta_0^2 \, (1 + a) \, (1 + 2a) \, (2 + \alpha)^2 \, h^{3/\alpha}}{(1 + \sigma_\perp) \, (1 - \sigma_-)} Y^{1+2a}(\mu)$$

$$+ \frac{\beta_0 \, (1 + a) \, (2 + \alpha)}{\alpha \, (1 - \sigma_-) \, h^{1/\alpha}} Y^{1+a}(\mu) \left[\frac{2\alpha \, (2 + \alpha)}{1 - \mu^2} + \frac{2}{hG} \frac{\mathrm{d} h}{\mathrm{d} \mu} \frac{\mathrm{d} G}{\mathrm{d} \mu} \right],$$

$$1 + \sigma_\perp = 1 - (1 + 2a) \, \beta_0 \Delta, \quad 1 - \sigma_- = 1 + \beta_0 \Delta,$$

$$\Delta = \frac{a}{1 + a} Y^{1+a}, \quad Y = \frac{h^{2+4/\alpha}}{G^2},$$

$q = 3 \, (2 + 4/\alpha) \, (1 + a) \, /5 - 2 - 6/\alpha$, and $V_A^2 = B_0^2/4\pi\rho_0$ is the Alfvén speed.

As in the general case, we need only seek solutions of Eq. (3.23) that are up-down symmetric or antisymmetric. The symmetric solutions are even in μ, have $0, 2, 4, \ldots 2j, \ldots$ nodes in the interval $-1 < \mu < 1$, and are determined by the boundary conditions $\mathrm{d}\xi/\mathrm{d}\mu|_{\mu=0} = \mathrm{d}\xi/\mathrm{d}\mu|_{\mu=1} = 0$. The odd in μ, or antisymmetric, solutions have $1, 3, 5, \ldots 2j + 1, \ldots$ nodes in the interval $-1 < \mu < 1$ and are determined by the boundary conditions $\xi(\mu = 0) = \xi(\mu = 1) = 0$.

As follows from the discussion in Section 3.3, to determine the ballooning stability of the equilibrium and the corresponding beta limit it is enough to consider only the second even and first odd eigenmodes of Eq. (3.23) with right hand side equal to zero.

Results of a numerical solution of Eq. (3.23) with periodic boundary conditions are shown in Figs. 3-1 - 3-3 for anisotropy parameters $a = -\frac{1}{4}, \frac{1}{10}$ and 5. The solid lines are with the right hand side retained and the dashed and dashed-dotted lines are with the right hand side set to zero. As expected, the behavior of the eigenvalues clearly reflects the presence of the firehose ($\beta_{\mathrm{fh}} = 3$ for $a = -\frac{1}{4}$) and mirror mode ($\beta_{\mathrm{mm}} = \frac{110}{12}$ for $a = \frac{1}{10}$ and $\beta_{\mathrm{mm}} = \frac{6}{55}$ for $a = 5$) beta limits at the values given by Eq. (3.20). As in the case of isotropic pressure [20] the first even eigenmode of the
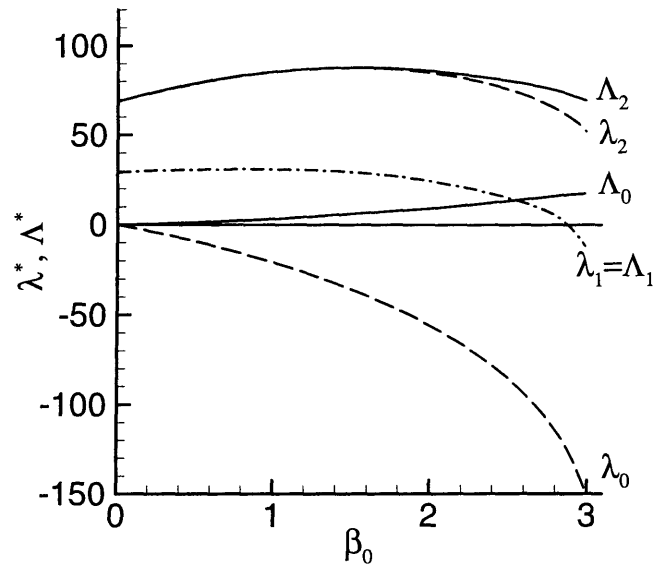
Figure 3-1: Eigenvalues λ^* and Λ^* for the first and second even and the first odd eigenfunctions versus β_0 as obtained by numerically solving Eq. (3.23) with (solid lines) and without (dashed and dashed-dotted lines) right-hand side for periodic boundary conditions and $a = -1/4$.
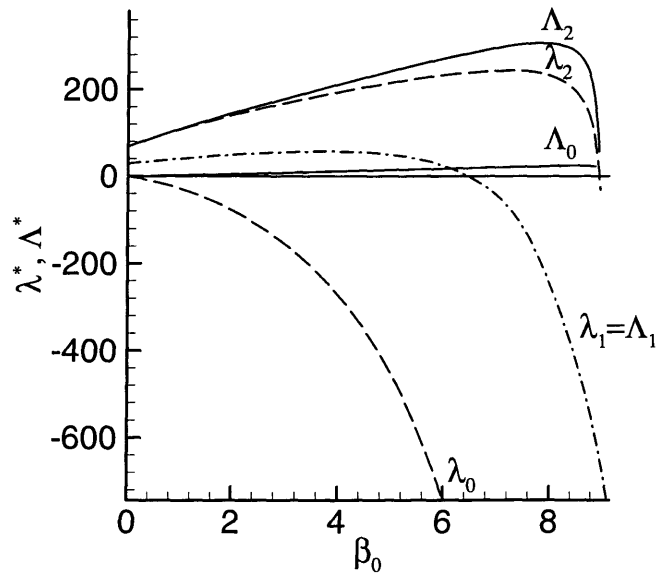
Figure 3-2: Same as Figure 3-1 but for $a = 1/10$.
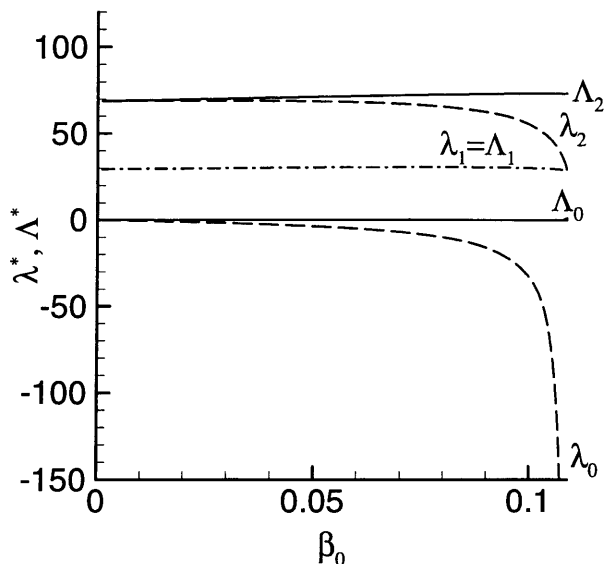
Figure 3-3:   Same as Figure 3-1 but for $a = 5$.

homogeneous differential form of Eq. (3.23) (without the right hand side) is unstable for any beta, while the first odd eigenmode and the second even eigenmode are stable up to some critical beta - possibly below the corresponding firehose or mirror mode beta limit. The eigenvalues of the integro-differential form of Eq. (3.23) (i.e. with the right hand side) are bigger than the corresponding eigenvalues of the homogeneous equation for all betas, because of the stabilizing influence of plasma compressibility. In particular, the lowest even mode of the integro-differential equation is stable for all betas up to a critical value.

It is interesting to notice a transition which occurs when the value of the anisotropy parameter $a = \frac{7}{2}$. As is shown in Appendix C the solutions of homogeneous analog of Eq. (3.23) at $\mu \ll 1$ and $\beta \to \beta_{mm}$ oscillate for $a < \frac{7}{2}$. Following Newcomb's analysis of stability of the screw pinch [46] it can be shown that such oscillatory behavior corresponds to instability. As in the Suydam/Newcomb analysis, absence of local oscillatory behavior does not necessarily imply stability. However our numerical analysis shows that for $a > \frac{7}{2}$ ballooning modes are stable for all betas up to β_{mm}. We conclude, therefore, that for these equilibria and for $p_\perp/p_\parallel > 1$, the beta limit is

59

set by the mirror instability if $p_\perp/p_\parallel > 8$ (i.e. $a > \frac{7}{2}$) and is set by the ballooning mode if $p_\perp/p_\parallel < 8$ (i.e. $a < \frac{7}{2}$).

3.5 The Case of "Tied Field Lines" or the Planetary Magnetosphere Case

In this section we apply the results obtained in the previous sections to the case of dipolar magnetic field produced by planetary [14, 47] or solar [30] dynamo activity with a highly conducting surface so that magnetic field lines are "tied" to it. The "tied" field line boundary condition means that the plasma displacement is equal to zero ($\xi = 0$) at the surface of the planet or star. Ballooning modes are suspected to be a source of many interesting phenomena occurring in such plasmas. In particular, in the absence of plasma compressibility, they have been suggested as being responsible for the localized depletions of thermal plasma around Jupiter observed by the Voyager 2 spacecraft in 1979 [14].

We use the anisotropic plasma pressure stability analysis as described and developed in the previous sections, but with the difference that now $\xi\,(\mu = \pm 1) = 0$ for all cases. This change in the boundary conditions leads to the observation that we can not consider the interchange mode anymore, as the plasma displacement would be equal to zero for all μ in this case. Moreover, both symmetric and antisymmetric eigenfunctions of the ballooning equation (3.23) have $\xi\,(\mu = \pm 1) = 0$ as a boundary condition. It can be shown that although the relationships $\lambda_{2j} \leq \Lambda_{2j} \leq \lambda_{2j+2} \leq \Lambda_{2j+2}$ and $\lambda_{2j+1} = \Lambda_{2j+1}$ between the eigenvalues of the full ballooning equation and ballooning equation with right hand side equal to zero are still valid, the general analysis of Appendix A for the most practically interesting and subtle case of $\lambda_0 < 0 < \lambda_2$ fails for the case of "tied" field lines. As a result it is necessary to solve the full integro-differential equation (3.23) to determine the ballooning stability of the equilibrium.

Results of the numerical solution of the Eq. (3.23) for the field line "tied" boundary conditions are shown on Figs. 3-4 - 3-6 for $a = -\frac{1}{4}$, $\frac{1}{10}$ and 5. All even ballooning

modes are more stable than those found with periodic boundary conditions because of the additional stabilizing influence of magnetic field line bending. As in the case of periodic boundary conditions ballooning modes become unstable at some critical betas below the mirror mode beta limit β_{mm} for $a < \frac{7}{2}$ and are stable up to the β_{mm} for $a > \frac{7}{2}$.

The ballooning stability of anisotropic plasma pressure equilibria with "tied" field line boundary conditions was studied in Refs. [25] and [26], where the ballooning equation was derived kinetically. The authors conjectured that the first odd ballooning mode was the most unstable solution and, therefore, dropped the integral term associated with plasma compressibility (without giving a simple, analytically tractable fluid expression for it). They then solved the differential ballooning equation, which coincides with our Eq. (3.11). Although their conjecture is appealing, a mathematically rigorous proof does not exist, so in general the full integro-differential ballooning equation must be solved. The argument of Ref. [25] can be understood in the following way. Although the stabilizing influence of magnetic field line bending is stronger for the first odd mode than for the first even mode, unlike even modes, odd modes are not subject to the stabilizing influence of plasma compressibility, which increases with beta. At the same time the instability driving term also increases with beta. So for large beta Ref. [25] argued that the first odd mode would be more unstable than the first even mode. However, at high plasma pressures the curvature becomes beta dependent, and for strong anisotropies, the critical betas for the onset of the mirror mode and firehose instabilities become small. As a result, the preceding argument may not hold and the first even ballooning mode could actually determine the ballooning beta limit for strong anisotropy. Indeed, as we can see from Figs. 3-4 - 3-6 for $a = -\frac{1}{4}$ and $\frac{1}{10}$, the first odd mode becomes unstable first; however, for $a = 5$ the first even mode is always less stable than the first odd mode. This same behavior is also seen for the periodic boundary condition case of Figs. 3-1 - 3-3. It should also be pointed out that the low beta equilibrium used in Ref. [26] is not a self-consistent global equilibrium since the direction of the magnetic field as well as its magnitude must change as beta increases [1, 15]. As a result, the order unity critical beta for the
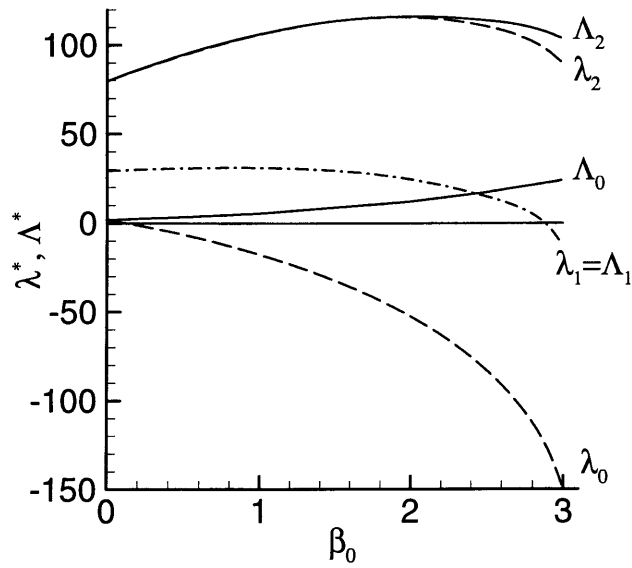
Figure 3-4: Same as Figure 3-1 except "tied" field line boundary conditions are employed; $a = -1/4$.
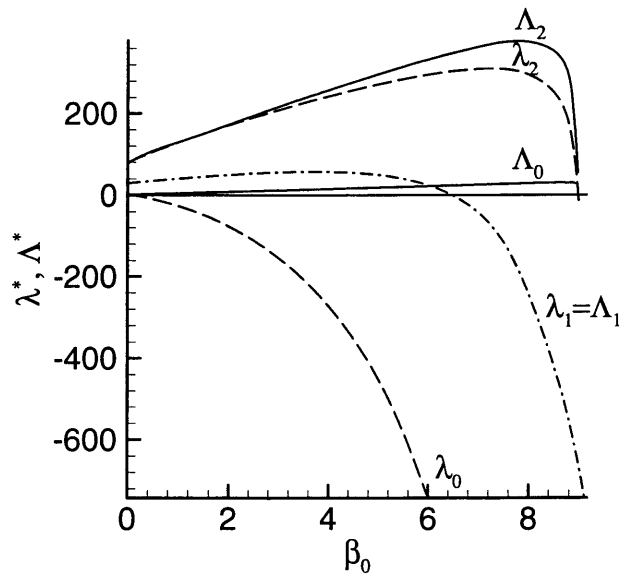
Figure 3-5: Same as Figure 3-2 except "tied" field line boundary conditions are employed; $a = 1/10$.
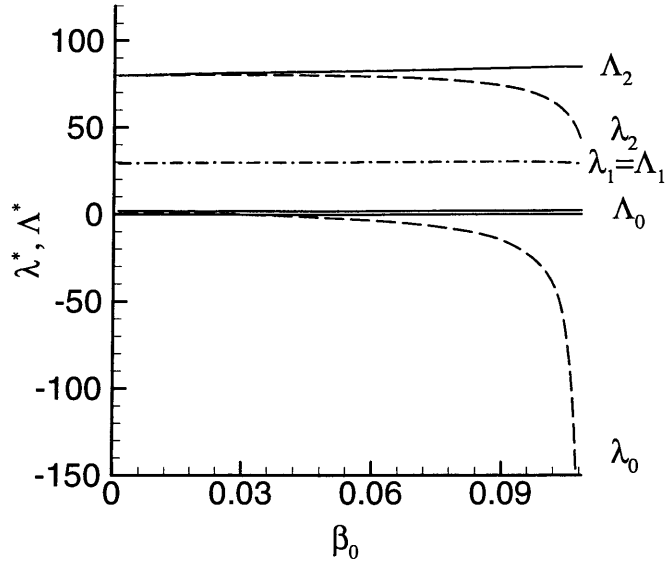
Figure 3-6: Same as Figure 3-3 except "tied" field line boundary conditions are employed; $a = 5$.

onset of ballooning instability found in Ref. [26] is not self-consistently determined.

3.6 Conclusions

Stability of plasma equilibrium in a dipolar magnetic field is important for both laboratory experiments (such as LDX) and planetary and astrophysical applications. In this chapter stability of a general anisotropic plasma pressure equilibrium in a dipole magnetic field was investigated. The Kruskal-Oberman form of the Energy Principle was rewritten, using a Schwarz inequality, to give a relatively simple "fluid" form of MHD Energy Principle. This expression was minimized with respect to the component of plasma displacement in the toroidal direction to give a finite beta interchange stability condition and an integro-differential ballooning equation. A "simplified differential ballooning equation" - the ballooning equation without the integral term - was also considered. It was shown that important relationships between the eigenvalues of these two equations exist - as in the isotropic pressure case [18].

The general stability theory was then applied to a more specific plasma equilibrium

with the perpendicular plasma pressure proportional to the parallel plasma pressure, namely $p_\perp = (1 + 2a)\, p_\parallel$. It was found that when the plasma displacement was restricted to be periodic, the plasma equilibrium is ballooning stable if it is interchange stable and the first odd and second even modes of the "simplified ballooning equation" are stable. So for the case of periodic boundary conditions it was not necessary to solve the entire integro-differential ballooning equation to determine ballooning stability of the equilibrium. It was only necessary to consider the homogeneous differential ballooning equation. Unlike the tokamak case where there are regions of favorable and unfavorable magnetic field line curvature, magnetic field line curvature of the dipole field is always unfavorable. On the other hand, unlike the tokamak case, magnetic field lines are closed for a dipole equilibrium, which provides a stabilizing plasma compressibility term (for the even modes) in addition to the usual magnetic field line bending stabilization.

Finally, the stability of the separable point dipole plasma equilibrium of Ref. [15] was investigated. Both the full integro-differential ballooning equation and the simplified differential equation were solved numerically for periodic boundary conditions and for the case of "tied" field lines to check the predictions of the theory. It was found that for periodic boundary conditions the equilibrium is interchange stable for all plasma betas and ballooning stable for all betas up to some critical value, which is below the mirror mode beta limit β_{mm} when the pressure anisotropy parameter $a < \frac{7}{2}$ (i.e. $p_\perp / p_\parallel < 8$) and is equal to β_{mm} for $a > \frac{7}{2}$ (i.e. $p_\perp / p_\parallel > 8$). Ballooning modes were found to be more stable with "tied" field line boundary conditions because of the additional field lines bending.

Chapter 4

Kinetic Stability of Electrostatic Plasma Modes in a Dipole Magnetic Field

4.1 Introduction

Unlike tokamaks, where both favorable and unfavorable field line curvature regions exist, so that the curvature can be favorable "on average", field line curvature for magnetic dipoles is unfavorable everywhere. On the other hand, plasma compressibility due to the closed field lines (or equivalently, large trapped particle populations) plays a very important stabilizing role for dipoles and is not present in tokamaks. It has recently been shown that plasma equilibria in dipolar magnetic fields have favorable ideal MHD [19, 20] and hybrid fluid-kinetic [27] stability properties.

Of course, many phenomena can not be described by ideal MHD. In particular, the orderings used to derive the basic MHD equations are not always adequate and so in many cases kinetic theory must be employed. Kinetic approaches to the problem were used in Refs. [10, 21, 31, 32, 33]. Ref. [10] considers collisionless electrostatic modes in closed field line multipole devices with regions of average favorable curvature, for the mode frequency between magnetic and diamagnetic drift frequencies.

Ref. [31] assumes magnetic and diamagnetic drift frequencies to be of the same order and studies collisionless electrostatic drift frequency modes for plasmas confined in dipolar fields. In Ref. [32] the authors consider an electromagnetic treatment of collisionless plasmas in the Earth's magnetosphere. Refs. [21, 33], on the other hand, study electrostatic plasma modes in a regime of intermediate collisionality, where the collision frequency is smaller than transit or bounce frequencies, but larger than the mode, magnetic drift, and diamagnetic drift frequencies. This regime is of interest for the Levitated Dipole Experiment [9] which is expected [48] to obtain plasma with a density $N \sim 10^{13} \, cm^{-3}$ and temperatures $T_e \sim T_i \sim 100 \, eV$ or more, in a magnetic field $B \sim 2 \, kG$ in a machine of dimension $D \sim 1 \, m$.

In Ref. [36] it is shown that ion collisional "dissipative" effects, in particular the so-called gyro-relaxation effects, are extremely important in determining stability of the plasma to electrostatic modes for the collisionality regime under consideration. Gyro-relaxation effects describe the collisional relaxation of a perturbed distribution function which is anisotropic, or isotropic but non-Maxwellian in energy, towards a Maxwellian. These collisional effects may either dissipate, or generate (inverse dissipation), energy and the resulting effects lead to mode growth or damping depending on the wave energy. For example, energy dissipation destabilizes negative energy waves. We will simply use the term "dissipation" without regard to the sign. In some cases gyro-relaxation effects can destabilize otherwise stable modes and so must be considered when choosing the LDX operational regime (in particular, the temperature and density profiles). Up to now, gyro-relaxation effects have been only studied for plasmas in a straight magnetic field or in the cylindrical magnetic field of a Z-pinch [36] (where the magnetic field is constant along the field line).

In this chapter, we extend the treatment of Refs. [21, 33] to the case of the arbitrary ratio of the electron and the ion equilibrium temperatures and to retain ion collisional effects. We show that the ion perpendicular heat conduction effects are negligible compared to the ion gyro-relaxation effects and develop a procedure for evaluating the latter for the case of arbitrary magnetic fields with closed field lines. We then obtain the electrostatic dispersion relation and determine the stable regions,

which can be conveniently described in terms of d and η, with η the ratio of gradients of the equilibrium temperature and density, and d the ratio of the diamagnetic and magnetic drift frequencies and proportional to the gradient of plasma pressure.

We begin by solving the gyro-kinetic equation in Sec. 4.2 by using the intermediate collisionality ordering. It is necessary to work to higher order than previous treatments to determine the leading collisional correction to the ion distribution function. Once this is done, the perturbed particle densities can be found and the quasineutrality condition formed to obtain the dispersion relation and to show that the electrostatic modes are flute-like for the ordering employed. These details are described in Sec. 4.3. The dispersion relation allows two classes of electrostatic modes: (i) "low-frequency" modes, with a frequency of the order of the magnetic and diamagnetic drift frequencies, and (ii) "high-frequency" modes, with a frequency much larger than the magnetic drift frequency. These two cases are considered in Secs. 4.4 and 4.5, respectively. In some cases the two classes of mode couple and this situation is described in Sec. 4.6. Finally, the results are summarized in Sec. 4.7. Appendices D through G provide details of the solution procedure and analysis.

4.2 Solution of the Gyrokinetic Equation

To derive and solve the gyrokinetic equation we adopt the following orderings:

$$\Omega_j \gg \omega_{bj} \gg \nu_{cj} \gg \omega \gtrsim \omega_{dj} \sim \omega_{*j}, \tag{4.1}$$

where Ω_j, $\omega_{bj} \sim \boldsymbol{v}_j \cdot \boldsymbol{\nabla}$, ν_{cj}, ω_{dj}, and ω_{*j} denote the cyclotron, bounce (transit), collision, magnetic drift, and diamagnetic drift frequencies, respectively, and ω is the mode frequency. The subscript j denotes different particle species, $j = i, e$.

Assuming the equilibrium electrostatic potential vanishes or that we are in the $\boldsymbol{E} \times \boldsymbol{B}$ drifting frame, the orderings (4.1) lead to Maxwellian equilibrium distribution functions,

$$f_{Mj}(E, \psi) \equiv N_j \left(M_j / 2\pi T_j \right)^{3/2} e^{-M_j E / T_j}, \tag{4.2}$$

to lowest order in ρ_j/D, with ρ_j the gyroradius and D the equilibrium scale length. Here, $N_j(\psi)$, $T_j(\psi)$, M_j and $E = v^2/2$ are the species density, temperature, mass and energy, respectively, and ψ is the the poloidal magnetic flux function. To next order in ρ_j/D the unperturbed distribution function has diamagnetic corrections, giving

$$f_{0j} = f_{Mj} + \frac{1}{\Omega_j} \boldsymbol{v} \times \hat{\boldsymbol{n}} \cdot \boldsymbol{\nabla} f_{Mj} \qquad (4.3)$$

to the order we require. In Eq. (4.3) $\hat{\boldsymbol{n}} = \boldsymbol{B}/|\boldsymbol{B}|$ is the unit vector along the equilibrium magnetic field $\boldsymbol{B} = \boldsymbol{\nabla}\psi \times \boldsymbol{\nabla}\zeta$, with ζ the toroidal coordinate.

We employ the eikonal approximation to determine the perturbed distribution function f_{1j} by taking [49, 50]

$$f_{1j} = \left(-\frac{Z_j e \hat{\Phi}_1}{T_j} f_{Mj} + h_j e^{iL_j} \right) e^{iS - i\omega t}. \qquad (4.4)$$

In Eq. (4.4) $Z_j e$ is the species charge, $\Phi_1 = \hat{\Phi}_1 e^{iS - i\omega t}$ is the perturbed electrostatic potential, $S = S(\psi, \zeta)$ is the eikonal [49], $L_j = (\boldsymbol{v} \cdot \hat{\boldsymbol{n}} \times \boldsymbol{k}_\perp)/\Omega_j$ and $\boldsymbol{k}_\perp = \boldsymbol{\nabla} S$. The portion of the perturbed distribution function denoted by h_j is *gyrophase independent* and satisfies the following gyrokinetic equation

$$v_\parallel \hat{\boldsymbol{n}} \cdot \boldsymbol{\nabla} h_j - i \left(\omega - \boldsymbol{v}_{dj} \cdot \boldsymbol{k}_\perp \right) h_j = \left\langle e^{-iL_j} C_{1j} \left(h_j e^{iL_j} \right) \right\rangle_\phi + \hat{Q} J_0 \left(\frac{k_\perp v_\perp}{\Omega_j} \right), \qquad (4.5)$$

in energy $(v^2/2)$, magnetic moment $(\mu = v_\perp^2/2B)$, and gyrophase (ϕ) variables. In Eq. (4.5) "parallel" and "perpendicular" refer to a direction along and across the magnetic field $\boldsymbol{B}$, and gyrophase averaging is defined as $\langle \ldots \rangle_\phi = (2\pi)^{-1} \oint (\ldots) \, d\phi$. The magnetic drift velocity $\boldsymbol{v}_{dj}$ is given by

$$\boldsymbol{v}_{dj} \equiv \hat{\boldsymbol{n}} \times \left(\frac{v_\perp^2}{2\Omega_j} \boldsymbol{\nabla} \ln B + \frac{v_\parallel^2}{\Omega_j} \boldsymbol{\kappa} \right) \qquad (4.6)$$

with $\boldsymbol{\kappa} \equiv \hat{\boldsymbol{n}} \cdot \boldsymbol{\nabla} \hat{\boldsymbol{n}}$ the magnetic field line curvature. The terms on the right hand side of Eq. (4.5) are the linearized collision operator C_{1j} and

$$\hat{Q} \equiv -\mathrm{i}\frac{Z_j e}{T_j} f_{Mj} \left\{ \omega - \omega_{*j} \left[1 + \eta_j \left(\frac{M_j E}{T_j} - \frac{3}{2} \right) \right] \right\} \hat{\Phi}_1, \tag{4.7}$$

with

$$\omega_{*j} \equiv \frac{c\ell T_j}{Z_j e N_j} \frac{\mathrm{d}\, N_j}{\mathrm{d}\,\psi}, \qquad \eta_j \equiv \frac{\mathrm{d}\, \ln T_j\,(\psi)\,/\mathrm{d}\,\psi}{\mathrm{d}\, \ln N_j\,(\psi)\,/\mathrm{d}\,\psi}, \tag{4.8}$$

where $k_\zeta \equiv \boldsymbol{k}_\perp \cdot \hat{\boldsymbol{\zeta}} = \ell/R$ with $\hat{\boldsymbol{\zeta}}$ the unit vector in the toroidal direction, c is the speed of light, R is the cylindrical radial coordinate, $\ell \gg 1$ the toroidal mode number and J_0 is the Bessel function of the first kind. The linearized Fokker-Planck collision operator C_{1j} is given to the required order by $C_{1e} = C_{1ee} + C_{1ei}$ for the electron kinetic equation and $C_{1i} = C_{1ii}$ for the ion kinetic equation, where C_{1jj} denotes the like particle contribution and C_{1ei} is the electron-ion term.

We solve Eq. (4.5) by expanding $h_j = h_{1j} + h_{2j} + h_{3j} + \ldots$ in accordance with our orderings (4.1). Suppressing the index j to simplify notation, we find to the lowest order

$$v_\parallel \hat{\boldsymbol{n}} \cdot \boldsymbol{\nabla} h_1 = 0, \tag{4.9}$$

so that $h_1 = h_1\,(E, \mu, \psi)$. To second order

$$v_\parallel \hat{\boldsymbol{n}} \cdot \boldsymbol{\nabla} h_2 = C_1\,(h_1), \tag{4.10}$$

which upon annihilation of the left hand side requires h_1 to be the perturbed Maxwellian [50]

$$h_1 = f_M \left(\alpha\,(\psi) + \beta\,(\psi) \frac{Mv^2}{2T} \right), \tag{4.11}$$

where $\alpha\,(\psi)$ and $\beta\,(\psi)$ are to be determined. Using expression (4.11) in Eq. (4.10) gives $v_\parallel \hat{\boldsymbol{n}} \cdot \boldsymbol{\nabla} h_2 = 0$ so that $h_2 = h_2\,(E, \mu, \psi)$. To determine α and β we use the third order equation

$$-\mathrm{i}\left(\omega - \boldsymbol{v}_d \cdot \boldsymbol{k}_\perp\right) h_1 + v_\parallel \hat{\boldsymbol{n}} \cdot \boldsymbol{\nabla} h_3 = C_1\left(h_2\right) + \hat{Q} J_0\left(\frac{k_\perp v_\perp}{\Omega}\right), \qquad (4.12)$$

where $J_0(z) \approx 1 - z^2/4$ since we assume $k_\perp v_\perp / \Omega \ll 1$. Integrating Eq. (4.12) over all $\boldsymbol{v}$ with weighting function v^q with $q = 0, 2$ and then averaging over poloidal angle θ to annihilate both the h_2 and h_3 terms, we obtain a pair of equations for α and β:

$$\left\langle \int \mathrm{d}^3 v\, v^q \left[\left(\omega - \boldsymbol{v}_d \cdot \boldsymbol{k}_\perp\right) h_1 - \mathrm{i}\hat{Q}\left(1 - \frac{k_\perp^2 v_\perp^2}{4\,\Omega^2}\right)\right]\right\rangle_\theta = 0, \qquad q = 0, 2, \qquad (4.13)$$

where $\langle \ldots \rangle_\theta = V^{-1} \oint \left[(\ldots)\,\mathrm{d}\theta / \left(\boldsymbol{B} \cdot \boldsymbol{\nabla}\theta\right)\right]$ with $V(\psi) \equiv \oint \left[\mathrm{d}\theta / \left(\boldsymbol{B} \cdot \boldsymbol{\nabla}\theta\right)\right]$.

Performing the integrations in Eq. (4.13) and solving the resulting linear system for α and β we find

$$\alpha = \frac{Ze\left\langle \hat{\Phi}_1 \right\rangle_\theta}{T} G_1 + \frac{Ze\left\langle b\hat{\Phi}_1 \right\rangle_\theta}{T} G_2,$$

$$\beta = \frac{Ze\left\langle \hat{\Phi}_1 \right\rangle_\theta}{2T} H_1 + \frac{Ze\left\langle b\hat{\Phi}_1 \right\rangle_\theta}{2T} H_2, \qquad (4.14)$$

where

$$G_1 = \frac{\omega^2 - \left[\left(1 - \frac{3}{2}\eta\right)\omega_* + \frac{10}{3}\langle \omega_d \rangle_\theta\right]\omega + \frac{5}{6}\left(4 - 3\eta\right)\omega_*\langle \omega_d \rangle_\theta}{\omega^2 - \frac{10}{3}\omega\langle \omega_d \rangle_\theta + \frac{5}{3}\langle \omega_d \rangle_\theta^2},$$

$$G_2 = \frac{\frac{5}{12}\left(2\langle \omega_d \rangle_\theta - 3\eta\omega_*\right)\omega - \frac{5}{12}\left(2 - 3\eta\right)\omega_*\langle \omega_d \rangle_\theta}{\omega^2 - \frac{10}{3}\omega\langle \omega_d \rangle_\theta + \frac{5}{3}\langle \omega_d \rangle_\theta^2},$$

$$H_1 = \frac{\left(\frac{4}{3}\langle \omega_d \rangle_\theta - 2\eta\omega_*\right)\omega - \left(\frac{4}{3} - 2\eta\right)\omega_*\langle \omega_d \rangle_\theta}{\omega^2 - \frac{10}{3}\omega\langle \omega_d \rangle_\theta + \frac{5}{3}\langle \omega_d \rangle_\theta^2},$$

$$H_2 = \frac{-\frac{2}{3}\omega^2 + \left(\frac{2}{3} + \frac{7}{3}\eta\right)\omega_*\omega - \frac{5}{3}\eta\,\omega_*\langle \omega_d \rangle_\theta}{\omega^2 - \frac{10}{3}\omega\langle \omega_d \rangle_\theta + \frac{5}{3}\langle \omega_d \rangle_\theta^2}$$

and

$$b \equiv \left(k_\perp^2 T / M\Omega^2 \right) \ll 1, \qquad \omega_d \equiv \frac{k_\zeta T}{M\Omega} \left[\hat{\zeta} \cdot \hat{n} \times (\nabla \ln B + \kappa) \right], \tag{4.15}$$

with [21]

$$\langle \omega_d \rangle_\theta = -\frac{c\ell T}{ZeV} \frac{dV}{d\psi}. \tag{4.16}$$

To account for collisional effects it is necessary to determine h_2 for the ions ($h_2 \propto M^{1/2}$, as will be shown shortly, so collisional effects can be neglected for electrons). The equation for h_2 is obtained from Eq. (4.12) by annihilating the h_3 term by multiplying by $B/v_\parallel$ and averaging over a closed trajectory orbits for both trapped and passing particles to obtain

$$\left\langle \frac{B}{v_\parallel} \left[i \left(\omega - v_d \cdot k_\perp \right) h_1 + C_1 \left(h_2 \right) + \hat{Q} \right] \right\rangle_\theta = 0. \tag{4.17}$$

It is possible to solve Eq. (4.17) by employing a variational procedure. To do so we consider the functional

$$\Lambda \left(g \right) \equiv \left\langle \int d^3 v\, g\, C_{1ii} \left(g\, f_M \right) \right\rangle_\theta + 2 \left\langle \int d^3 v\, g \left[i \left(\omega - v_d \cdot k_\perp \right) h_1 + \hat{Q} \right] \right\rangle_\theta \tag{4.18}$$

and define a class of trial functions

$$g/f_{Mi} = \sum_{m=0}^{\infty} a_m L_m^{(1/2)} \left(x \right) + \left(x - \frac{3}{2} \frac{x_\perp}{B \left\langle 1/B \right\rangle_\theta} \right) \sum_{m=0}^{\infty} b_m L_m^{(5/2)} \left(x \right), \tag{4.19}$$

with $L_m^{(n+1/2)} \left(x \right)$ the generalized Laguerre (Sonine) polynomials [51, 52], $x \equiv M_i v^2 / 2T_i$, $x_\perp \equiv M_i v_\perp^2 / 2T_i$, and $a_m \left(\psi \right)$ and $b_m \left(\psi \right)$ unknown coefficients to be determined variationally. By substituting g from Eq. (4.19) into the functional (4.18) and varying the resulting expression with respect to the a_m and b_m, we can determine the unknown coefficients and, thereby, obtain a good approximation to the solution of Eq. (4.17).

It is clear from Eq. (4.17) that any solution is determined up to a perturbed

Maxwellian which corresponds to a_0 and a_1 being arbitrary. To determine a_0 and a_1 it is necessary to go to the fourth order expansion of the gyrokinetic Eq. (4.5). After integrating this fourth order equation in velocity space with the weighting functions v^q $(q = 0, 2)$ and averaging over poloidal angle to annihilate h_3 and h_4 terms we obtain the following pair of constraints on h_2:

$$\left\langle \int \mathrm{d}^3 v \, v^q \left(\omega - \boldsymbol{v}_d \cdot \boldsymbol{k}_\perp \right) h_2 \right\rangle_\theta = 0, \qquad q = 0,\, 2. \tag{4.20}$$

These two equations fully determine a_0 and a_1. A detailed solution of Eq. (4.17) is given in Appendix D.

We remark that the form (4.19) of the trial function is motivated by the case of $B(\theta)$=const, for which we can solve Eq. (4.17) without recourse to the variational principle by simply expanding the solution in an infinite series in Legendre $P_n \left(v_\parallel / v \right)$ and generalized Laguerre polynomials. In this case the solution depends only on P_0 and P_2. Moreover, it is possible to obtain accurate solutions by truncating the expansions in Laguerre polynomials [53] at a_3 and b_1. For our problem such truncation provides a solution with a precision better than 10%.

4.3 Electrostatic Dispersion Relation

To evaluate the perturbed electron and ion densities N_{1j} we substitute h_1 from Eq. (4.11) and h_2 in the form (4.19), with the coefficients from Appendix D, into Eq. (4.4) for the perturbed distribution function f_1 and integrate over all velocities. Then, using the quasineutrality condition $N_{1e} = Z_i N_{1i}$ we obtain the following eigenmode equation

$$-\hat{\Phi}_1\left(\boldsymbol{r}\right)\left(1+\tau\right)+\left\langle\hat{\Phi}_1\left(\boldsymbol{r}\right)\right\rangle_\theta\left[\tau\left(G_{1i}+\frac{3}{4}H_{1i}\right)+\left(G_{1e}+\frac{3}{4}H_{1e}\right)\right]$$
$$+\left\langle b_i\hat{\Phi}_1\left(\boldsymbol{r}\right)\right\rangle_\theta\tau\left[G_{2i}+\frac{3}{4}H_{2i}\right]-b_i\left\langle\hat{\Phi}_1\left(\boldsymbol{r}\right)\right\rangle_\theta\tau\left[\frac{1}{2}G_{1i}+\frac{5}{8}H_{1i}\right]$$
$$+\left[a_0+\frac{3}{2}\left(b_0+b_1\right)\left(1-\frac{1}{B\left\langle1/B\right\rangle_\theta}\right)\right]\frac{T_e}{e}=0, \tag{4.21}$$

where a_0, b_0 and b_1 are given in Appendix D and $\tau\equiv Z_iT_e/T_i$.

Averaging Eq. (4.21) over poloidal angle and subtracting the result from Eq. (4.21) we find

$$\frac{\left\langle\hat{\Phi}_1\left(\boldsymbol{r}\right)\right\rangle_\theta-\hat{\Phi}_1\left(\boldsymbol{r}\right)}{\left\langle\hat{\Phi}_1\left(\boldsymbol{r}\right)\right\rangle_\theta}=\frac{b_i-\left\langle b_i\right\rangle_\theta}{2}\frac{\tau}{1+\tau}\left[G_{1i}+\frac{5}{4}H_{1i}\right]$$
$$-\frac{3\left(b_0+b_1\right)}{2\left(1+\tau\right)}\left(\frac{T_e}{e\left\langle\hat{\Phi}_1\right\rangle_\theta}\right)\left[1-\frac{1}{B\left\langle1/B\right\rangle_\theta}\right], \tag{4.22}$$

where, as a consequence of our orderings, the second term on the right hand side is of the order of ω_{di}/ν_{ii} and therefore is larger than the first term on the right hand side which is of the order of b_i. Expanding $\hat{\Phi}_1=\hat{\Phi}_1^0+\hat{\Phi}_1^1+\hat{\Phi}_1^2+\dots$ in the small parameter ω_{di}/ν_{ii} and substituting the expansion into Eq. (4.22) we see that $\hat{\Phi}_1^0=\left\langle\hat{\Phi}_1^0\right\rangle_\theta$, that is, the electrostatic modes are flute-like to the leading order. For completeness, we note that the next order correction is given by

$$\frac{\left\langle\hat{\Phi}_1^1\left(\boldsymbol{r}\right)\right\rangle_\theta-\hat{\Phi}_1^1\left(\boldsymbol{r}\right)}{\left\langle\hat{\Phi}_1^0\left(\boldsymbol{r}\right)\right\rangle_\theta}=-\mathrm{i}\frac{\left\langle\omega_{di}\right\rangle_\theta}{\nu_{ii}}\left[1-\frac{1}{B\left\langle1/B\right\rangle_\theta}\right]S \tag{4.23}$$

with

$$S \equiv \frac{5}{48} \frac{9\kappa_2 - 10}{\kappa_1^2 \left(249\kappa_1^2 - 160\right)} \frac{1}{\lambda^2 - \frac{10}{3}\lambda + \frac{5}{3}} \left[\left(489\kappa_1^2 - 320\right)\lambda^2 \right.$$
$$- \left(d \frac{8\eta\left(117\kappa_1^2 - 80\right) + 489\kappa_1^2 - 320}{1 + \eta} + 517\kappa_1^2 - 320 \right)\lambda$$
$$\left. + d\frac{\eta\left(447\kappa_1^2 - 320\right) + 517\kappa_1^2 - 320}{1 + \eta} \right] = O\left(1\right), \qquad (4.24)$$

where

$$\lambda \equiv \frac{\omega}{\langle\omega_{di}\rangle_\theta}, \qquad d \equiv \frac{\omega_{*i}\left(1 + \eta\right)}{\langle\omega_{di}\rangle_\theta} = -\frac{\mathrm{d}\ln p}{\mathrm{d}\ln V} \qquad (4.25)$$

with p plasma pressure, $\kappa_1^2 \equiv \left(\langle 1/B^2 \rangle_\theta / \langle 1/B \rangle_\theta^2\right)$, and $\kappa_2 \equiv \left(\langle\omega_{di}/B\rangle_\theta / \langle\omega_{di}\rangle_\theta \langle 1/B \rangle_\theta\right)$. The quantity d is defined as in Ref. [21] and will be positive outside the peak pressure location and negative near the levitated ring in LDX. We take in Eq. (4.24) $\tau = 1$ for simplicity so that $\eta_i = \eta_e \equiv \eta$.

Substituting expressions for G_1, G_2, H_1, H_2, a_0, b_0, b_1 into Eq. (4.21), noticing that $\omega_{*e} = -\tau\omega_{*i}$, $\langle\omega_{de}\rangle_\theta = -\tau\langle\omega_{di}\rangle_\theta$, taking $\tau = constant$, and annihilating the small ballooning component $\hat{\Phi}_1^1$ of the predominantly flute-like modes by integrating $\langle\ldots\rangle_\theta$, the *electrostatic dispersion relation* is found to be

$$\left[\left(d - \frac{5}{3}\right)\lambda^2 + \frac{5\left(\tau - 1\right)}{3}\left(\frac{d}{1 + \eta} - 1\right)\lambda + \frac{5\tau}{9}\left(d\frac{3\eta - 7}{1 + \eta} + 5\right)\right]\frac{1 + \tau}{2} + \frac{\langle b_i \rangle_\theta}{2}\lambda^4$$
$$+ \mathrm{i}\frac{\langle\omega_{di}\rangle_\theta}{\nu_{ii}}\frac{\lambda^2 + \frac{10}{3}\tau\lambda + \frac{5}{3}\tau^2}{\lambda^2 - \frac{10}{3}\lambda + \frac{5}{3}}\left[c_3\,\lambda^3 + c_2\left(d, \eta\right)\lambda^2 + c_1\left(d, \eta\right)\lambda + c_0\left(d, \eta\right)\right] = 0, (4.26)$$

where we neglect all terms of order $\langle b_i \rangle_\theta \lambda^n$ with $n \leq 3$ since $\langle\omega_{di}\rangle_\theta / \nu_{ii} \gg \langle b_i \rangle_\theta$ for our orderings.

The coefficients c_0 to c_3, in their most general form, are rather cumbersome expressions and are given in Appendix F. These expressions can be considerably simplified by evaluating κ_1 and κ_2 for the point dipole equilibrium of Ref. [1]. In this case we find that $\kappa_1 \approx 1.079$, $\kappa_2 = 7/6$ and the c_j's become simply

$$c_0\left(d,\eta\right) = d\,\frac{1.96\,\eta - 1.32}{1+\eta},$$

$$c_1\left(d,\eta\right) = 1.32 - d\,\frac{1.94\,\eta - 0.01}{1+\eta},$$

$$c_2\left(d,\eta\right) = -0.01 - d\,\frac{0.02\,\eta + 0.008}{1+\eta},$$

$$c_3 = 0.0084. \tag{4.27}$$

Before solving the dispersion relation (4.26) we make the following observations. First, the $\langle b_i \rangle_\theta \lambda^4$ term corresponds to finite Larmor radius effects and so we will refer to it as the "FLR" term. Second, the $O\left(\omega_{di}/\nu_{ii}\right)$ terms are "dissipative" and have been described by Mikhailovskii [36] as "gyro-relaxation" terms. Notice, that the sign of the dissipation is sensitive to d and η. They describe the collisional relaxation of a perturbed distribution function which is anisotropic, or isotropic but non-Maxwellian, towards a Maxwellian, and in some cases can lead to instability. In Braginskii's description [53] these physical effects arise from the ion viscosity tensor, but for the orderings (4.1) Mikhailovskii points out [36] that they are not described accurately enough by his fluid equations. Third, were we to keep $e^{\pm iL}$ terms in the collision term of Eq. (4.12), we would obtain terms of the order of $O\left(\nu_{ii}b_i/\omega_{di}\right)$ in the dispersion relation (4.26) describing cross-field ion heat conduction [36]. These "heat conduction" terms have been evaluated, but since, within our ordering scheme, they are much smaller than the $O\left(\omega_{di}/\nu_{ii}\right)$ terms [36], they have been neglected in the dispersion relation. Both the ion gyro-relaxation and ion thermal conduction effects have only been evaluated by Mikhailovskii [36] for a plasma in a straight magnetic field.

Examining the dispersion relation (4.26) we find that it has two classes of solutions: one corresponding to low frequency "drift" modes with $\omega \sim \langle \omega_{di} \rangle_\theta$ (or $\lambda \sim 1$), and the other to high frequency "MHD-like" modes with $\omega \gg \langle \omega_{di} \rangle_\theta$ (or $\lambda \gg 1$).

For the "drift" modes all the "FLR" and "gyro-relaxation" terms in Eq. (4.26) can be neglected in the leading order. However, the "gyro-relaxation" terms provide

small imaginary corrections to the mode frequency and so modify the mode stability in an important way in next order. For the "MHD-like" mode $\lambda \gg 1$, and the first term in Eq. (4.26) can be balanced by either the "FLR" term or the leading (order λ^3) "gyro-relaxation" term, depending on which is larger. In the next sections we consider the stability of these modes in greater detail.

4.4 Low Frequency Modes: Entropy Modes

We start by considering the low frequency modes with $\lambda \sim 1$ ($\omega \sim \langle \omega_{di} \rangle_\theta$). To the lowest order we drop the "gyro-relaxation" and "FLR" terms in the dispersion relation (4.26) to find

$$\lambda_0 = \frac{5(\tau-1)\left(1 - \frac{d}{1+\eta}\right) \pm 5\sqrt{(\tau-1)^2\left(1 - \frac{d}{1+\eta}\right)^2 - \frac{4\tau}{5}\left(d - \frac{5}{3}\right)\left(d\frac{3\eta-7}{1+\eta} + 5\right)}}{6\left(d - \frac{5}{3}\right)}.$$

(4.28)

It is clear that the modes can be either stable or unstable depending on the sign of the expression under the square root, $\tau = 1$ being the most unstable among all possible $\tau > 0$. Considering the most unstable $\tau = 1$ case, it can be easily shown that instability occurs for $-1 < \eta < \frac{2}{3}$ when $\frac{5(1+\eta)}{7-3\eta} < d < \frac{5}{3}$, for $\frac{2}{3} < \eta < \frac{7}{3}$ when $\frac{5}{3} < d < \frac{5(1+\eta)}{7-3\eta}$, and for $\eta < -1$ and $\eta > \frac{7}{3}$ when $d < \frac{5(1+\eta)}{7-3\eta}$ and $d > \frac{5}{3}$. The growth rate is $\gamma \equiv Im\,\omega \sim \langle \omega_{di} \rangle_\theta$. Figs. 4-1 - 4-4 illustrate the situation described, showing the unstable regions in black and the stable regions in white for $\tau = 0.5$, 1, 2 and 10. The gray regions are stable according to (4.28), but will be discussed further in the following paragraphs. As expected from Eq. (4.28), the case of $\tau = 1$ is the most unstable, while that of $\tau = 10$ is the most stable among the cases shown.

These modes are the so-called "entropy modes", discussed (for a Z-pinch equilibrium) by Kadomtsev [39] in 1959 and later studied by other workers [36, 54, 55, 56]. In recent stability analysis of magnetic dipoles [21, 33] they were referred to as "drift-temperature-gradient modes".

An important characteristic of these modes is that the perturbations of particle
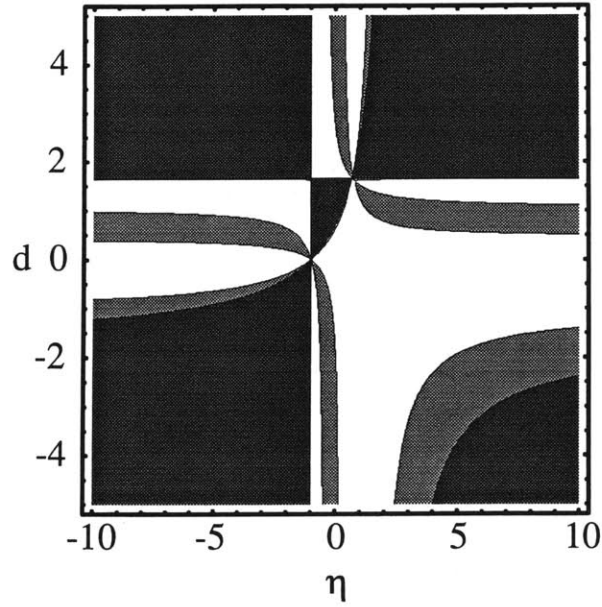
Figure 4-1: Stability diagram for the entropy mode for the point dipole equilibrium of Ref. [1] with $\tau = 1$. Shown in black are the regions unstable in the absence of the ion gyro-relaxation effects, in gray are the regions unstable due to the ion gyro-relaxation effects but stable otherwise, and in white are the stable regions.
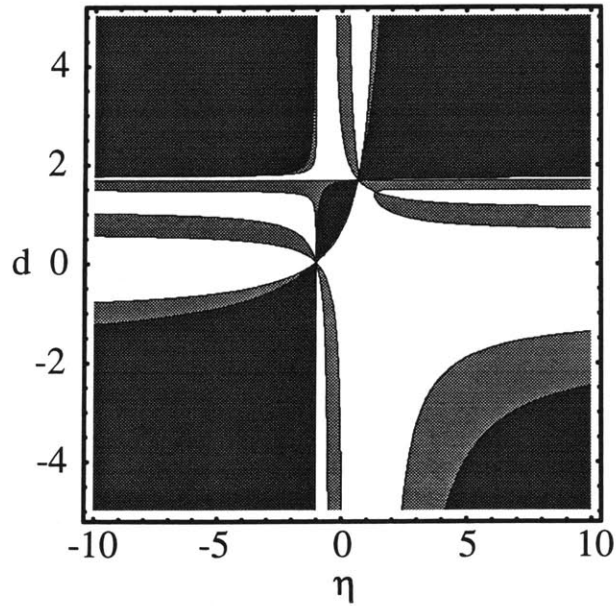
Figure 4-2: Same as in Figure 4-1 but for $\tau = 2$.
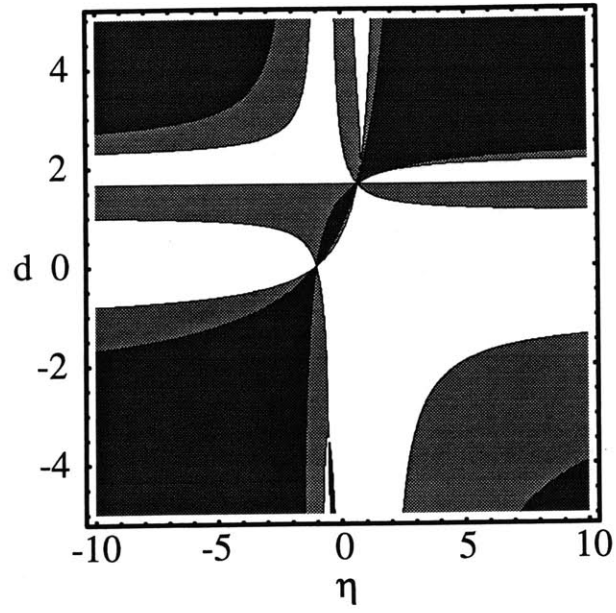
Figure 4-3:   Same as in Figure 4-1 but for $\tau = 10$.
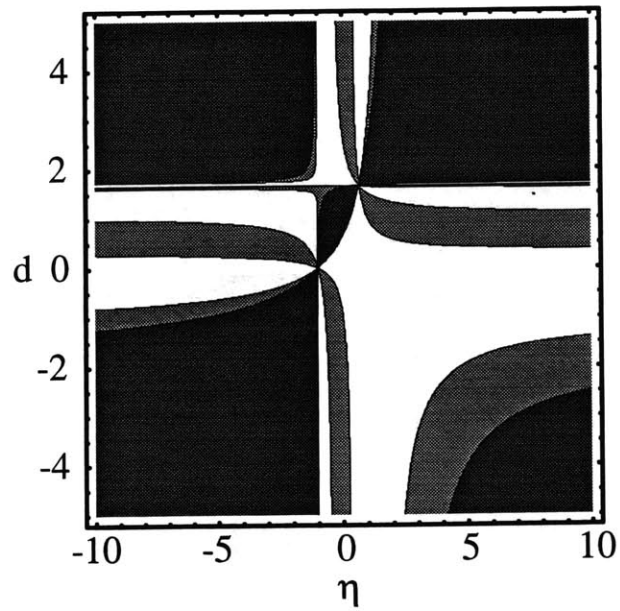
Figure 4-4:   Same as in Figure 4-1 but for $\tau = 1/2$.

densities and temperatures occur in such a way that the perturbation of the total ion plus electron pressure is zero to the leading order. By analogy with the ideal gas, where the entropy per particle is $s = \ln\left(T^{5/2}/p\right) + const$, with T and p the gas pressure and temperature, we note that these modes perturb the entropy of the system. This situation is quite different from that of ideal MHD, which assumes an adiabatic equation of state and, consequently, constant entropy. When entropy modes are stable, they occur as two waves propagating toroidally with phase velocities of the order of $\langle \omega_{di} \rangle_\theta / k_\zeta$. Both electrons and ions oscillate radially owing to the $\boldsymbol{B} \times \boldsymbol{\nabla} \Phi_1$ and $\boldsymbol{B} \times \boldsymbol{\nabla} p_{1j}$ drifts, where p_{1j} is the perturbed pressure of the species j. As the density perturbations propagate toroidally, temperature perturbations propagate toroidally as well,and result in the electron plus ion pressure remaining constant. The diamagnetic heat flows are responsible for the temperature perturbations [39] and the radial flow of heat (in the $\boldsymbol{B} \times \boldsymbol{\nabla} T_{1j}$ direction [39, 53], with T_{1j} the perturbed temperature of the species j).

Under some circumstances, density perturbations can acquire a phase shift of $\pm\,\pi/2$ with respect to the electrostatic potential perturbations, in which case for one of the modes particles $\boldsymbol{E} \times \boldsymbol{B}$ drift in such a way as to increase the potential perturbation and the mode grows. Taking $\tau = 1$ for simplicity, Eq. (4.28) can be rewritten as

$$\lambda_0 = \pm\sqrt{\frac{5}{9}\frac{5 + 7\frac{\mathrm{d}\ln p}{\mathrm{d}\ln V} - 10\frac{\mathrm{d}\ln T}{\mathrm{d}\ln V}}{\frac{5}{3} + \frac{\mathrm{d}\ln p}{\mathrm{d}\ln V}}}, \tag{4.29}$$

which is identical to Eq. (30) in Ref. [39]. From this form we can see that if $d = -\,\mathrm{d}\ln p/\mathrm{d}\ln V < 5/3$ (which is the stability condition for the high frequency MHD-like mode considered in the next section) the entropy mode is stable if

$$\frac{\mathrm{d}\ln T}{\mathrm{d}\ln V} < \frac{1}{2} + \frac{7}{10}\frac{\mathrm{d}\ln p}{\mathrm{d}\ln V}. \tag{4.30}$$

That is, for a given value of pressure gradient the temperature can not increase too quickly. If it does, the mode becomes unstable causing a transfer of heat in the radial direction until the temperature gradient satisfies inequality (4.30). Notice

that entropy mode is unstable even in the absence of the temperature gradient if $5/7 < -\mathrm{d}\ln p/\mathrm{d}\ln V < 5/3$, indicating that the name drift-temperature-gradient mode [21, 33] is somewhat misleading.

Next, we consider the $O\left(\langle\omega_{di}\rangle_\theta/\nu_{ii}\right)$ gyro-relaxation effects. They were originally considered in Refs. [57, 58] in connection with the problem of plasma heating, where an adiabatic change in the magnetic field brings about a change in perpendicular plasma pressure due to the conservation of the particle magnetic moment μ. Collisions try to annihilate the resulting pressure anisotropy so the effect is accompanied by energy dissipation (or inverse dissipation). More generally, such relaxation processes take place whenever the ion distribution function is anisotropic or isotropic but non-Maxwellian. Gyro-relaxation effects were described in Refs. [36, 56] in conjunction with entropy modes for plasmas in a straight magnetic field or in the cylindrical magnetic field of a Z-pinch.

Taking gyro-relaxation effects into account and solving perturbatively leads to additional imaginary terms in the entropy mode frequency:

$$\lambda = \lambda_0 - \frac{i}{(1+\tau)\left[\left(d-\frac{5}{3}\right)\lambda_0 + \frac{5(\tau-1)}{6}\left(\frac{d}{1+\eta}-1\right)\right]}\frac{\langle\omega_{di}\rangle_\theta}{\nu_{ii}}\frac{\lambda_0^2 + \frac{10}{3}\tau\lambda_0 + \frac{5}{3}\tau^2}{\lambda_0^2 - \frac{10}{3}\lambda_0 + \frac{5}{3}} \times$$
$$\left[c_3\left(d,\eta\right)\lambda_0^3 + c_2\left(d,\eta\right)\lambda_0^2 + c_1\left(d,\eta\right)\lambda_0 + c_0\left(d,\eta\right)\right], \qquad (4.31)$$

where we are only interested in the sign of these new terms in the stable regions of Eq. (4.28). For the case of the point dipole equilibrium [1] ($\kappa_1 \approx 1.079$ and $\kappa_2 = 7/6$) the unstable regions are shown in Figs. 4-1 - 4-4 in gray. As can be seen, gyro-relaxation effects can destabilize an otherwise stable entropy mode. Moreover, notice that as the black unstable regions shrink as τ departs from unity, the gray unstable regions tend to expand in size so the improvement in stability obtained by neglecting the gyro-relaxation terms is misleading. However, the instability growth rate due to these gyro-relaxation terms is much smaller than that for the entropy mode: $\gamma \sim \langle\omega_{di}\rangle_\theta^2/\nu_{ii} \ll \langle\omega_{di}\rangle_\theta$. The appearance of the additional unstable regions due to gyro-

relaxation effects can be understood from the point of view of small amplitude mode energy and power dissipation by gyro-relaxation effects, whereby a negative (positive) energy mode is driven unstable by positive (negative) energy dissipation [59, 60, 61]. A detailed analysis for a Z-pinch equilibrium is given in Appendix G.

4.5 High Frequency Modes: MHD-like Scaling

Next, we consider high frequency modes with $\lambda \gg 1$ ($\omega \gg \langle \omega_{di} \rangle_\theta$). In this section we assume $\tau = 1$ for simplicity. The high frequency modes are obtained by balancing the first term in dispersion relation (4.26) by the larger of the FLR or leading gyro-relaxation terms:

$$\left(d - \frac{5}{3}\right) + \frac{\langle b_i \rangle_\theta}{2}\lambda^2 + \mathrm{i}\,\frac{\langle \omega_{di} \rangle_\theta}{\nu_{ii}}\,c_3\lambda = 0. \tag{4.32}$$

Although, within our orderings, $(\langle \omega_{di} \rangle_\theta / \nu_{ii}) \gg \langle b_i \rangle_\theta$, the gyro-relaxation term can be either bigger or smaller than the FLR term because the numerical coefficient $c_3 \ll 1$ (see appendix F).

Equation (4.32) can be easily solved to give

$$\lambda = \frac{-\mathrm{i}\,\sigma \pm \sqrt{2\,\langle b_i \rangle_\theta \left(\frac{5}{3} - d\right) - \sigma^2}}{\langle b_i \rangle_\theta}, \tag{4.33}$$

where we introduce $\sigma \equiv \langle \omega_{di} \rangle_\theta\, c_3/\nu_{ii} \ll 1$. For $|d - 5/3| \gg (\sigma^2/\langle b_i \rangle_\theta)$ we obtain a mode with the MHD-like scaling (and stability threshold):

$$\lambda \approx \pm\sqrt{-\frac{2\left(d - \frac{5}{3}\right)}{\langle b_i \rangle_\theta}}. \tag{4.34}$$

It is clear from Eqs. (4.33) and (4.34) that the high frequency mode is stable for $d < \frac{5}{3}$ and unstable otherwise. This stability condition coincides with the well-known MHD interchange stability condition for a rotationally symmetric system with closed field lines (see, for example, Refs. [1, 19, 20]). Indeed, if we evaluate the frequency of the MHD flute mode using the MHD energy principle [18] ($\omega^2 = W/H$, with W

81

the plasma plus magnetic field potential energy and $\omega^2 H$ the *perpendicular* kinetic energy [20]) we would obtain an expression identical to Eq. (4.34). For these reasons we call the high frequency mode the MHD-like mode.

In the opposite limit $|d - 5/3| \ll (\sigma^2/\langle b_i \rangle_\theta)$ the MHD-like mode splits into two high frequency MHD-like modes with

$$\lambda_L \approx \mathrm{i}\frac{\left(d - \frac{5}{3}\right)}{\sigma}, \qquad \lambda_U \approx -\mathrm{i}\frac{2\,\sigma}{\langle b_i \rangle_\theta}. \tag{4.35}$$

The MHD splitting occurs at $|d - 5/3| \sim (\sigma^2/\langle b_i \rangle_\theta)$. Notice, that only the lower frequency mode, λ_L, can be unstable and again requires $d > 5/3$ for instability. Consequently, even though the gyro-relaxation effect does not alter the stability condition of the MHD-like mode, it does change the mode's character from reactive to dissipative and appreciably lowers its growth rate, thereby making it easier to satisfy our $\lambda \ll \nu_{ii}/\langle \omega_{di} \rangle_\theta$ ordering.

4.6 Coupling between MHD-like and Entropy Modes

Examining expressions (4.28), (4.33), (4.34), and (4.35) for the eigenfrequencies of the entropy and MHD-like modes we see that, when d approaches the "critical" value of $5/3$, the frequency of the entropy mode increases and that of the MHD-like mode decreases. Consequently, coupling between these modes is possible in the vicinity of $d = 5/3$. Since $\lambda \gg 1$, only the large λ limit of the $\langle \omega_{di} \rangle_\theta /\nu_{ii}$ terms need be retained in the dispersion relation (4.26) for the discussion of this section. Depending on the values of the parameters σ and $\langle b_i \rangle_\theta$ two different situations are possible. In the first case, the coupling between the entropy and the MHD-like modes occurs closer to $d = 5/3$ than the splitting of the branches of the MHD-like mode. As a result, only the lower frequency branch λ_L of the MHD-like mode couples with the two branches of the entropy mode, while the upper frequency branch λ_U does not. In the second case, the splitting of the two branches of the MHD-like mode would occur closer to $d = 5/3$ than the coupling between the entropy and the MHD-like modes. Consequently, both upper and lower frequency branches of the MHD-like

mode couple to the two branches of the entropy mode. Next, we illustrate these two situations in greater detail for $\tau = 1$ by considering the following simplified version of the dispersion relation (4.26):

$$\left(d - \frac{5}{3}\right)\lambda^2 + \frac{50}{9}\left(\frac{\eta - 2/3}{1 + \eta}\right) + \frac{\langle b_i \rangle_\theta}{2}\lambda^4 + i\,\sigma\lambda^3 = 0, \qquad (4.36)$$

where we have taken $d = 5/3$ in all terms except the first one.

The first of the situations described occurs when the $\langle b_i \rangle_\theta$ term is negligible at coupling in dispersion relation (4.36) and since splitting occurs before coupling as d approaches $5/3$. Noticing that at coupling the first, second, and the gyro-relaxation terms in (4.36) are of the same order (and λ is still larger than 1), we can easily find three modes that are coupled for $|d - 5/3| \lesssim \sigma^{2/3} \ll 1$ with frequencies of the order $\sigma^{-4/3} \gg 1$. The neglect of the $\langle b_i \rangle_\theta$ term that makes splitting occur before coupling requires $\langle b_i \rangle_\theta^3 \ll \sigma^4$.

The second situation occurs when the gyro-relaxation term in dispersion relation (4.36) is negligible. Requiring the first three terms in (4.36) to be of the same order we find that the modes couple at $|d - 5/3| \lesssim \langle b_i \rangle_\theta^{1/2} \ll 1$ and have frequencies of the order of $\langle b_i \rangle_\theta^{-1/4} \gg 1$. In this case splitting does not occur because the σ term is negligible if $\langle b_i \rangle_\theta^3 \gg \sigma^4$.

4.7 Conclusions

In this chapter electrostatic plasma modes have been investigated under the intermediate collisionality orderings (4.1) for an arbitrary axially symmetric plasma confined by a poloidal magnetic field with closed field lines. A kinetic treatment is employed and the appropriate linearized gyrokinetic equation solved. Finite ion Larmor radius effects and ion collisional dissipative effects are considered. A procedure for evaluating the collisional gyro-relaxation effects for the case of arbitrary variation of the magnetic field along the field line is developed and solved herein for the first time. The electrostatic dispersion relation we derive contains these new dissipative terms as important modifications .

The electrostatic modes are found to be of a flute type with a departure of the perturbed electrostatic potential Φ_1 from its average along a magnetic field line, $\langle\Phi_1\rangle_\theta$, of the order of $\langle\omega_{di}\rangle_\theta / \nu_{ii} \ll 1$. The dispersion relation permits two different classes of modes: high frequency MHD-like modes with $\omega \gg \langle\omega_{di}\rangle_\theta$ and low frequency entropy modes with $\omega \sim \langle\omega_{di}\rangle_\theta$. The lowest order low frequency mode is the entropy mode of Kadomtsev[39], also referred to as the "drift-temperature-gradient" mode in Refs. [33, 21]. The modes are strongly coupled in the vicinity of $-\mathrm{d}\ln p/\mathrm{d}\ln V = 5/3$.

The stability of the electrostatic modes is conveniently described in terms of two independent parameters: $\eta = \mathrm{d}\ln T/\mathrm{d}\ln N$ (assuming $T_e = T_i$) and $d = \omega_{*i}(1+\eta)/\langle\omega_{di}\rangle_\theta = -\mathrm{d}\ln p/\mathrm{d}\ln V$. The MHD-like mode is stable if $d < 5/3$ and unstable otherwise; the marginal stability condition being identical to the MHD interchange mode stability condition for such plasma systems [1, 19, 20]. The gyro-relaxation terms do not alter the stability condition, but they do reduce the growth rate of the MHD-like mode. Stability of the entropy mode depends on both d and η, with stable and unstable regions shown in white and black respectively in Figs. 4-1 - 4-4. The collisional ion gyro-relaxations effects we have considered modify the stability of the electrostatic modes considerably. However, even with these additional instability regions in the parametric d, η space, shown in Figs. 4-1 - 4-4 in gray, there is still a considerable part of the parametric space that remains stable. For $T_e \neq T_i$ the improved stability of the entropy mode is largely offset by the increased size of the gyro-relaxation unstable regions.

Chapter 5

Kinetic Stability of Electromagnetic Plasma Modes in a Dipole Magnetic Field

5.1 Introduction

In Chapter 4 the kinetic stability of electrostatic modes in a dipolar magnetic field was investigated. Strictly speaking, the electrostatic treatment applies only to the case of low beta plasma equilibria. In order to study the stability of finite beta equilibria the full electromagnetic problem must be solved. The solution of this electromagnetic problem is the subject of Chapter 5.

5.2 Solution of the Gyrokinetic Equation

To perform the electromagnetic derivation of the modes present in arbitrary $\beta \equiv$ (plasma pressure / magnetic pressure) plasma confined by a dipole magnetic field we adopt orderings [21, 33, 35], which are relevant to the LDX experiment currently under construction:

$$\Omega_j \gg \omega_{bj} \gg \nu_{cj} \gg \omega \gtrsim \omega_{dj} \sim \omega_{*j},$$ (5.1)

where Ω_j, $\omega_{bj} \sim \boldsymbol{v}_j \cdot \boldsymbol{\nabla}$, ν_{cj}, ω_{dj}, and ω_{*j} denote the cyclotron, bounce (transit), collision, magnetic drift, and diamagnetic drift frequencies, respectively, and ω is the mode frequency. The subscript j denotes different particle species, $j = i, e$.

Assuming that the equilibrium electrostatic potential vanishes or that we are in the $\boldsymbol{E} \times \boldsymbol{B}$ drifting frame, the unperturbed distribution function is given to the required accuracy by the expression [35]

$$f_{0j} = f_{Mj} + \frac{1}{\Omega_j} \boldsymbol{v} \times \hat{\boldsymbol{n}} \cdot \boldsymbol{\nabla} f_{Mj} \qquad (5.2)$$

with f_{Mj} the Maxwellian distribution function

$$f_{Mj}(E, \psi) \equiv N_j \left(M_j / 2\pi T_j\right)^{3/2} e^{-M_j E/T_j}, \qquad (5.3)$$

where $\hat{\boldsymbol{n}} = \boldsymbol{B}/|\boldsymbol{B}|$ is the unit vector along the equilibrium magnetic field $\boldsymbol{B} = \boldsymbol{\nabla}\psi \times \boldsymbol{\nabla}\zeta$, ψ is the poloidal magnetic flux coordinate and ζ is the toroidal coordinate, and with $N_j(\psi)$, $T_j(\psi)$, M_j and $E = v^2/2$ the species density, temperature, mass and energy, respectively.

Employing the eikonal approximation and following Refs. [49, 50, 62] we find that the perturbed distribution function f_{1j} is given by the expression

$$f_{1j} = \left(-\frac{Z_j e \hat{\Phi}}{T_j} f_{Mj} + g_j e^{iL_j}\right) e^{iS - i\omega t}, \qquad (5.4)$$

where $Z_j e$ is the species charge, $\Phi = \hat{\Phi} e^{iS - i\omega t}$ is the perturbed electrostatic potential, $S = S(\psi, \zeta)$ is the eikonal [49], $L_j = (\boldsymbol{v} \cdot \hat{\boldsymbol{n}} \times \boldsymbol{k}_\perp)/\Omega_j$, $\boldsymbol{k}_\perp = \boldsymbol{\nabla} S$ and g_j is a *gyrophase independent* function satisfying the following gyrokinetic equation [49, 50]:

$$v_\parallel \hat{\boldsymbol{n}} \cdot \boldsymbol{\nabla} g_j - i\left(\omega - \boldsymbol{v}_{dj} \cdot \boldsymbol{k}_\perp\right) g_j = \left\langle e^{-iL_j} C_{1j}\left(g_j e^{iL_j}\right)\right\rangle_\phi$$
$$-i\frac{Z_j e}{T_j} f_{Mj}\left(\omega - \omega_{*j}^T\right)\left[J_0(a_j)\left(\hat{\Phi} - \frac{v_\parallel}{c}\hat{A}_\parallel\right) + J_1(a_j)\frac{v_\perp}{k_\perp}\frac{\delta\hat{B}_\parallel}{c}\right]. \qquad (5.5)$$

In Eq. (5.5) "parallel" and "perpendicular" refer to the directions along and across the

magnetic field $\boldsymbol{B}$, $A_\parallel = \hat{A}_\parallel e^{iS-i\omega t}$ and $\delta B_\parallel = \delta \hat{B}_\parallel e^{iS-i\omega t}$ are the parallel components of the perturbed vector potential and magnetic field, respectively, and averaging over the gyrophase ϕ is defined as $\langle \dots \rangle_\phi = (2\pi)^{-1} \oint (\dots) \, d\phi$. In addition, the magnetic drift velocity $\boldsymbol{v}_{dj}$ is given by

$$\boldsymbol{v}_{dj} \equiv \hat{n} \times \left(\frac{v_\perp^2}{2\Omega_j} \boldsymbol{\nabla} \ln B + \frac{v_\parallel^2}{\Omega_j} \boldsymbol{\kappa} \right) \tag{5.6}$$

with $\boldsymbol{\kappa} \equiv \hat{n} \cdot \boldsymbol{\nabla}\hat{n}$ the magnetic field line curvature, $J_0(a_j)$ and $J_1(a_j)$ are the Bessel functions of the first kind with $a_j \equiv k_\perp v_\perp / \Omega_j$, and

$$\omega_{*j} \equiv \frac{ck_\zeta RT_j}{Z_j eN_j} \frac{d\,N_j}{d\,\psi}, \qquad \eta_j \equiv \frac{d\,\ln T_j(\psi)/d\,\psi}{d\,\ln N_j(\psi)/d\,\psi}, \tag{5.7}$$

with

$$\omega_{*j}^T \equiv \omega_{*j} \left[1 + \eta_j \left(\frac{M_j E}{T_j} - \frac{3}{2} \right) \right], \tag{5.8}$$

where $k_\zeta \equiv \boldsymbol{k}_\perp \cdot \hat{\boldsymbol{\zeta}}$ with $\hat{\boldsymbol{\zeta}}$ the unit vector in the toroidal direction, c is the speed of light, and R is the cylindrical radial coordinate. The linearized Fokker-Planck collision operator C_{1j} is given to the required order by $C_{1e} = C_{1ee} + C_{1ei}$ for the electron kinetic equation and $C_{1i} = C_{1ii}$ for the ion kinetic equation, where C_{1jj} denotes the like particle contribution and C_{1ei} is the electron-ion term.

To solve the gyrokinetic equation (5.5) it is convenient to introduce an auxiliary potential $\hat{\Psi}$ and function h_j such that[50]

$$\hat{A}_\parallel = \frac{c}{i\omega} \hat{n} \cdot \boldsymbol{\nabla}\hat{\Psi} \tag{5.9}$$

and

$$g_j = \frac{Z_j e \hat{\Psi}}{T_j} f_{Mj} \left(1 - \frac{\omega_{*j}^T}{\omega} \right) + h_j. \tag{5.10}$$

Assuming $L \ll 1$ and neglecting the perpendicular collisional heat conduction effects [35], allows us to rewrite $\left\langle e^{-iL_j} C_{1j} \left(g_j e^{iL_j} \right) \right\rangle_\phi \approx C_{1j}(g_j) \approx C_{1j}(h_j)$, giving the

following equation for h_j:

$$v_\parallel \hat{\boldsymbol{n}} \cdot \boldsymbol{\nabla} h_j - \mathrm{i} \left(\omega - \boldsymbol{v}_{dj} \cdot \boldsymbol{k}_\perp \right) h_j = C_{1j} \left(h_j \right) + \hat{Q}_j, \tag{5.11}$$

where

$$\hat{Q}_j \equiv -\mathrm{i} \frac{Z_j e}{T_j} f_{Mj} \left(\omega - \omega_{*j}^T \right) \left[J_0 \left(a_j \right) \hat{\Phi} + \mathrm{i} \left(J_0 \left(a_j \right) - 1 \right) \frac{v_\parallel}{\omega} \hat{\boldsymbol{n}} \cdot \boldsymbol{\nabla} \hat{\Psi} \right.$$
$$\left. + J_1 \left(a_j \right) \frac{v_\perp}{k_\perp} \frac{\delta \hat{B}_\parallel}{c} - \left(1 - \frac{\boldsymbol{v}_{dj} \cdot \boldsymbol{k}_\perp}{\omega} \right) \hat{\Psi} \right]. \tag{5.12}$$

We solve Eq. (5.11) by expanding $h_j = h_{1j} + h_{2j} + h_{3j} + \ldots$ in accordance with our orderings (5.1) and following the procedure developed in Ref. [35]. To the lowest order we find

$$v_\parallel \hat{\boldsymbol{n}} \cdot \boldsymbol{\nabla} h_{1j} = 0, \tag{5.13}$$

so that $h_{1j} = h_{1j} \left(E, \mu, \psi \right)$. To second order

$$v_\parallel \hat{\boldsymbol{n}} \cdot \boldsymbol{\nabla} h_{2j} = C_1 \left(h_{1j} \right). \tag{5.14}$$

Upon annihilation of the left hand side this equation requires h_{1j} to be a perturbed Maxwellian

$$h_{1j} = f_{Mj} \left(\alpha_j \left(\psi \right) + \beta_j \left(\psi \right) \frac{M_j v^2}{2 T_j} \right). \tag{5.15}$$

The quantities $\alpha_j \left(\psi \right)$ and $\beta_j \left(\psi \right)$ are then determined by annihilating the h_{2j} and h_{3j} terms in the third order version of Eq. (5.11):

$$\left\langle \int \mathrm{d}^3 v \, v^q \left[\left(\omega - \boldsymbol{v}_{dj} \cdot \boldsymbol{k}_\perp \right) h_{1j} - \mathrm{i} \hat{Q}_j \right] \right\rangle_\theta = 0, \qquad q = 0, 2, \tag{5.16}$$

where $\langle \ldots \rangle_\theta = V^{-1} \oint \left[\left(\ldots \right) \mathrm{d}\theta / \left(\boldsymbol{B} \cdot \boldsymbol{\nabla} \theta \right) \right]$ with $V \equiv \oint \left[\mathrm{d}\theta / \left(\boldsymbol{B} \cdot \boldsymbol{\nabla} \theta \right) \right]$.

Assuming $a_j \ll 1$, expanding $J_0 \left(a_j \right) \approx 1 - a_j^2/4$, $J_1 \left(a_j \right) \approx a_j/2 - a_j^3/16$, introduc-

ing dimensionless variables $\tilde{\Phi}_j \equiv Z_j e\, \hat{\Phi}/T_j$, $\tilde{\Psi}_j \equiv Z_j e\, \hat{\Psi}/T_j$, $\delta\tilde{B}_\parallel \equiv \delta\hat{B}_\parallel/B$, performing the velocity space integrations in Eq. (5.16), and solving the resulting linear system of equations for α_j and β_j we find

$$
\alpha_j = \left\langle \tilde{\Phi}_j - \tilde{\Psi}_j \right\rangle_\theta G_{1j} + \left[\left\langle \delta\tilde{B}_\parallel \right\rangle_\theta + \frac{\left\langle \omega_{dj}\, \tilde{\Psi}_j \right\rangle_\theta}{\omega} - \frac{\left\langle b_j\, \tilde{\Phi}_j \right\rangle_\theta}{2} \right] G_{2j} + \left\langle b_j\, \delta\tilde{B}_\parallel \right\rangle_\theta G_{3j},
$$

$$(5.17)$$

$$
\beta_j = \left\langle \tilde{\Phi}_j - \tilde{\Psi}_j \right\rangle_\theta H_{1j} + \left[\left\langle \delta\tilde{B}_\parallel \right\rangle_\theta + \frac{\left\langle \omega_{dj}\, \tilde{\Psi}_j \right\rangle_\theta}{\omega} - \frac{\left\langle b_j\, \tilde{\Phi}_j \right\rangle_\theta}{2} \right] H_{2j} + \left\langle b_j\, \delta\tilde{B}_\parallel \right\rangle_\theta H_{3j},
$$

where

$$
G_{1j} = \frac{\omega^2 - \left[\left(1 - \tfrac{3}{2}\eta_j\right) \omega_{*j} + \tfrac{10}{3}\left\langle \omega_{dj} \right\rangle_\theta \right]\omega + \tfrac{5}{6}\left(4 - 3\eta_j\right)\omega_{*j}\left\langle \omega_{dj} \right\rangle_\theta}{\omega^2 - \tfrac{10}{3}\omega\left\langle \omega_{dj} \right\rangle_\theta + \tfrac{5}{3}\left\langle \omega_{dj} \right\rangle_\theta^2},
$$

$$
G_{2j} = \frac{\tfrac{5}{6}\left(3\,\eta_j\,\omega_{*j} - 2\left\langle \omega_{dj} \right\rangle_\theta\right)\omega + \tfrac{5}{6}\left(2 - 3\eta_j\right)\omega_{*j}\left\langle \omega_{dj} \right\rangle_\theta}{\omega^2 - \tfrac{10}{3}\omega\left\langle \omega_{dj} \right\rangle_\theta + \tfrac{5}{3}\left\langle \omega_{dj} \right\rangle_\theta^2},
$$

$$
G_{3j} = \frac{\tfrac{1}{2}\omega^2 - \tfrac{1}{4}\left(11\eta_j + 2\right)\omega_{*j}\,\omega + \tfrac{35}{12}\,\eta_j\,\omega_{*j}\left\langle \omega_{dj} \right\rangle_\theta}{\omega^2 - \tfrac{10}{3}\omega\left\langle \omega_{dj} \right\rangle_\theta + \tfrac{5}{3}\left\langle \omega_{dj} \right\rangle_\theta^2},
$$

$$
H_{1j} = \frac{\left(\tfrac{2}{3}\left\langle \omega_{dj} \right\rangle_\theta - \eta_j\,\omega_{*j}\right)\omega - \left(\tfrac{2}{3} - \eta_j\right)\omega_{*j}\left\langle \omega_{dj} \right\rangle_\theta}{\omega^2 - \tfrac{10}{3}\omega\left\langle \omega_{dj} \right\rangle_\theta + \tfrac{5}{3}\left\langle \omega_{dj} \right\rangle_\theta^2},
$$

$$
H_{2j} = \frac{\tfrac{2}{3}\omega^2 - \left(\tfrac{2}{3} + \tfrac{7}{3}\eta_j\right)\omega_{*j}\,\omega + \tfrac{5}{3}\eta_j\,\omega_{*j}\left\langle \omega_{dj} \right\rangle_\theta}{\omega^2 - \tfrac{10}{3}\omega\left\langle \omega_{dj} \right\rangle_\theta + \tfrac{5}{3}\left\langle \omega_{dj} \right\rangle_\theta^2},
$$

$$
H_{3j} = \frac{-\tfrac{2}{3}\omega^2 + \left[\left(\tfrac{2}{3} + \tfrac{5}{2}\eta_j\right)\omega_{*j} + \tfrac{1}{3}\left\langle \omega_{dj} \right\rangle_\theta\right]\omega - \left(\tfrac{1}{3} + \tfrac{11}{6}\eta_j\right)\omega_{*j}\left\langle \omega_{dj} \right\rangle_\theta}{\omega^2 - \tfrac{10}{3}\omega\left\langle \omega_{dj} \right\rangle_\theta + \tfrac{5}{3}\left\langle \omega_{dj} \right\rangle_\theta^2},
$$

and

$$
b_j \equiv \left(k_\perp^2 T_j/M_j\Omega_j^2\right) \ll 1, \qquad \omega_{dj} \equiv \frac{T_j}{M_j\Omega_j}k_\zeta\left[\hat{\boldsymbol{\zeta}} \cdot \hat{\boldsymbol{n}} \times \left(\boldsymbol{\nabla}\ln B + \boldsymbol{\kappa}\right)\right], \qquad (5.18)
$$

with[21]

$$\langle \omega_{dj} \rangle_\theta = -\frac{c k_\zeta R T_j}{Z_j e V} \frac{\mathrm{d}V}{\mathrm{d}\psi}.$$ (5.19)

Knowing α_j and β_j the perturbed distribution function for each species can now be obtained by using the expression

$$f_{1j} = \left[-\tilde{\Phi}_j + \tilde{\Psi}_j \left(1 - \frac{\omega_{*j}^T}{\omega} \right) e^{iL_j} + \left(\alpha_j + \beta_j \frac{M_j v^2}{2 T_j} \right) e^{iL_j} \right] f_{Mj} \, e^{iS - i\omega t}.$$ (5.20)

Introducing $\tau \equiv Z_i T_e / T_i$ we see that $\tilde{\Phi}_e = -\tilde{\Phi}_i/\tau$, $\tilde{\Psi}_e = -\tilde{\Psi}_i/\tau$, $\omega_{*e} = -\tau\omega_{*i}$, $\omega_{de} = -\tau\omega_{di}$, and, assuming $\tau = \text{constant}$, $\eta_e = \eta_i \equiv \eta$. To take into consideration the smallness of the ratio of the electron to ion masses, $M_e/M_i \ll 1$, we set $b_e = 0$ in all the formulas to follow.

5.3 Quasineutrality and Ampere Equation

To proceed, we construct the quasineutrality equation and two components of the Ampere equation in terms of the three unknowns, $\tilde{\Phi}_i$, $\tilde{\Psi}_i$ and $\delta\tilde{B}_\parallel$. Combining these three equations will ultimately allow us to obtain a second order integro-differential equation for the electromagnetic eigenmodes of the system.

The quasineutrality equation and the perpendicular Ampere equation both take the form of one dimensional integral equations, coupling $\tilde{\Phi}_i(l)$, $\tilde{\Psi}_i(l)$ and $\delta\tilde{B}_\parallel(l)$, where l is arc length along the magnetic field lines. These equations are, however, of a trivial nature and permit exact solution for $\tilde{\Phi}_i(l)$ and $\delta\tilde{B}_\parallel(l)$ in terms of $\tilde{\Psi}_i(l)$. The remaining equation, which contains the parallel component of the Ampere law, is integro-differential in l. Using the solutions for $\tilde{\Phi}_i(l)$, $\delta\tilde{B}_\parallel(l)$ obtained from the quasineutrality and perpendicular Ampere equation, we finally obtain a single, integro-differential ballooning equation for $\tilde{\Psi}_i$. These steps are described in more detail below.

Using expression (5.20) for the perturbed distribution function f_{1j} in the quasineu-

trality condition

$$\sum_{j=i,e} Z_j \int \mathrm{d}^3 v f_{1j} = 0 \qquad (5.21)$$

we obtain the following equation:

$$
-\frac{1+\tau}{\tau} Y + \left[G_{1i} + \frac{3}{2} H_{1i} + \frac{1}{\tau} \left(G_{1e} + \frac{3}{2} H_{1e} \right) \right] \langle Y \rangle_\theta - \left(G_{2i} + \frac{3}{2} H_{2i} \right) \frac{\left\langle b_i \tilde{\Phi}_i \right\rangle_\theta}{2}
$$
$$
+ \left[G_{2i} + \frac{3}{2} H_{2i} - G_{2e} - \frac{3}{2} H_{2e} \right] \langle X \rangle_\theta + \left(G_{3i} + \frac{3}{2} H_{3i} \right) \left\langle b_i \delta \tilde{B}_\parallel \right\rangle_\theta \qquad (5.22)
$$
$$
-\frac{b_i}{2} \left[\left(G_{1i} + \frac{5}{2} H_{1i} \right) \langle Y \rangle_\theta + \left(G_{2i} + \frac{5}{2} H_{2i} \right) \langle X \rangle_\theta + \left(1 - \frac{\omega_{*i}(1+\eta)}{\omega} \right) \tilde{\Psi}_i \right] = 0,
$$

where we have used the relations between electron and ion variables described at the end of Sec. 5.2, and introduced

$$
Y \equiv \tilde{\Phi}_i - \tilde{\Psi}_i, \qquad \langle X \rangle_\theta \equiv \left\langle \delta \tilde{B}_\parallel \right\rangle_\theta + \frac{\left\langle \omega_{di} \tilde{\Psi}_i \right\rangle_\theta}{\omega}. \qquad (5.23)
$$

The radial component of the perturbed Ampere equation, [49, 50]

$$
\mathrm{i}\, k_\zeta \, \delta \hat{B}_\parallel = \frac{4\pi}{c} \sum_{j=i,e} \int \mathrm{d}^3 v \, v_\psi \, f_{1j}, \qquad (5.24)
$$

gives, after some straightforward algebra, the following expression for the normalized perturbed parallel magnetic field $\delta \tilde{B}_\parallel$:

$$
\delta \tilde{B}_\parallel = \frac{\beta}{2(1+\tau)} \Bigg\{ (1+\tau) \frac{\omega_{*i}(1+\eta)}{\omega} \tilde{\Psi}_i - \left[G_{1i} + \frac{5}{2} H_{1i} - G_{1e} - \frac{5}{2} H_{1e} \right] \langle Y \rangle_\theta
$$
$$
- \left[G_{2i} + \frac{5}{2} H_{2i} + \tau \left(G_{2e} + \frac{5}{2} H_{2e} \right) \right] \langle X \rangle_\theta + \left(G_{2i} + \frac{5}{2} H_{2i} \right) \frac{\left\langle b_i \tilde{\Phi}_i \right\rangle_\theta}{2} \qquad (5.25)
$$
$$
- \left(G_{3i} + \frac{5}{2} H_{3i} \right) \left\langle b_i \delta \tilde{B}_\parallel \right\rangle_\theta + \frac{b_i}{2} \left[\left(G_{1i} + \frac{7}{2} H_{1i} \right) \langle Y \rangle_\theta + \left(G_{2i} + \frac{7}{2} H_{2i} \right) \langle X \rangle_\theta \right.
$$
$$
\left. + \left(1 - \frac{\omega_{*i}(1+2\eta)}{\omega} \right) \tilde{\Psi}_i \right] \Bigg\},
$$

91

where $\beta \equiv 8\pi \left(1 + \tau\right) N_i T_i / B^2$.

The perturbed parallel current $\hat{j}_\parallel$ is most conveniently evaluated from the parallel component of the perturbed Ampere equation by using

$$\frac{\mathrm{i}\,c}{4\pi\omega} \boldsymbol{B} \cdot \boldsymbol{\nabla} \left(\frac{k_\perp^2}{B} \hat{A}_\parallel\right) = \frac{\mathrm{i}}{\omega} \boldsymbol{B} \cdot \boldsymbol{\nabla} \left(\frac{\hat{j}_\parallel}{B}\right) \tag{5.26}$$

and obtaining the expression for the right hand side of this equation by taking the moment $\sum\limits_{j=i,e} \int \mathrm{d}^3v \exp\left(\mathrm{i}\,L\right)$ of the gyrokinetic equation (5.5) [49, 50]. We hereby obtain the following equation [50]

$$\frac{\mathrm{i}\,c}{4\pi\omega} \boldsymbol{B} \cdot \boldsymbol{\nabla} \left(\frac{k_\perp^2}{B} \hat{A}_\parallel\right) = -\sum_{j=i,e} Z_j\, e\, \tilde{\Phi}_j \int \mathrm{d}^3v\, f_{Mj} \left[1 - \left(1 - \frac{\omega_{*j}^T}{\omega}\right) J_0^2\left(a_j\right)\right]$$

$$+ \sum_{j=i,e} \frac{Z_j^2\, e^2}{T_j} \frac{\delta\hat{B}_\parallel}{c\,k_\perp} \int \mathrm{d}^3v\, f_{Mj}\, v_\perp \left(1 - \frac{\omega_{*j}^T}{\omega}\right) J_0\left(a_j\right) J_1\left(a_j\right) \tag{5.27}$$

$$+ \sum_{j=i,e} Z_j\, e \int \mathrm{d}^3v\, \frac{\boldsymbol{v}_d \cdot \boldsymbol{k}_\perp}{\omega} \hat{g}\, J_0\left(a_j\right) + \frac{\mathrm{i}}{\omega} \sum_{j=i,e} Z_j\, e \int \mathrm{d}^3v\, \hat{g}\, v_\parallel\, \hat{\boldsymbol{n}} \cdot \boldsymbol{\nabla} J_0\left(a_j\right).$$

On substituting the appropriate expressions for $\hat{g}$, this yields a third equation relating $\tilde{\Phi}_i$, $\tilde{\Psi}_i$ and $\delta\tilde{B}_\parallel$, namely:

$$\frac{\rho_i^2\, V_A^2}{2\,\omega^2} \boldsymbol{B} \cdot \boldsymbol{\nabla} \left(\frac{k_\perp^2}{B^2} \boldsymbol{B} \cdot \boldsymbol{\nabla}\tilde{\Psi}_i\right) = -\left[(1+\tau)\frac{\omega_{*i}\left(1+\eta\right)}{\omega} + \frac{3}{2}\,b_i \left(1 - \frac{\omega_{*i}\left(1+2\eta\right)}{\omega}\right)\right] \delta\tilde{B}_\parallel$$

$$+ \frac{\omega_{di}}{\omega} \left\{ \left(G_{1i} + \frac{5}{2}H_{1i} - G_{1e} - \frac{5}{2}H_{1e}\right) \langle Y \rangle_\theta + \left[G_{2i} + \frac{5}{2}H_{2i} + \tau\left(G_{2e} + \frac{5}{2}H_{2e}\right)\right] \langle X \rangle_\theta \right.$$

$$- (1+\tau)\frac{\omega_{*i}\left(1+\eta\right)}{\omega}\tilde{\Psi}_i - \left(G_{2i} + \frac{5}{2}H_{2i}\right)\frac{\left\langle b_i\, \tilde{\Phi}_i \right\rangle_\theta}{2} + \left(G_{3i} + \frac{5}{2}H_{3i}\right)\left\langle b_i\, \delta\tilde{B}_\parallel \right\rangle_\theta \tag{5.28}$$

$$- \frac{b_i}{2}\xi \left[\left(G_{1i} + \frac{7}{2}H_{1i}\right) \langle Y \rangle_\theta + \left(G_{2i} + \frac{7}{2}H_{2i}\right) \langle X \rangle_\theta + \left(1 - \frac{\omega_{*i}\left(1+2\eta\right)}{\omega}\right)\tilde{\Psi}_i\right] \right\}$$

$$- b_i\, \tilde{\Phi}_i \left(1 - \frac{\omega_{*i}\left(1+\eta\right)}{\omega}\right)$$

where $\rho_i \equiv c\left(2M_i T_i\right)^{1/2} / \left(Z_i e B\right)$ is the ion gyroradius, $V_A \equiv B^2/\left(4\pi M_i N_i\right)$ is the Alfvén speed, $\xi \equiv 1 + \omega_{\nabla B i}/\omega_{di}$, and

$$\omega_{\nabla Bi} \equiv \frac{T_i}{M_i \Omega_i} k_\zeta \left(\hat{\zeta} \cdot \hat{n} \times \nabla \ln B \right), \qquad \omega_{\kappa i} \equiv \frac{T_i}{M_i \Omega_i} k_\zeta \left(\hat{\zeta} \cdot \hat{n} \times \kappa \right). \qquad (5.29)$$

Equations (5.22), (5.25) and (5.28) now form a coupled set of equations for the three field variables $\tilde{\Phi}_i$, $\tilde{\Psi}_i$ and $\delta \tilde{B}_\parallel$. In the next section we describe how equations (5.22) and (5.25) can be used to eliminate the electrostatic potential $\tilde{\Phi}_i$ and the magnetic compression $\delta \tilde{B}_\parallel$, leaving an integro-differential ballooning equation for $\tilde{\Psi}_i$ as the eigenmode equation for the system.

5.4 Electromagnetic Dispersion Relation for the Odd Modes

As the physical system under consideration is symmetric with respect to the equatorial plane of the magnetic dipole, plasma modes in such a system must be either symmetric or antisymmetric with respect to this plane [20, 27]. More precisely, as the coefficients in the quasineutrality condition (5.22) and the two components of the Ampere equation (5.25) and (5.28) are symmetric with respect to the equatorial plane, the variables $\delta \tilde{B}_\parallel$, $\tilde{\Phi}_i$ and $\tilde{\Psi}_i$ are (simultaneously) either symmetric or anti-symmetric with respect to this plane. In this section we derive a dispersion relation for the antisymmetric, or odd, electromagnetic modes, so that all the averages $\langle \ldots \rangle_\theta$ of $\delta \tilde{B}_\parallel$, $\tilde{\Phi}_i$ and $\tilde{\Psi}_i$, with arbitrary symmetric weighting functions, are equal to zero. For simplicity, here and in the following sections, we consider the case of $\tau = 1$, which can be readily generalized to arbitrary τ.

For the odd modes, equations (5.22), (5.25) and (5.28) can be simplified considerably. It follows then from the quasineutrality condition that

$$\tilde{\Phi}_i = \left[1 - \frac{b_i}{4} \left(1 - \frac{\omega_{*i} (1 + \eta)}{\omega} \right) \right] \tilde{\Psi}_i, \qquad (5.30)$$

the radial component of the Ampere equation gives

93

$$\delta \tilde{B}_{\parallel} = \frac{\beta}{2} \left[\frac{\omega_{*i}(1+\eta)}{\omega} + \frac{b_i}{4} \left(1 - \frac{\omega_{*i}(1+2\eta)}{\omega} \right) \right] \tilde{\Psi}_i, \tag{5.31}$$

while the parallel component of the Ampere equation can be rewritten as

$$\frac{\rho_i^2 V_A^2}{2} \boldsymbol{B} \cdot \boldsymbol{\nabla} \left(\frac{k_\perp^2}{B^2} \boldsymbol{B} \cdot \boldsymbol{\nabla} \tilde{\Psi}_i \right) = -2\omega^2 \left[\frac{\omega_{*i}(1+\eta)}{\omega} + \frac{3}{4} b_i \left(1 - \frac{\omega_{*i}(1+2\eta)}{\omega} \right) \right] \delta \tilde{B}_{\parallel}$$

$$-\omega \omega_{di} \left[2\frac{\omega_{*i}(1+\eta)}{\omega} + \frac{\xi}{2} b_i \left(1 - \frac{\omega_{*i}(1+2\eta)}{\omega} \right) \right] \tilde{\Psi}_i - b_i \omega^2 \left(1 - \frac{\omega_{*i}(1+\eta)}{\omega} \right) \tilde{\Phi}_i. \tag{5.32}$$

Substituting expression (5.30) for $\tilde{\Phi}_i$ and expression (5.31) for $\delta \tilde{B}_{\parallel}$ into Eq. (5.32), assuming $k_\perp \approx k_\zeta = \ell/R$ with $\ell \gg 1$ the toroidal mode number, dropping the terms of order $b_i^2 \ll 1$, using the expression for the magnetic field line curvature

$$\boldsymbol{\kappa} = \frac{4\pi}{B^2} \boldsymbol{\nabla} \left(p + \frac{B^2}{8\pi} \right) \tag{5.33}$$

and the equality

$$\omega_{*i}(1+\eta) \frac{\beta}{2} = 2\omega_{\kappa i} - \omega_{di}, \tag{5.34}$$

we eventually obtain the electromagnetic ballooning equation for the odd modes:

$$R^2 B^2 \boldsymbol{B} \cdot \boldsymbol{\nabla} \left(\frac{\boldsymbol{B} \cdot \boldsymbol{\nabla} \tilde{\Psi}_i}{R^2 B^2} \right) + 4\pi \left(2\boldsymbol{\kappa} \cdot \boldsymbol{\nabla} p + \rho \Lambda^2 \right) \tilde{\Psi}_i = 0, \tag{5.35}$$

where $\rho \equiv N_i M_i$ is plasma density and the generalized eigenvalue Λ^2 is defined as

$$\Lambda^2 \equiv \omega^2 - \omega \left[\omega_{*i}(1+\eta) - \left(\frac{5}{2}\omega_{\kappa i} - \omega_{\nabla Bi} \right) \right] - \omega_{*i}(1+2\eta) \left(\frac{5}{2}\omega_{\kappa i} - \omega_{\nabla Bi} \right). \tag{5.36}$$

Equation (5.35) is the generalization of the well known ballooning equation for odd ideal MHD modes in an axially symmetric poloidal magnetic field with closed field lines, derived, for example, in Ref. [20]. The only difference is that our generalized

equation (5.35) has Λ^2 in place of ω^2. The additional terms in Λ^2 as given by Eq. (5.36) describe the finite Larmor radius (FLR) diamagnetic and magnetic drift corrections to the ideal MHD result. They can be either stabilizing or destabilizing depending on the values of parameters ω_{*i}, $\omega_{\kappa i}$, η and β. We notice that in the limit of zero field line curvature, $\kappa = 0$, expression (5.36) coincides with the expression (10.8) obtained in Ref. [36] for the case of straight magnetic field lines.

We may rewrite Eq. (5.36) in the form

$$\Lambda^2 = \left[\omega - \frac{\omega_{*pi} - \omega_{gi}}{2}\right]^2 - \Delta\left(\omega_{gi}, \omega_{*pi}\right), \qquad (5.37)$$

where $\Delta\left(\omega_{gi}, \omega_{*pi}\right) \equiv \left(\omega_{gi}^2 + \omega_{*pi}^2 + \sigma\,\omega_{gi}\,\omega_{*pi}\right)/4$ with $\omega_{gi} \equiv \frac{5}{2}\omega_{\kappa i} - \omega_{\nabla Bi}$, $\omega_{*pi} \equiv \omega_{*i}\left(1 + \eta\right)$ and $\sigma \equiv 2\left(1 + 3\eta\right)/\left(1 + \eta\right)$. FLR effects stabilize (destabilize) the odd ideal MHD ballooning modes if $\left\langle \Delta\tilde{\Psi}_i^2 \right\rangle_\theta > 0$ (< 0). Rewriting Δ as

$$\Delta = \left(\omega_{gi} + \sigma\frac{\omega_{*pi}}{2}\right)^2 + \omega_{*pi}^2\left(1 - \frac{\sigma^2}{4}\right) \qquad (5.38)$$

we see that for $-2 < \sigma < 2$ or equivalently for $-1/2 < \eta < 0$, $\Delta > 0$ and FLR effects are always stabilizing. On the other hand, for $\sigma > 2$ ($\eta > 0$ or $\eta < -1$) or $\sigma < -2$ ($-1 < \eta < -1/2$) the quantity Δ may change sign along the field line so that stabilization or destabilization by the FLR effects depends on the eigenfunction $\tilde{\Psi}_i$ of Eq. (5.35).

5.5 Electromagnetic Dispersion Relation for the Even Modes

Next, we turn our attention to the more involved case of the even modes. First, we notice from Eq. (5.9) that the auxiliary potential $\hat{\Psi}$ is defined up to an arbitrary constant. A convenient way to choose this constant is to require $\left\langle \tilde{\Phi}_i \right\rangle_\theta = \left\langle \tilde{\Psi}_i \right\rangle_\theta$ or $\langle Y \rangle_\theta = 0$, which simplifies Eqs. (5.22), (5.25) and (5.28) considerably.

Then, averaging the quasineutrality condition (5.22) over poloidal angle θ, solving

the resulting equation for $\left\langle b_i \tilde{\Phi}_i \right\rangle_\theta$ and substituting this quantity back into Eq. (5.22) we find

$$\tilde{\Phi}_i = \tilde{\Psi}_i + \frac{\langle b_i \rangle_\theta - b_i}{4} \left(G_{2i} + \frac{5}{2} H_{2i} \right) \langle X \rangle_\theta + \frac{\left\langle b_i \tilde{\Psi}_i \right\rangle_\theta - b_i \tilde{\Psi}_i}{4} \left(1 - \frac{\omega_{*i}(1+\eta)}{\omega} \right). \quad (5.39)$$

Notice that $Y = O(b_i)$. We next observe that $\tilde{\Phi}_i$ enters Eqs. (5.25) and (5.28) only in the combination $b_i \tilde{\Phi}_i$. Consequently, we can use the approximate equality

$$b_i \tilde{\Phi}_i \approx b_i \tilde{\Psi}_i \quad (5.40)$$

with accuracy $O(b_i)$.

We desire to solve the radial Ampere equation (5.25) for $\delta \tilde{B}_\parallel$. Noticing that the equation also contains the averaged quantities $\left\langle \delta \tilde{B}_\parallel \right\rangle_\theta$ and $\left\langle b_i \delta \tilde{B}_\parallel \right\rangle_\theta$, we proceed by first averaging the equation over poloidal angle with weighting functions 1 and b_i, solving the resulting linear system to find these averaged quantities, and then substituting them back into the radial Ampere equation. Finally, taking into account equality (5.40), an expression for $\delta \tilde{B}_\parallel$ is obtained in terms of $\tilde{\Psi}_i$. Substituting this expression for $\delta \tilde{B}_\parallel$ and $b_i \tilde{\Phi}_i$ from Eq. (5.40), into the parallel Ampere equation (5.28) we find the following integro-differential eigenmode equation for the even modes:

$$\frac{\rho_i^2 V_A^2}{2} \boldsymbol{B} \cdot \boldsymbol{\nabla} \left(\frac{\ell^2}{R^2 B^2} \boldsymbol{B} \cdot \boldsymbol{\nabla} \tilde{\Psi}_i \right) = -b_i \Lambda^2 \tilde{\Psi}_i - [\omega_{*i}(1+\eta)\beta + 2\omega_{di}] \times$$
$$\left[\omega_{*i}(1+\eta)\tilde{\Psi}_i - \frac{\Gamma}{2 + \Gamma \langle \beta \rangle_\theta} \left(2 \left\langle \omega_{di} \tilde{\Psi}_i \right\rangle_\theta + \omega_{*i}(1+\eta) \left\langle \beta \tilde{\Psi}_i \right\rangle_\theta \right) \right], \quad (5.41)$$

where Λ^2 is given by Eq. (5.36),

$$\Gamma \equiv \frac{15\lambda^4 - 5\left(d\frac{17\eta+7}{1+\eta} + 5 \right)\lambda^2 + 25d}{9\lambda^4 - 70\lambda^2 + 25}, \quad (5.42)$$

and we have introduced the dimensionless frequency $\lambda \equiv \omega / \langle \omega_{di} \rangle_\theta$ and $d \equiv$

96

$\omega_{*i}(1+\eta)/\langle\omega_{di}\rangle_\theta$. We have also dropped small terms of order $O\left(b_i\,\lambda\,\tilde{\Psi}_i\right)$ and $O\left(b_i\,\tilde{\Psi}_i\right)$ compared to $O\left(b_i\,\lambda^2\,\tilde{\Psi}_i\right)$, except in Λ^2, for compatibility with the odd mode equation (5.35). Such terms could only be important near the marginal stability boundary for the MHD mode if the frequency ω becomes of the order of ω_{di} and ω_{*i}. However, such low frequency solutions do not occur for the even MHD mode because (as discussed below) it couples to the entropy mode near marginality and remains at high frequency, i.e. $\lambda\gg1$.

Using definitions of ρ_i, V_A, ω_{*i}, ω_{di}, $\omega_{\nabla Bi}$, and η and expression (5.34) for β, as in Section 5.4, we can rewrite the ballooning equation (5.41) in the form

$$R^2B^2\boldsymbol{B}\cdot\boldsymbol{\nabla}\left(\frac{\boldsymbol{B}\cdot\boldsymbol{\nabla}\tilde{\Psi}_i}{R^2B^2}\right)+4\pi\left(2\boldsymbol{\kappa}\cdot\boldsymbol{\nabla}p+\rho\,\Lambda^2\right)\tilde{\Psi}_i=16\pi p\Gamma\left(\boldsymbol{\kappa}\cdot\boldsymbol{\nabla}\psi\right)\frac{\left\langle\frac{\boldsymbol{\kappa}\cdot\boldsymbol{\nabla}\psi}{R^2B^2}\tilde{\Psi}_i\right\rangle_\theta}{1+\frac{\Gamma}{2}\langle\beta\rangle_\theta}.$$
$$(5.43)$$

This form is identical to the ideal MHD ballooning equation for even modes [20], except that Λ^2 replaces ω^2 and Γ replaces the adiabatic index $\gamma=5/3$. In the limit $\omega\gg\langle\omega_{di}\rangle_\theta$ we find $\Lambda^2\approx\omega^2$ and $\Gamma\approx5/3=\gamma$ so that the ideal MHD limit is recovered.

As in the case of *electrostatic* modes in dipolar fields [35], equation (5.43) not only allows high-frequency ($\omega\gg\langle\omega_{di}\rangle_\theta$) MHD solutions, but also permits low frequency ($\omega\sim\langle\omega_{di}\rangle_\theta$) solutions. These are the entropy modes [39], which were also found in the electrostatic limit [35]. The two modes couple near $d=5/3$.

This fact can be demonstrated in the following way. Averaging equation (5.41) over poloidal angle we obtain the following equality

$$\frac{2\,d-2\Gamma}{2+\Gamma\,\langle\beta\rangle_\theta}\left(2\left\langle\hat{\omega}_d\tilde{\Psi}_i\right\rangle_\theta+d\left\langle\beta\tilde{\Psi}_i\right\rangle_\theta\right)+\frac{\Lambda^2}{\langle\omega_{di}\rangle_\theta^2}\left\langle b_i\tilde{\Psi}_i\right\rangle_\theta=0,\qquad(5.44)$$

where we introduce the normalized ion magnetic drift frequency $\hat{\omega}_d\equiv\omega_{di}/\langle\omega_{di}\rangle_\theta$. Using Eq. (5.44), equation (5.41) can be rewritten as

$$\frac{\rho_i^2 V_A^2}{2 \langle \omega_{di} \rangle_\theta^2} \boldsymbol{B} \cdot \boldsymbol{\nabla} \left(\frac{\ell^2}{R^2 B^2} \boldsymbol{B} \cdot \boldsymbol{\nabla} \tilde{\Psi}_i \right) = \frac{\Lambda^2}{\langle \omega_{di} \rangle_\theta^2} \left[\left\langle b_i \tilde{\Psi}_i \right\rangle_\theta \frac{d \, \beta \tilde{\Psi}_i + 2 \, \hat{\omega}_d \tilde{\Psi}_i}{d \left\langle \beta \tilde{\Psi}_i \right\rangle_\theta + 2 \left\langle \hat{\omega}_d \tilde{\Psi}_i \right\rangle_\theta} - b_i \tilde{\Psi}_i \right]$$

$$+ \Gamma \frac{d \, \beta + 2 \, \hat{\omega}_d}{2 + \Gamma \langle \beta \rangle_\theta} \left[d \left(\left\langle \beta \tilde{\Psi}_i \right\rangle_\theta - \langle \beta \rangle_\theta \tilde{\Psi}_i \right) + 2 \left(\left\langle \hat{\omega}_d \tilde{\Psi}_i \right\rangle_\theta - \tilde{\Psi}_i \right) \right]. \tag{5.45}$$

We now consider modes with frequencies which are not too large, namely $\lambda \ll b_i^{-1/2}$. Then the first term on the right hand side of Eq. (5.45) is of order $O\left(b_i \lambda^2 \tilde{\Psi}_i \right)$, while the other terms are of order $O\left(\tilde{\Psi}_i \right)$. Expanding $\tilde{\Psi}_i$ in the small parameter $b_i \lambda^2 \ll 1$, $\tilde{\Psi}_i = \tilde{\Psi}_i^{(1)} + \tilde{\Psi}_i^{(2)} + \ldots$, we find that $\tilde{\Psi}_i^{(1)} = $ constant (the proof is given in Appendix H), while $\tilde{\Psi}_i^{(2)} \sim b_i \lambda^2 \tilde{\Psi}_i^{(1)} \ll \tilde{\Psi}_i^{(1)}$, so that the low-frequency even modes are flutes to leading order. Using this fact in Eq. (5.44) and substituting the expression for Γ we obtain the following dispersion relation for these modes

$$\left(d - \frac{5}{3} \right) \lambda^2 + \frac{5}{9} \left(d \frac{3\eta - 7}{1 + \eta} + 5 \right) + \frac{\langle b_i \rangle_\theta}{2} \frac{1 + 5 \langle \beta \rangle_\theta / 6}{1 + d \langle \beta \rangle_\theta / 2} \lambda^4 = 0, \tag{5.46}$$

where we keep only the leading power of λ in the "b_i" term.

This dispersion relation is very similar to the electrostatic dispersion relation for plasmas confined in dipolar fields [21, 33, 35] and, as has already been mentioned, allows two classes of mode: the high frequency MHD mode and the low frequency entropy mode. The entropy mode [21, 33, 35] frequency is obtained by balancing the first two terms in Eq. (5.46), giving

$$\lambda_E = \pm \sqrt{\frac{5}{9} \frac{d \frac{3\eta - 7}{1 + \eta} + 5}{\frac{5}{3} - d}}. \tag{5.47}$$

Notice that the "b_i" terms in all equations can be neglected for the entropy mode so it is an *exact flute*. In this case it follows from Eqs. (5.9), (5.25), (5.39) and (5.46) that $\hat{A}_\parallel = \delta \hat{B}_\parallel = 0$ so that the entropy mode does not perturb the magnetic field and is therefore a purely electrostatic mode for arbitrary β. This result is not surprising as the mode does not perturb total plasma pressure [35, 39]. More details on the entropy mode are given in Refs. [35, 39].

In addition to the entropy mode, dispersion relation (5.46) permits the high frequency MHD mode, which is obtained by balancing the first and the last terms, giving $\lambda_{MHD} \sim b_i^{-1/2} |d - 5/3|^{1/2}$. As we assumed $\lambda \ll b_i^{-1/2}$ when deriving Eq. (5.46), this equation can only describe the MHD mode near $d = 5/3$, namely for $|d - 5/3| \ll 1$. We can therefore replace d by $5/3$ in the last term of Eq. (5.46) to obtain

$$\lambda_{MHD} = \pm \sqrt{-\frac{2\left(d - \frac{5}{3}\right)}{\langle b_i \rangle_\theta}}, \tag{5.48}$$

which shows that the MHD mode is stable for $d < 5/3$ and is unstable otherwise. Noticing [21, 35] that $d = -\mathrm{d}\ln p / \mathrm{d}\ln V$ with p plasma pressure and $V \equiv \oint \mathrm{d}l / B$ we see that the stability condition $d < 5/3$ is equivalent to the well known ideal MHD interchange stability condition (see for example Ref. [20])

$$\frac{1}{p}\frac{\mathrm{d}p}{\mathrm{d}\psi} + \frac{\gamma}{V}\frac{\mathrm{d}V}{\mathrm{d}\psi} < 0 \tag{5.49}$$

with $\gamma = 5/3$. This result is not surprising either because the MHD mode becomes flute-like as d approaches $5/3$.

It follows from Eqs. (5.47) and (5.48) that λ_E increases while λ_{MHD} decreases as d approaches $5/3$ so the two modes will couple. We can see from Eq. (5.46) that the coupling occurs (that is, all three terms are of the same order) when $|d - 5/3| \lesssim b_i^{1/2} \ll 1$ and the frequency of the modes obtained is $\lambda_c \sim b_i^{-1/4} \gg 1$. More precisely, Eq. (5.46) gives the expression

$$\lambda_{c\pm}^2 = \frac{\left(\frac{5}{3} - d\right) \pm \sqrt{\left(\frac{5}{3} - d\right)^2 - \langle b_i \rangle_\theta \frac{10}{9}\left(d\frac{3\eta - 7}{1 + \eta} + 5\right)}}{\langle b_i \rangle_\theta}, \tag{5.50}$$

which contains both the MHD, entropy, and coupled modes. Equation (5.50) shows that λ_{c-} is unstable whenever $d > 5/3$ for arbitrary η (MHD instability). If $d < 5/3$ the λ_{c-} mode is unstable when $d(3\eta - 7)/(1 + \eta) + 5 < 0$ (entropy instability). Both λ_{c+} and λ_{c-} modes are stable if

$$\left(d - \frac{5}{3}\right)^2 > \langle b_i \rangle_\theta \frac{10}{9} \left(d \frac{3\eta - 7}{1 + \eta} + 5\right) > 0 \tag{5.51}$$

and unstable if one of the inequalities in Eq. (5.51) does not hold. In this case the MHD stability boundary $d = 5/3$ gets modified by the FLR terms and stability requires

$$d = 5/3 \left[1 - 2\sqrt{\langle b_i \rangle_\theta \frac{\eta - 2/3}{\eta + 1}}\right] < 5/3, \tag{5.52}$$

where we have used $d \approx 5/3$ to simplify the expression under the square root. Consequently, coupling to the entropy mode *destabilizes* the even MHD mode in magnetic dipoles for $\eta < -1$ and $\eta > 2/3$. The inequalities for η guarantee that the expression under the square root in Eq. (5.52) is positive (if it is negative the entropy mode becomes unstable, see Eq. (5.47)).

5.6   Conclusions

In this chapter we used kinetic theory to investigate the electromagnetic plasma stability of an axisymmetric system having poloidal magnetic fields with closed field lines. Our results generalize the electrostatic results of Chapter 4. We have employed the intermediate collisionality ordering (5.1), appropriate for high density and low temperature LDX plasmas.

First, we solved the electromagnetic gyro-kinetic equation to leading order to show that the perturbed distribution function is a Maxwellian. This perturbed Maxwellian was then used to form the quasineutrality equation and two components of the Ampere equation. These gave a system of integro-differential equations for the perturbed electrostatic potential Φ, an auxiliary potential Ψ which is equivalent to the parallel component of the vector potential, and the parallel component of the perturbed magnetic field $\delta B_\parallel$. The quasineutrality equation and the radial component of the Ampere equation were solved to give Φ and $\delta B_\parallel$ in terms of Ψ. Substituting these expressions into the parallel component of the Ampere equation gave the integro-differential

ballooning equation for electromagnetic modes.

As in the ideal MHD case, described in Chapter 2, two types of modes can be obtained because of the symmetry of the equilibrium with respect to the equatorial plane, namely the symmetric (or even) and the antisymmetric (or odd) modes. The electromagnetic ballooning equation is particularly simple for the odd modes and is the ideal MHD ballooning equation with diamagnetic and magnetic drift modifications. These modifications are important near the marginal stability boundary and can be either stabilizing or destabilizing, depending on the plasma parameters. On the other hand, the electromagnetic ballooning equation for the even modes describes not only the ideal MHD mode, but also the low frequency entropy mode, described in detail in Chapter 4. As in the electrostatic case, the two modes couple near the marginal stability boundary for the MHD mode, which leads to a destabilization of the MHD mode in a narrow strip near the MHD stability boundary.

The entropy mode is essentially an electrostatic mode, perturbing neither plasma pressure nor magnetic field. Despite the fact that finite β effects modify the value of the parameter $d = \omega_{*i} \left(1 + \eta\right) / \langle \omega_{di} \rangle_\theta$, the stability diagrams obtained for this mode in Chapter 4 in terms of d and $\eta = \mathrm{d} \ln T / \mathrm{d} \ln N$ remain unchanged.

Chapter 6

Conclusion

In this thesis the stability of axisymmetric plasmas confined by poloidal magnetic fields has been studied. Typical examples are magnetospheric plasmas in planetary dipolar fields and the Levitated Dipole Experiment under construction at MIT.

The ideal MHD stability of isotropic pressure plasmas was investigated first (Chapter 2). The energy principle was used to study pressure driven modes which are intrinsic for unfavorable curvature dipolar magnetic fields. The interchange stability condition and an *integro-differential* ballooning equation were derived. It was observed that stability boundaries can be described in terms of a much simpler homogeneous *differential* equation, obtained by dropping the stabilizing compressional integral term from the ballooning equation. In particular, ballooning modes are stable whenever the equilibrium under consideration is interchange stable, and the lowest antisymmetric and the second lowest symmetric modes of the homogeneous *differential* equation are stable. For a dipolar field, interchange stability is guaranteed if the pressure decreases with radius more slowly than $r^{-20/3}$. The plasma and magnetic compression play a vital role in stabilizing pressure driven modes, allowing stable equilibria with arbitrarily large $\beta =$ (plasma pressure / magnetic pressure) to exist. The separable point dipole equilibrium of Ref. [1] is an example of such a class of equilibria.

Realizing that magnetospheric plasmas and the ECRH-heated LDX plasmas have anisotropic pressure, we have generalized the MHD formulation to account for such

situations (Chapter 3). We started with the Kruskal-Oberman form of the energy principle and used a Schwartz inequality to bound the complicated plasma compression contribution, which is given in terms of integrals along particle trajectories, by a much simpler fluid expression. We then derived a general anisotropic pressure interchange stability condition and an integro-differential ballooning equation, which reduce to the isotropic pressure expressions in the limit $p_\parallel \rightarrow p_\perp \rightarrow p$. Our results were then applied to the case of the separable point dipole, anisotropic pressure equilibria of Ref. [15], to show that it is interchange stable up to beta limits imposed by the mirror or firehose instabilities and is ballooning stable up to a beta limit which is typically close to these limits. A modified stability problem in which a "tied field line" boundary condition was implemented was also considered. This problem is relevant for atmospheric and solar plasma applications. Greater stability was found in this case due to the additional magnetic field line bending stabilization introduced by the "line tied" boundary conditions.

MHD theory is unable to describe many important stability issues, such as FLR effects and the stability of drift modes. Moreover, the collisional ordering of MHD is unsuitable for LDX plasmas. As a result, we employed an intermediate collisionality ordering with $\Omega \gg \omega_b \gg \nu_c \gg \omega \gtrsim \omega_d, \omega_*$ to study plasma stability kinetically. The electrostatic stability of low beta equilibria was investigated first (Chapter 4). Two types of modes were found; namely the high frequency MHD and low frequency entropy modes. Electrostatically, both of these modes are flutes to leading order in our small expansion parameters. The stability of these modes can be described in terms of two parameters, $d \equiv \omega_{*i} \left(1 + \eta\right) / \langle \omega_{di} \rangle_\theta$ and $\eta = \mathrm{d} \ln T / \mathrm{d} \ln N$. The MHD mode is stable for $d < 5/3$, which is consistent with the interchange stability condition found in the ideal MHD analysis of Chapter 2. The entropy modes were shown to be unstable in certain regions of d, η space as shown in Figs. 4-1 - 4-4. The influence of collisional effects on plasma stability was then studied. We found that gyro-relaxation effects are important and can destabilize portions of the otherwise stable regions of d, η space for the entropy waves. However, large areas in d, η parametric space remain stable and suitable for LDX operation.

Finally, a fully electromagnetic kinetic analysis of arbitrary beta equilibria was performed in Chapter 5 and a generalized integro-differential ballooning equation was derived. For antisymmetric modes this equation reproduces the ideal MHD ballooning equation, but with FLR corrections to the inertial term due to magnetic and diamagnetic drifts. These FLR corrections can be stabilizing or destabilizing close to the ideal stability boundary, depending on the plasma parameters. For the even modes this ballooning equation permits two classes of solutions; namely an ideal MHD ballooning mode and an entropy mode. These modes are coupled near the ideal MHD stability boundary in a similar manner to the electrostatic analysis of Chapter 4. As in that case, coupling to the entropy mode destabilizes the MHD mode near its stability boundary. The entropy mode remains essentially electrostatic in nature, but plasma β effects modify the unperturbed magnetic field contributions to $d = \omega_{*pi}/\langle\omega_{di}\rangle_\theta$ and thereby change its value from the $\beta \to 0$ limit. However, the entropy mode stability diagrams in d and $\eta = \mathrm{d}\ln T/\mathrm{d}\ln N$ parametric space shown in Figures 4-1 - 4-4 remain unchanged.

Future theoretical work (both analytical and numerical) on plasma stability in a dipole magnetic field might extend the work of this thesis in the following ways: (i) by investigating linear stability of higher temperature (or lower density) plasmas in which the ions (primarily) respond in a collisionless manner (i.e. $\omega \gg \nu_{ii}$), and (ii) by developing a nonlinear stability theory for plasmas of different collisionality.

The first of these goals originates from the fact that many plasmas of interest are less collisional than that considered in this thesis. For example planetary and stellar magnetospheric plasmas are usually collisionless. In the case of LDX, just after being created, a low-density ECRH-heated plasma is expected to have a small population of very energetic electrons, which barely collide with the background plasma. Neutral gas injection is then expected to produce a relatively cold and dense plasma, as considered in Chapters 4 and 5 of this thesis. After further heating, this plasma will first become less collisional (collisionless ions) and then, if the temperature is high enough, fully collisionless. Stability of collisionless plasmas has already been investigated in multipole devices in a number of works, for example [10, 31, 32, 63], while the stability

105

of three component plasmas (i.e. with an energetic particle population of either ions or electrons in a "cold" background ion-electron plasma) has been studied in other devices [64, 65, 66, 67]. In Refs. [64, 65, 66] a highly energetic electron population interacted with a cold background in the bumpy torus devices. In Ref. [67] energetic ion populations destabilized otherwise stable waves in tokamaks. Plasma stability in dipole fields, in the intermediate regime of collisionality (i.e. collisional electrons but collisionless ions, $\nu_e \gg \omega \gg \nu_{ii}$), is currently under investigation by J. Kesner [48].

The second extension must be achieved in order to understand turbulent plasma transport and to be able to interpret and predict experimental results. To achieve this goal numerical solution of gyro-kinetic equations and particle simulations [68] will be invaluable in order to model anomalous transport in dipole confined plasmas. Of course, analytic work will be required to formulate the reduced kinetic descriptions necessary for modelling and to identify potentially dangerous instabilities which can drive anomalous losses.

Appendix A

Ordering of Eigenvalues and Proof of Equation (3.17)

In this appendix it is shown that the eigenvalues Λ_j of the general integro-differential ballooning equation (3.10) are greater than or equal to the corresponding eigenvalues λ_j of the corresponding differential equation (3.11), such that $\Lambda_{2j+1} = \lambda_{2j+1}$ and $\lambda_{2j} \leq \Lambda_{2j} \leq \lambda_{2j+2} \leq \Lambda_{2j+2}$, for $j = 0, 1, 2, \ldots$. Moreover, the ballooning stability condition of Eq. (3.17) is derived for a particular case .

First, we notice that Eq. (3.11) is a Sturm-Liouville equation and so for specified boundary conditions its eigenfunctions, ξ_j, form a complete set of functions with corresponding eigenvalues, λ_j, which are all distinct and can be arranged into an infinite, increasing sequence. As the even and odd eigenfunctions have different (periodic) boundary conditions, they form two different sets of functions, and the corresponding eigenvalues form two different increasing sequences, namely $\lambda_0 < \lambda_2 < \cdots < \lambda_{2j} < \cdots$ and $\lambda_1 < \lambda_3 < \cdots < \lambda_{2j+1} < \cdots$, where even (odd) indices correspond to even (odd) eigenfunctions. These eigenfunctions can be normalized in such a way that

$$\langle \xi_i \xi_j \rangle_\theta = \oint \left\{ \frac{\mathrm{d}l}{B} \frac{4\pi\rho}{R^2 B^2} \xi_i \xi_j \right\} = \delta_{ij}. \tag{A.1}$$

If we now consider a solution ξ of Eq. (3.10), then we can generalize the treatment of Ref. [18] to prove that $\lambda_{2j} \leq \Lambda_{2j} \leq \lambda_{2j+2} \leq \Lambda_{2j+2}$ by writing

$$\xi = \sum_j b_j \xi_j, \tag{A.2}$$

as well as

$$D \equiv (\boldsymbol{\kappa} \cdot \boldsymbol{\nabla}\psi)\left[\Sigma_-\Gamma_1 + \Gamma_2\right]/\rho = \sum_j a_j \xi_j. \tag{A.3}$$

Then from Eqs. (3.10), (3.11), (A.2) and (A.3) it follows that

$$\sum_j (\Lambda - \lambda_j)\, b_j \xi_j = f(\psi) \sum_j a_j \xi_j, \tag{A.4}$$

where

$$f(\psi) = \frac{\oint (\mathrm{d}l/B)\left\{(\boldsymbol{\kappa}\cdot\boldsymbol{\nabla}\psi/B^2 R^2)\,\xi\left[\Sigma_-\Gamma_1 + \Gamma_2\right]\right\}}{\oint (\mathrm{d}l/B)\left\{\Gamma_3 + 4\pi\Gamma_1^2/B^2\,(1+\sigma_\perp)\right\}}. \tag{A.5}$$

Multiplying Eq. (A.4) by ξ_i and using Eq. (A.1) we find

$$b_j = \frac{a_j}{\Lambda - \lambda_j} f(\psi). \tag{A.6}$$

Rewriting Eq. (A.5) as

$$f(\psi) = \frac{\langle D\xi\rangle_\theta}{4\pi \oint (\mathrm{d}l/B)\left\{\Gamma_3 + 4\pi\Gamma_1^2/B^2\,(1+\sigma_\perp)\right\}},$$

noticing that $\langle D\xi\rangle_\theta = \sum_j a_j b_j$, and using Eq. (A.6) we find

$$F(\Lambda) = \sum_j \frac{a_j^2}{\Lambda - \lambda_j} = 4\pi \oint \frac{\mathrm{d}l}{B}\left\{\Gamma_3 + \frac{4\pi\Gamma_1^2}{B^2\,(1+\sigma_\perp)}\right\}. \tag{A.7}$$

We must require $1 + \sigma_\perp > 0$ for a mirror mode stable equilibrium. Moreover, $\Gamma_3 \equiv p_\perp + \frac{3}{4}p_\parallel - C = -\int \mathrm{d}^3 v\, \epsilon^2\,(\partial F/\partial\epsilon) \geq 0$ for $\partial F/\partial\epsilon < 0$, a condition necessary for the derivation of the Kruskal-Oberman energy principle. As a result $F(\Lambda) \geq 0$. Also, it is clear that $\mathrm{d}F(\Lambda)/\mathrm{d}\Lambda < 0$ and, by plotting both sides of Eq. (A.7), $\lambda_0 \leq \Lambda_0 \leq \lambda_2 \leq \Lambda_2 \cdots$.

It is possible to develop our analysis further and to find a criterion for ballooning

mode stability for the case when perpendicular and parallel pressures are proportional, that is $p_\perp = (1 + 2a) \, p_\parallel$. Using Eq. (3.13) and introducing the expansion coefficients a_j in a form slightly different from that of Eq. (A.3) by letting $a_j \rightarrow (2a + 5/2) \, \hat{p} \, (\psi) \, a_j$ so that

$$D \equiv (\boldsymbol{\kappa} \cdot \boldsymbol{\nabla}\psi) \left[(1 + 2a) \, \Sigma_- - 2a\right] (2a + 5/2) \, \hat{p} \, (\psi) \, w/\rho$$

$$= (2a + 5/2) \, \hat{p} \, (\psi) \sum_j a_j \xi_j,$$

we may rewrite Eq. (A.7) as

$$F(\Lambda) = \sum_j \frac{a_j^2}{\Lambda - \lambda_j} = \frac{4\pi}{\hat{\gamma}\hat{p}\,(\psi)} \oint \frac{\mathrm{d}l}{B} \left\{ w + \frac{4\pi \, \hat{\gamma} \, (1 + 2a)^2 \, \hat{p}\,(\psi) \, w^2}{B^2 \, (1 + \sigma_\perp)} \right\}$$

$$\equiv 4\pi \left(\frac{V\,(\psi)}{\hat{\gamma}\hat{p}\,(\psi)} + L\,(\psi) \right) \tag{A.8}$$

where $V\,(\psi)$ and $L\,(\psi)$ are defined after Eq. (3.17). Field line averaging Eq. (3.15) with the right hand side equal to zero (and $\Lambda \rightarrow \lambda_j$, $\xi \rightarrow \xi_j$) for periodic boundary conditions gives the following relation between its eigenfunctions and eigenvalues

$$\lambda_j \, \langle \xi_j \rangle_\theta + a_j \hat{p}' \, (\psi) = 0. \tag{A.9}$$

As a result

$$F(0) = -\sum_j \frac{a_j^2}{\lambda_j} = \frac{4\pi}{\hat{p}'\,(\psi)} \oint \frac{\mathrm{d}l}{B} \left\{ \frac{\boldsymbol{\kappa} \cdot \boldsymbol{\nabla}\psi}{B^2 R^2} w \left[(1 + 2a) \, \Sigma_- - 2a\right] \right\}$$

$$\equiv \frac{4\pi}{\hat{p}'\,(\psi)} U\,(\psi). \tag{A.10}$$

From Eqs. (A.8) and (A.10), and the relation $U\,(\psi) = L\,(\psi)\,\hat{p}'\,(\psi) - V'\,(\psi)$ proven in Appendix B, we obtain Eq. (3.17).

Finally, notice that Eqs. (A.9), (A.10), and, therefore, Eq. (3.17) are not valid for field line tied boundary condition since $\boldsymbol{B} \cdot \boldsymbol{\nabla} \xi$ does not vanish at the equatorial plane.

Appendix B

Proof of the Relation

$$U\left(\psi\right) = L\left(\psi\right)\hat{p}'\left(\psi\right) - V'\left(\psi\right)$$

In this appendix the relationship $U\left(\psi\right) = L\left(\psi\right)\hat{p}'\left(\psi\right) - V'\left(\psi\right)$ is derived.

Using Ampere's law to express current in terms of magnetic field we find

$$\frac{1}{c}\boldsymbol{J} \times \boldsymbol{B} = \frac{1}{4\pi}\left(\boldsymbol{\nabla} \times \boldsymbol{B}\right) \times \boldsymbol{B} = \frac{B^2}{4\pi}\left[\hat{\boldsymbol{n}} \cdot \boldsymbol{\nabla}\hat{\boldsymbol{n}} - \left(\overleftrightarrow{I} - \hat{\boldsymbol{n}}\hat{\boldsymbol{n}}\right) \cdot \boldsymbol{\nabla}\ln B\right].$$

where $\hat{\boldsymbol{n}}$ is a unit vector along magnetic field and $\overleftrightarrow{I}$ is a unit tensor. Noticing that

$$\frac{1}{c}\left(\boldsymbol{J} \times \boldsymbol{B}\right) \cdot \boldsymbol{\nabla}\psi = -\frac{R^2 B^2}{4\pi}\boldsymbol{\nabla} \cdot \left(\frac{\boldsymbol{\nabla}\psi}{R^2}\right), \tag{B.1}$$

the magnetic field line curvature $\boldsymbol{\kappa} \equiv \hat{\boldsymbol{n}} \cdot \boldsymbol{\nabla}\hat{\boldsymbol{n}}$ becomes

$$\boldsymbol{\kappa} \cdot \boldsymbol{\nabla}\psi = \boldsymbol{\nabla}\psi \cdot \boldsymbol{\nabla}\ln B - R^2\boldsymbol{\nabla} \cdot \left(\frac{\boldsymbol{\nabla}\psi}{R^2}\right). \tag{B.2}$$

Rewriting

$$\frac{2\boldsymbol{\nabla}\psi \cdot \boldsymbol{\nabla}\ln B}{R^2 B^2} = -\frac{1}{w}\boldsymbol{\nabla} \cdot \left(\frac{w\boldsymbol{\nabla}\psi}{R^2 B^2}\right) + \frac{\boldsymbol{\nabla}\psi \cdot \boldsymbol{\nabla}w}{wR^2 B^2} + \frac{1}{B^2}\boldsymbol{\nabla} \cdot \left(\frac{\boldsymbol{\nabla}\psi}{R^2}\right)$$

and using $w = \left(B_0/B\right)^{2a}$ we find

111

$$2\left(1+a\right)\frac{\boldsymbol{\nabla}\psi\cdot\boldsymbol{\nabla}\ln B}{R^{2}B^{2}}=\frac{1}{B^{2}}\boldsymbol{\nabla}\cdot\left(\frac{\boldsymbol{\nabla}\psi}{R^{2}}\right)-\frac{1}{w}\boldsymbol{\nabla}\cdot\left(\frac{w\boldsymbol{\nabla}\psi}{R^{2}B^{2}}\right). \tag{B.3}$$

We may also write the force balance equation as

$$\frac{1}{c}\boldsymbol{J}\times\boldsymbol{B}=\boldsymbol{\nabla}\overleftrightarrow{P}=\boldsymbol{\nabla}p_{\perp}+\hat{\boldsymbol{n}}\boldsymbol{B}\cdot\boldsymbol{\nabla}\left(\frac{p_{\parallel}-p_{\perp}}{B}\right)+\left(p_{\parallel}-p_{\perp}\right)\hat{\boldsymbol{n}}\cdot\boldsymbol{\nabla}\hat{\boldsymbol{n}}.$$

Using Eqs. (B.1), (3.13), the definitions of σ_- and $\sigma_\perp$, and the fact that $\left(\boldsymbol{\nabla}\psi\cdot\boldsymbol{\nabla}\psi\right)=R^{2}B^{2}$ we find

$$4\pi R^{2}\left(1+2a\right)\hat{p}'\left(\psi\right)w+\sigma_{\perp}\left(\boldsymbol{\nabla}\psi\cdot\boldsymbol{\nabla}\ln B\right)+\sigma_{-}\left(\boldsymbol{\kappa}\cdot\boldsymbol{\nabla}\psi\right)$$

$$=-R^{2}\boldsymbol{\nabla}\cdot\left(\frac{\boldsymbol{\nabla}\psi}{R^{2}}\right). \tag{B.4}$$

Combining Eqs. (B.2) through (B.4) to remove the $\boldsymbol{\nabla}\psi\cdot\boldsymbol{\nabla}\ln B$ and $\boldsymbol{\nabla}\cdot\left(\boldsymbol{\nabla}\psi/R^{2}\right)$ terms we find

$$\frac{\boldsymbol{\kappa}\cdot\boldsymbol{\nabla}\psi}{R^{2}B^{2}}w\left[\frac{1-\sigma_-}{1+\sigma_\perp}\left(1+2a\right)+1\right]$$

$$=\frac{4\pi\left(1+2a\right)^{2}w^{2}\hat{p}'\left(\psi\right)}{B^{2}\left(1+\sigma_\perp\right)}-\boldsymbol{\nabla}\cdot\left(\frac{w\boldsymbol{\nabla}\psi}{R^{2}B^{2}}\right), \tag{B.5}$$

which upon field line averaging using $\oint dl/B$ gives the required expression $U\left(\psi\right)=L\left(\psi\right)\hat{p}'\left(\psi\right)-V'\left(\psi\right)$.

Appendix C

Ballooning Stability in the Mirror Mode Limit

This appendix investigates the ballooning stability of the anisotropic pressure point dipole equilibrium of Ref. [15] in the limit $\beta \to \beta_{\mathrm{mm}}$ following Newcomb's analysis of the stability of a screw pinch [46].

For $0 < \delta\beta \equiv (\beta_{\mathrm{mm}} - \beta) \to 0$ and $0 < \mu \ll 1$ the homogeneous version of the ballooning equation (3.23) can be written as

$$
\frac{\mathrm{d}^2\xi}{\mathrm{d}\,\mu^2} + \left\{ \frac{1+2a}{2\,(1+a)} \left[\lambda^* + \frac{(\alpha+2)^2\,(1+a)}{a} \right] \right.
$$
$$
\left. + \frac{2\,(2+\alpha)^2\,(1+a)^2}{4a^3\delta\beta + (2+\alpha)^2\,(1+a)^2\,(1+2a)\,\mu^2} \right\} \xi = 0. \tag{C.1}
$$

Notice that the last term in curly brackets becomes infinite at $\mu = 0$ and $\beta = \beta_{\mathrm{mm}}$. Introducing $\epsilon^2 = 4a^3\delta\beta/\left[(2+\alpha)^2\,(1+a)^2\,(1+2a)\right]$, changing variables to $t = \mu/\epsilon$, and taking the limit of small ϵ and $\lambda^* = 0$, Eq. (C.1) can be rewritten as

$$
\frac{\mathrm{d}^2\xi}{\mathrm{d}\,\mu^2} + \frac{2}{1+2a}\frac{\xi}{1+t^2} = 0. \tag{C.2}
$$

Equation (C.2) can be solved analytically to find

$$\xi(t) \ = \ C_1 \ {}_2F_1 \left[-\frac{1}{4} + d, -\frac{1}{4} - d; \frac{1}{2}; -t^2 \right]$$

$$+ C_2 \, t \, {}_2F_1 \left[\frac{1}{4} + d, \frac{1}{4} - d; \frac{3}{2}; -t^2 \right], \qquad\qquad (C.3)$$

where ${}_2F_1 [a, b; c; t]$ is a hypergeometric function, $d = \sqrt{4a^2 - 12a - 7}/(4 + 8a)$, and C_1 and C_2 are constants determined by the boundary conditions. The first term on the right hand side of Eq. (C.3) represents an even solution, while the second term represents an odd one. Solution (C.3) can be rewritten for $t \gg 1$ to obtain

$$\xi(t) \approx C_1 \left\{ (A_1 + A_2) \, t^{1/2 - 2d} \left[1 - \frac{d^2 - \frac{1}{16}}{1 + 2d} \frac{1}{t^2} \right] \right.$$

$$\left. + (B_1 + B_2) \, t^{1/2 + 2d} \left[1 - \frac{d^2 - \frac{1}{16}}{1 - 2d} \frac{1}{t^2} \right] \right\}, \qquad\qquad (C.4)$$

where

$$A_1 = \Gamma \left(\tfrac{1}{2} \right) \Gamma \left(-2d \right) / \left(\Gamma \left(-\tfrac{1}{4} - d \right) \Gamma \left(\tfrac{3}{4} - d \right) \right),$$

$$A_2 = \Gamma \left(\tfrac{1}{2} \right) \Gamma \left(2d \right) / \left(\Gamma \left(-\tfrac{1}{4} + d \right) \Gamma \left(\tfrac{3}{4} + d \right) \right),$$

$$B_1 = \Gamma \left(\tfrac{3}{2} \right) \Gamma \left(-2d \right) / \left(\Gamma \left(\tfrac{1}{4} - d \right) \Gamma \left(\tfrac{5}{4} - d \right) \right),$$

$$B_2 = \Gamma \left(\tfrac{3}{2} \right) \Gamma \left(2d \right) / \left(\Gamma \left(\tfrac{1}{4} + d \right) \Gamma \left(\tfrac{5}{4} + d \right) \right),$$

and Γ denotes a Gamma function. As d is imaginary for $a < \frac{7}{2}$, the solution (C.4) of the ballooning equation (C.2) oscillates about zero at large t (which still means small μ if $\epsilon \ll 1$). According to the Newcomb analysis [46], the existence of this oscillatory behavior implies that the ballooning modes are unstable for $a < \frac{7}{2}$ as $\beta \to \beta_{\mathrm{mm}}$.

Appendix D

Evaluation of the Second Order Solution h_2 of the Ion Gyrokinetic Equation (4.5)

This appendix describes the technique for solving Eq. (4.17). The procedure uses a variational principle and minimizes the functional $\Lambda(g)$ given by Eq. (4.18) to determine the coefficients of the trial function (4.19). As is mentioned in the text, we truncate by assuming $a_m = 0$ for $m \geq 4$ and $b_m = 0$ for $m \geq 2$. The minimization allows us to obtain a system of linear equations for the unknown coefficients a_2, a_3 and b_0, b_1, while the coefficients a_0, a_1 must be found from Eq. (4.20).

We begin by noticing that we may rewrite certain terms in Eq. (4.17) using

$$
\mathrm{i}\left(\omega - \boldsymbol{v}_d \cdot \boldsymbol{k}_\perp\right) h_1 + \hat{Q} = -f_M \left[X_2\, L_0^{(1/2)}(x) + X_3\, L_1^{(1/2)}(x) + 2X_0\, L_2^{(1/2)}(x) \right]
$$
$$
- f_M P_2\left(\frac{v_\parallel}{v}\right) x \left[\left(\frac{7}{4}X_0 + X_1\right) L_0^{(5/2)}(x) - \frac{1}{2}X_0 L_1^{(5/2)}(x) \right], \qquad \text{(D.1)}
$$

where

115

$$X_0 = \frac{1}{3}\,i\,\omega_d\, H_1 \frac{Ze\left\langle \hat{\Phi}_1 \right\rangle_\theta}{T}, \qquad X_1 = \frac{1}{3}\,i\,\omega_d\, G_1 \frac{Ze\left\langle \hat{\Phi}_1 \right\rangle_\theta}{T},$$

$$X_2 = i\left\{ (\omega - \omega_*)\,\hat{\Phi}_1 + \left[\omega_d \left(G_1 + \frac{5}{4}H_1 \right) - \omega \left(G_1 + \frac{3}{4}H_1 \right) \right] \left\langle \hat{\Phi}_1 \right\rangle_\theta \right\} \frac{Ze}{T}, \quad \text{(D.2)}$$

$$X_3 = i\left\{ \omega_*\eta\hat{\Phi}_1 + \left[\frac{1}{2}\omega H_1 - \omega_d \left(\frac{2}{3}G_1 + \frac{5}{3}H_1 \right) \right] \left\langle \hat{\Phi}_1 \right\rangle_\theta \right\} \frac{Ze}{T},$$

and $x = (Mv^2/2T)$. We suppress the index i (for ions) to simplify the notation. Substituting g from Eq.(4.19) into the functional (4.18) and using matrix elements from Appendix E we arrive at the following expression for Λ:

$$\frac{\Lambda}{N\nu_{ii}} = -\left[\frac{3}{2}a_2^2 + \frac{9}{4}a_2\,a_3 + \frac{93}{32}a_3^2 + \frac{9}{10}\frac{1}{\kappa_1^2}b_0^2 + \frac{27}{20}\frac{1}{\kappa_1^2}b_0\,b_1 + \left(\frac{315}{32}\frac{1}{\kappa_1^2} - 6 \right) b_1^2 \right]$$

$$-\frac{1}{\nu_{ii}}\left[\frac{15}{2}\left\langle X_0\right\rangle_\theta\,a_2 - 15\left\langle X_0\right\rangle_\theta\,b_1 + \frac{21}{8}\frac{\left\langle X_0/B\right\rangle_\theta}{\left\langle 1/B\right\rangle_\theta}b_0 + \frac{99}{8}\frac{\left\langle X_0/B\right\rangle_\theta}{\left\langle 1/B\right\rangle_\theta}b_1 \right. \qquad \text{(D.3)}$$

$$\left. +\frac{3}{2}\frac{\left\langle X_1/B\right\rangle_\theta}{\left\langle 1/B\right\rangle_\theta}b_0 - 3\frac{\left\langle X_2/B\right\rangle_\theta}{\left\langle 1/B\right\rangle_\theta}b_0 - 3\frac{\left\langle X_2/B\right\rangle_\theta}{\left\langle 1/B\right\rangle_\theta}b_1 + 3\frac{\left\langle X_3/B\right\rangle_\theta}{\left\langle 1/B\right\rangle_\theta}b_0 - \frac{9}{2}\frac{\left\langle X_3/B\right\rangle_\theta}{\left\langle 1/B\right\rangle_\theta}b_1 \right],$$

with $\kappa_1^2 \equiv \left\langle 1/B^2\right\rangle_\theta / \left\langle 1/B\right\rangle_\theta^2$ and $\nu_{ii} = \left(4\sqrt{\pi}Z_i^4 e^4 N_i \ln\Lambda/3M_i^{1/2}T_i^{3/2} \right)$ the ion-ion collision frequency. Finding an extremum of the above expression with respect to a_2, a_3, b_0, b_1 we obtain a system of four linear equations for these coefficients, which may be solved to find

$$a_2 = \frac{155}{44}\frac{\left\langle X_0\right\rangle_\theta}{\nu_{ii}}, \qquad a_3 = \frac{15}{11}\frac{\left\langle X_0\right\rangle_\theta}{\nu_{ii}}, \qquad \text{(D.4)}$$

$$b_0 = -\frac{1}{\nu_{ii}}\frac{5}{9\kappa_1^2}\left[\frac{21}{8}\frac{\left\langle X_0/B\right\rangle_\theta}{\left\langle 1/B\right\rangle_\theta} + \frac{3}{2}\frac{\left\langle X_1/B\right\rangle_\theta}{\left\langle 1/B\right\rangle_\theta} - 3\frac{\left\langle X_2/B\right\rangle_\theta}{\left\langle 1/B\right\rangle_\theta} + 3\frac{\left\langle X_3/B\right\rangle_\theta}{\left\langle 1/B\right\rangle_\theta} \right]$$

$$-\frac{1}{\nu_{ii}}\frac{15}{16}\frac{1}{249\kappa_1^2 - 160}\left[160\left\langle X_0\right\rangle_\theta - 111\frac{\left\langle X_0/B\right\rangle_\theta}{\left\langle 1/B\right\rangle_\theta} + 12\frac{\left\langle X_1/B\right\rangle_\theta}{\left\langle 1/B\right\rangle_\theta} \right. \qquad \text{(D.5)}$$

$$\left. +8\frac{\left\langle X_2/B\right\rangle_\theta}{\left\langle 1/B\right\rangle_\theta} + 72\frac{\left\langle X_3/B\right\rangle_\theta}{\left\langle 1/B\right\rangle_\theta} \right],$$

and

$$b_1 = \frac{1}{\nu_{ii}} \frac{5}{4} \frac{1}{249\kappa_1^2 - 160} \left[160 \langle X_0 \rangle_\theta - 111 \frac{\langle X_0/B \rangle_\theta}{\langle 1/B \rangle_\theta} + 12 \frac{\langle X_1/B \rangle_\theta}{\langle 1/B \rangle_\theta} \right.$$
$$\left. + 8 \frac{\langle X_2/B \rangle_\theta}{\langle 1/B \rangle_\theta} + 72 \frac{\langle X_3/B \rangle_\theta}{\langle 1/B \rangle_\theta} \right]. \tag{D.6}$$

We notice that Λ is independent of a_0, a_1. These coefficients must be found from constraint (4.20), which can be evaluated to give

$$a_0 = \frac{20\, a_2 - (9\,\kappa_2 - 10)\, [3\, b_0\, (\lambda - 1) - 7\, b_1]}{4\, (3\, \lambda^2 - 10\lambda - 5)}, \tag{D.7}$$

and

$$a_1 = \frac{(9\,\kappa_2 - 10)\, [2\, b_0\, (2\,\lambda - 1) - 7\, b_1\, (\lambda - 1)] - 20\, a_2\, (\lambda - 1)}{4\, (3\, \lambda^2 - 10\lambda - 5)}, \tag{D.8}$$

where $\lambda \equiv \omega / \langle \omega_d \rangle_\theta$ and $\kappa_2 \equiv (\langle \omega_d/B \rangle_\theta / \langle \omega_d \rangle_\theta \langle 1/B \rangle_\theta)$.

Appendix E

Matrix Elements of the Linearized Fokker-Planck Ion-Ion Collision Operator

To obtain the matrix elements it is convenient to use the Landau form of the linearized collision operator C_{1ii}, namely

$$C_{1ii}(f_{1i}) = \nabla_v \cdot \left(\gamma f_{Mi} \int d^3 v' f'_{Mi} Q \cdot (\nabla_v g - \nabla_{v'} g') \right), \tag{E.1}$$

where $g = f_{1i}/f_{Mi}$, $\gamma = 2\pi Z_i^4 e^4 \ln \Lambda / M_i^2$, $\ln \Lambda$ is the Coulomb logarithm, $Q = w^{-3}(w^2 I - ww) = \nabla_w \nabla_w w$ with $w = v - v'$, $w = |w|$, and f'_{Mi} and g' are the functions f_{Mi} and g with v replaced by v'.

It is then convenient to define the following matrix elements:

$$H_{mm'}\left(\frac{1}{2},\frac{1}{2}\right) \equiv \int d^3 v \, L_m^{(1/2)}(x) \, C_{1ii}\left\{ L_{m'}^{(1/2)}(x) \, f_{Mi}(x) \right\}, \tag{E.2}$$

$$H_{mm'}\left(\frac{1}{2},\frac{5}{2}\perp\right) \equiv \int d^3 v \, L_m^{(1/2)}(x) \, C_{1ii}\left\{ x_\perp L_{m'}^{(5/2)}(x) \, f_{Mi}(x) \right\}, \tag{E.3}$$

$$H_{mm'}\left(\frac{1}{2},\frac{5}{2}\right) \equiv \int d^3 v \, L_m^{(1/2)}(x) \, C_{1ii}\left\{ x L_{m'}^{(5/2)}(x) \, f_{Mi}(x) \right\}, \tag{E.4}$$

$$H_{mm'}\left(\frac{5}{2}, \frac{5}{2}\right) \equiv \int d^3v\, x\, L_m^{(5/2)}\left(x\right) C_{1ii}\left\{x\, L_{m'}^{(5/2)}\left(x\right) f_{Mi}\left(x\right)\right\}, \tag{E.5}$$

$$H_{mm'}\left(\frac{5}{2}, \frac{5}{2}\perp\right) \equiv \int d^3v\, x\, L_m^{(5/2)}\left(x\right) C_{1ii}\left\{x_\perp\, L_{m'}^{(5/2)}\left(x\right) f_{Mi}\left(x\right)\right\}, \tag{E.6}$$

and

$$H_{mm'}\left(\frac{5}{2}\perp, \frac{5}{2}\perp\right) \equiv \int d^3v\, x_\perp L_m^{(5/2)}\left(x\right) C_{1ii}\left\{x_\perp L_{m'}^{(5/2)}\left(x\right) f_{Mi}\left(x\right)\right\}, \tag{E.7}$$

where $L_m^{(n+1/2)}\left(x\right)$ are generalized Laguerre polynomials, $x = M_i v^2/2T_i$, and $x_\perp = M_i v_\perp^2/2T_i$. The linearized collision operator C_{1ii} is self-adjoint so that

$$H_{mm'}\left(i_1, i_2\right) = H_{mm'}\left(i_2, i_1\right) \tag{E.8}$$

for arbitrary i_1, i_2.

The technique for calculating the necessary matrix elements is well known and was described in detail in Ref. [69], although some of the matrix elements given there were calculated incorrectly. The procedure is to evaluate the integrals of the form (E.2)-(E.7) by replacing the Laguerre polynomials by the functions

$$F \equiv (1-\xi)^{-\frac{2n+3}{2}} \exp\left(-\frac{x\,\xi}{1-\xi}\right) = \sum_{m=0}^{\infty} \xi^m L_m^{(n+1/2)}\left(x\right) \tag{E.9}$$

and

$$G \equiv (1-\eta)^{-\frac{2n'+3}{2}} \exp\left(-\frac{x\,\eta}{1-\eta}\right) = \sum_{m'=0}^{\infty} \eta^{m'} L_{m'}^{(n'+1/2)}\left(x\right). \tag{E.10}$$

The expressions obtained are then expanded in Taylor series in ξ and η and the required matrix elements are identified using expressions (E.9) and (E.10).

After some extremely tedious algebra it is possible to obtain

$$\sum_{m,\,m'=0}^{\infty} \xi^m \, \eta^{m'} \, H_{mm'} \left(\frac{1}{2}, \frac{1}{2} \right) = -\frac{3}{2} N_i \nu_{ii} \, \frac{\xi^2 \, \eta^2}{(1 - \xi\,\eta) \left(1 - \frac{\xi+\eta}{2} \right)^{3/2}}, \qquad \text{(E.11)}$$

so that

$$H_{mm'} \left(\frac{1}{2}, \frac{1}{2} \right) = -\frac{3}{2} N_i \nu_{ii} \begin{pmatrix} 0 & 0 & 0 & 0 & 0 & \vdots \\ 0 & 0 & 0 & 0 & 0 & \vdots \\ 0 & 0 & 1 & \frac{3}{4} & \frac{15}{32} & \vdots \\ 0 & 0 & \frac{3}{4} & \frac{31}{16} & \frac{201}{128} & \vdots \\ 0 & 0 & \frac{15}{32} & \frac{201}{128} & \frac{2929}{1024} & \vdots \\ & & \cdots\cdots\cdots\cdots\cdots\cdots\cdots & & \end{pmatrix}. \qquad \text{(E.12)}$$

In a similar way,

$$\sum_{m,\,m'=0}^{\infty} \xi^m \, \eta^{m'} \, H_{mm'} \left(\frac{1}{2}, \frac{5}{2} \perp \right) = 2 N_i \nu_{ii} \, \frac{\xi^2 \, \eta}{(1 - \xi\,\eta)^2 \, (1 - \eta) \left(1 - \frac{\xi+\eta}{2} \right)^{5/2}} \times$$
$$\left(1 - \frac{1}{2}\xi - \frac{15}{8}\eta + \frac{3}{8}\xi\eta + \frac{1}{2}\eta^2 + \frac{9}{8}\xi\eta^2 + \frac{1}{4}\xi^2\eta - \frac{5}{8}\xi^2\eta^2 - \frac{1}{4}\xi\eta^3 \right), \qquad \text{(E.13)}$$

gives

$$H_{mm'} \left(\frac{1}{2}, \frac{5}{2} \perp \right) = 2 N_i \nu_{ii} \begin{pmatrix} 0 & 0 & 0 & 0 & 0 & \vdots \\ 0 & 0 & 0 & 0 & 0 & \vdots \\ 0 & 1 & \frac{3}{8} & -\frac{3}{8} & -\frac{251}{256} & \vdots \\ 0 & \frac{3}{4} & \frac{75}{32} & \frac{9}{8} & -\frac{495}{1024} & \vdots \\ 0 & \frac{15}{32} & \frac{513}{256} & \frac{1073}{256} & \frac{19383}{8192} & \vdots \\ & & \cdots\cdots\cdots\cdots\cdots\cdots\cdots & & \end{pmatrix}; \qquad \text{(E.14)}$$

121

$$\sum_{m,\,m'=0}^{\infty} \xi^m\,\eta^{m'}\,H_{mm'}\left(\frac{5}{2},\frac{5}{2}\right) = -6N_i\nu_{ii}\,\frac{\xi\,\eta}{(1-\xi)\,(1-\eta)\,(1-\xi\,\eta)^3}\,\times$$

$$\frac{1}{64\left(1-\frac{\xi+\eta}{2}\right)^{7/2}}\Bigg[64 + 311\,\xi\,\eta - 291\,\xi^2\,\eta^2 + 41\,\xi^3\,\eta^3 + 35\,\xi^4\,\eta^4$$

$$-\,(\xi+\eta)\left(152 + 67\,\xi\,\eta - 178\,\xi^2\,\eta^2 + 79\,\xi^3\,\eta^3\right)$$

$$+\left(\xi^2+\eta^2\right)\left(92 - 50\,\xi\,\eta - 4\,\xi^2\,\eta^2 + 10\,\xi^3\,\eta^3\right)$$

$$-\left(\xi^3+\eta^3\right)\left(16 - 12\,\xi\,\eta + 4\,\xi^2\,\eta^2\right)\Bigg], \qquad\qquad \text{(E.15)}$$

gives

$$H_{mm'}\left(\frac{5}{2},\frac{5}{2}\right) = -6N_i\nu_{ii}\begin{pmatrix} 0 & 0 & 0 & 0 & 0 & \vdots \\ 0 & 1 & \frac{3}{8} & -\frac{3}{8} & -\frac{251}{256} & \vdots \\ 0 & \frac{3}{8} & \frac{207}{64} & \frac{63}{32} & \frac{21}{2048} & \vdots \\ 0 & -\frac{3}{8} & \frac{63}{32} & \frac{1001}{128} & \frac{2985}{512} & \vdots \\ 0 & -\frac{251}{256} & \frac{21}{2048} & \frac{2985}{512} & \frac{1038919}{65536} & \vdots \\ & & \cdots\cdots\cdots\cdots\cdots & & \end{pmatrix}; \qquad \text{(E.16)}$$

and

$$\sum_{m,\,m'=0}^{\infty} \xi^m\,\eta^{m'}\,H_{mm'}\left(\frac{5}{2}\perp,\frac{5}{2}\perp\right) = -\frac{2}{5}N_i\nu_{ii}\,\frac{1}{(1-\xi)\,(1-\eta)\,(1-\xi\,\eta)^3}\,\times$$

$$\frac{1}{8\left(1-\frac{\xi+\eta}{2}\right)^{7/2}}\Bigg[8 + 84\,\xi\,\eta + 255\,\xi^2\,\eta^2 - 255\,\xi^3\,\eta^3 + 37\,\xi^4\,\eta^4 + 31\xi^5\eta^5$$

$$-\,(\xi+\eta)\left(16 + 142\,\xi\,\eta + 43\,\xi^2\,\eta^2 - 149\,\xi^3\,\eta^3 + 68\xi^4\eta^4\right)$$

$$+\left(\xi^2+\eta^2\right)\left(10 + 76\,\xi\,\eta - 44\,\xi^2\,\eta^2 - 2\,\xi^3\,\eta^3 + 8\xi^4\eta^4\right)$$

$$-\left(\xi^3+\eta^3\right)\left(2 + 12\,\xi\,\eta - 9\,\xi^2\,\eta^2 + 3\xi^3\eta^3\right)\Bigg], \qquad\qquad \text{(E.17)}$$

gives

$$H_{mm'}\left(\frac{5}{2}\perp,\frac{5}{2}\perp\right) = -\frac{2}{5}N_i\nu_{ii}\begin{pmatrix} 1 & \frac{3}{4} & \frac{15}{32} & \frac{35}{128} & \vdots \\ \frac{3}{4} & \frac{175}{16} & \frac{809}{128} & \frac{155}{512} & \vdots \\ \frac{15}{32} & \frac{809}{128} & \frac{33969}{1024} & \frac{98889}{4096} & \vdots \\ \frac{35}{128} & \frac{155}{512} & \frac{98889}{4096} & \frac{1260999}{16384} & \vdots \\ & \cdots\cdots\cdots\cdots\cdots\cdots\cdots & & \end{pmatrix}. \tag{E.18}$$

Finally, notice from the definitions (E.3) - (E.6) that

$$
\begin{aligned}
H_{mm'}\left(\frac{1}{2},\frac{5}{2}\right) &= \frac{3}{2}H_{mm'}\left(\frac{1}{2},\frac{5}{2}\perp\right), \\
H_{mm'}\left(\frac{5}{2},\frac{5}{2}\perp\right) &= \frac{2}{3}H_{mm'}\left(\frac{5}{2},\frac{5}{2}\right).
\end{aligned} \tag{E.19}
$$

A generating function for matrix elements $H_{mm'}(1/2,1/2)$ can also be found in Ref. [70].

Appendix F

Coefficients c_0 to c_3 in the Electrostatic Dispersion Relation (4.26)

This appendix gives the most general form of the coefficients c_0 to c_3 that appear in the dispersion relation (4.26):

$$c_0(d, \eta) = \frac{25}{3168} \frac{d}{\kappa_1^2 \left(249 \, \kappa_1^2 - 160\right)} \left[20584 \, \kappa_1^4 \, \frac{3\,\eta - 2}{1 + \eta} + 704 \left(9 \, \kappa_2 - 10\right)^2 \right. \quad \text{(F.1)}$$

$$\left. -\kappa_1^2 \frac{\eta \left(31185\kappa_2^2 - 69300\kappa_2 + 78180\right) + 110187\kappa_2^2 - 244860\kappa_2 + 109580}{1 + \eta} \right],$$

$$c_1(d, \eta) = \frac{5}{3168} \frac{1}{\kappa_1^2 \left(249 \, \kappa_1^2 - 160\right)} \times$$

$$\left\{ 205840\kappa_1^4 - 3520 \left(9\kappa_2 - 10\right)^2 + \left(550935\kappa_2^2 - 1224300\kappa_2 + 547900\right) \kappa_1^2 \right. \quad \text{(F.2)}$$

$$+ \frac{d}{1 + \eta} \left[\left(785862\kappa_2^2 - 1746360\kappa_2 + 970200\right) \kappa_1^2 - 7040 \left(9\kappa_2 - 10\right)^2 \right.$$

$$\left. \left. -\eta \left(308760\kappa_1^4 - 3 \left(376299\kappa_2^2 - 836220\kappa_2 + 530700\right) \kappa_1^2 + 10560 \left(9\kappa_2 - 10\right)^2\right) \right] \right\},$$

125

$$c_2\left(d,\eta\right) = -\frac{5}{288}\frac{\left(9\kappa_2-10\right)^2}{\kappa_1^2\left(249\,\kappa_1^2-160\right)}\left[882\kappa_1^2-640\right.$$

$$\left.+d\,\frac{8\,\eta\,\left(147\kappa_1^2-80\right)+525\kappa_1^2-320}{1+\eta}\right], \tag{F.3}$$

and

$$c_3 = \frac{25}{288}\frac{\left(105\kappa_1^2-64\right)\left(9\kappa_2-10\right)^2}{\kappa_1^2\left(249\,\kappa_1^2-160\right)}, \tag{F.4}$$

where the definitions of d, η, κ_1, and κ_2 are given in Sec. 4.3.

Our theory is valid for any axially symmetric plasma confined in a magnetic field with closed lines, in particular for a Z-pinch and for the point dipole of Ref. [1]. The difference between these two cases manifests itself in the values of κ_1 and κ_2 and, consequently, of the coefficients c_0 to c_3. So, for the Z-pinch $\kappa_1 = \kappa_2 = 1$ and $c_3^{pinch} = 0.04$, while for the point dipole $\kappa_1 = 1.079$, $\kappa_2 = 7/6$ and $c_3^{dipole} = 0.0084 \ll c_3^{pinch}$. As the coefficient c_3 is particularly important for the MHD-like mode and in determining the coupling between the MHD-like and the entropy modes, we see that the two cases can be rather different.

Appendix G

Understanding the Influence of the Gyro-relaxation Effects on the Entropy Mode Stability

In this appendix we describe destabilization of the entropy mode by the gyro-relaxation process in terms of the small amplitude mode energy and power dissipated by the these processes. It is well known (see for example Refs. [59, 60, 61]) that if the mode has negative energy, that is, if the energy of the system in the presence of the mode is smaller than the energy without the mode, then dissipation can drive the mode unstable by taking energy from the system to make the mode grow. Similarly, a positive energy mode can be driven unstable by supplying energy (inverse dissipation). We follow the formalism of Ref. [61] which, strictly speaking, is valid only for the case of spatially homogeneous and time-independent equilibria. However, it is clear that such formalism can be also applied to the case of Z-pinch where $\boldsymbol{B} \cdot \boldsymbol{\nabla}|\boldsymbol{B}| = 0$. From the entropy mode point of view, the Z-pinch is quite similar to the magnetic dipole as seen by comparing Figs. 4-1 and G-1 (the reason for the signs in Fig. G-1 will be explained shortly). Consequently, in this appendix we consider a Z-pinch to demonstrate all the physics behind the phenomenon. For simplicity we assume $\tau = 1$.

As follows from Ref. [61], the energy density of the small amplitude mode can be found from the following expression
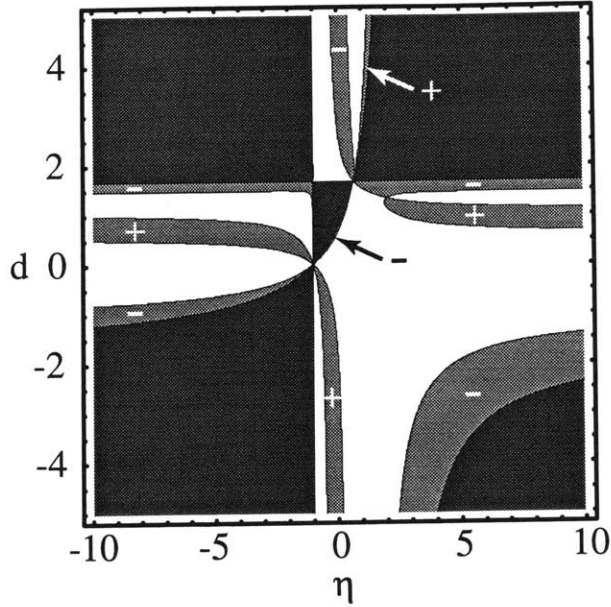
Figure G-1: Same as in Figure 4-1, but for a Z-pinch equilibrium with $\tau = 1$. The "+" sign denotes unstable regions due to gyro-relaxation effects on the entropy mode with positive energy, while the "-" sign indicates similar regions with negative energy.

$$w = \frac{k_\zeta^2 |\Phi_1|^2}{16\pi} \left(\lambda \frac{\partial \chi_{\zeta\zeta}^h}{\partial \lambda} \right) \Big|_{\lambda_\pm}, \qquad (G.1)$$

while the dissipated power density can be conveniently evaluated using the equation

$$p = \frac{k_\zeta^2 |\Phi_1|^2}{8\pi} \left(-i\lambda \chi_{\zeta\zeta}^a \right) \Big|_{\lambda_\pm}, \qquad (G.2)$$

where $\chi_{\zeta\zeta}^h$ and $\chi_{\zeta\zeta}^a$ are the ζ, ζ components of the Hermitian and anti-Hermitian parts of the susceptibility tensor defined by the equation

$$\sum_{j=i,e} Z_j e N_{1j} = -\frac{1}{4\pi} \left(\boldsymbol{k}_\perp \cdot \overset{\leftrightarrow}{\chi} \cdot \boldsymbol{k}_\perp \right) \Phi_1, \qquad (G.3)$$

with $\boldsymbol{k}_\perp \approx \boldsymbol{k}_\zeta$, and the expressions in the parenthesis in Eqs. (G.1) and (G.2) must be evaluated at the entropy mode frequencies

$$\lambda_\pm = \pm\sqrt{\frac{5}{9}\frac{d\frac{3\eta-7}{1+\eta}+5}{\frac{5}{3}-d}} \qquad (G.4)$$

(recall Eq. (4.28) at $\tau = 1$).

Using the Z-pinch limit of the perturbed particle densities N_{1j}, Eq. (G.3) and neglecting the FLR terms it is easy to obtain the expression for the required component of the susceptibility tensor:

$$\chi_{\zeta\zeta} = \frac{2}{k_\zeta^2\lambda_D^2}\left[1 - \frac{1}{2}\left(G_{1i} + \frac{3}{4}H_{1i} + G_{1e} + \frac{3}{4}H_{1e}\right) - \frac{a_0}{2N}\frac{T}{e\hat{\Phi}_1}\right], \qquad (G.5)$$

with $\lambda_D \equiv (T/4\pi e^2 N)^{1/2}$ Debye length, T and N equilibrium temperature and density (the same for both electrons and ions), and G_{1j}, H_{1j}, $j = e, i$, and a_0 given in Sec. 4.2 and Appendix D, correspondingly. Rewriting Eq. (G.5) in terms of λ, d and η we can obtain

$$\chi_{\zeta\zeta}^h = \frac{2}{k_\zeta^2\lambda_D^2}\frac{\left(d - \frac{5}{3}\right)\lambda^2 + \frac{5}{9}\left(d\frac{3\eta-7}{1+\eta}+5\right)}{\lambda^4 - \frac{70}{9}\lambda^2 + \frac{25}{9}} \qquad (G.6)$$

and

$$-\mathrm{i}\chi_{\zeta\zeta}^a = \frac{2}{k_\zeta^2\lambda_D^2}\frac{\omega_{di}}{\nu_{ii}}\frac{c_3\lambda^3 + c_2\left(d,\eta\right)\lambda^2 + c_1\left(d,\eta\right)\lambda + c_0\left(d,\eta\right)}{\left(\lambda^2 - \frac{10}{3}\lambda + \frac{5}{3}\right)^2}, \qquad (G.7)$$

where c_0 to c_3 are given in Appendix F and must be evaluated at $\kappa_1 = \kappa_2 = 1$.

Using expression (G.6) in Eq. (G.1) we calculate the mode energy density w throughout the parametric space d, η and indicate only its sign in Fig. G-2. The regions with $w > 0$ (positive energy mode) are shown in white while those with $w < 0$ (negative energy mode) are shown in gray. The black regions indicate the unstable regions of the entropy mode in the absence of gyro-relaxation effects where the weak growth theory described does not apply. Notice, that as $\chi_{\zeta\zeta}^h$ contains only even powers of λ, w has the same sign for both stable branches, λ_+ and λ_-, of the entropy mode.

Substituting $-\mathrm{i}\chi_{\zeta\zeta}^a$ from Eq. (G.7) into Eq. (G.2) we calculate the sign of the
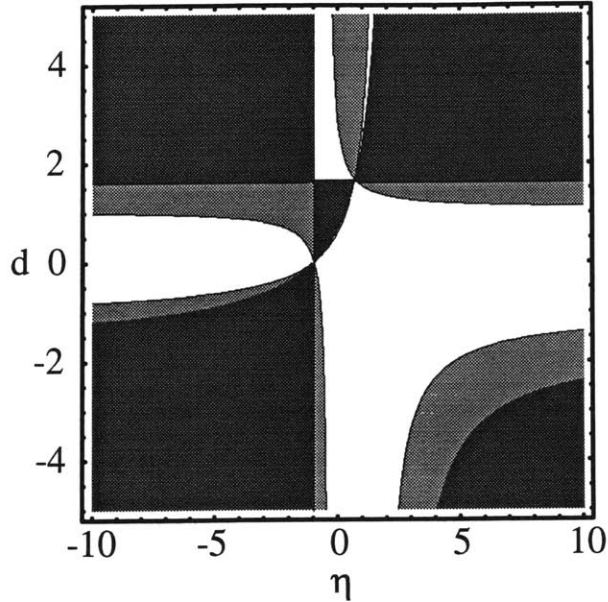
Figure G-2: Regions of positive (white) and negative (gray) small amplitude mode energy density for the entropy mode for a Z-pinch equilibrium with $\tau = 1$. The black regions are unstable in the absence of gyro-relaxation as in Figures 4-1 - 4-4 and G-1.

dissipated power density p and show it in Figs. G-3 and G-3 for λ_+ and λ_-, correspondingly. White shows the regions with $p > 0$ (positive energy dissipation), gray those with $p < 0$ (negative energy dissipation), and black the instability regions for the entropy mode without gyro-relaxation effects.

It follows from Figs. G-1, G-2, G-3 and G-4 that the instability regions due to gyro-relaxation effects (gray regions of Fig. G-1) correspond to the overlapping gray regions of Fig. G-2 (negative energy mode) and white regions of Fig. G-4 (positive energy dissipation) and, conversely, the white regions of Fig. G-2 (positive energy mode) and gray regions of Fig. G-4 (negative energy dissipation). Consequently, gyro-relaxation effects drive both positive and negative energy modes unstable depending upon whether they provide inverse dissipation or dissipation. Following this observation, we mark the gray regions of Fig. G-1 with "+" or "-" according to the sign of w and to indicate whether the regions correspond to positive or negative energy waves, respectively. Notice, that only the λ_- branch of the entropy mode (Fig. G-4)
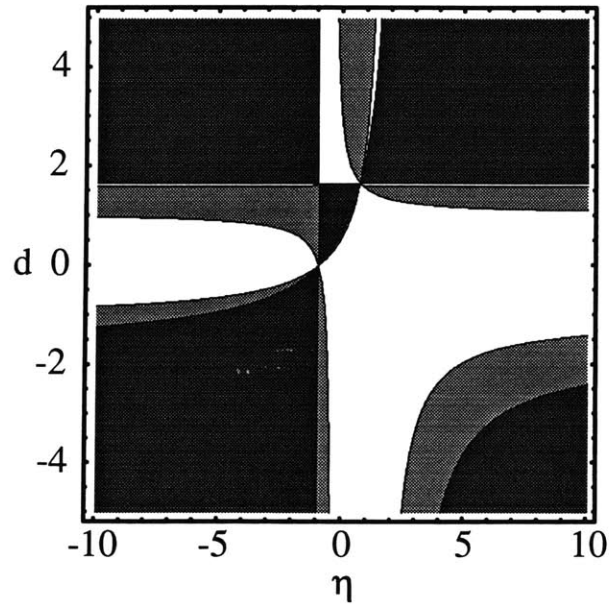
Figure G-3: Power dissipated by the gyro-relaxation effects for the λ_+ branch of the entropy mode for a Z-pinch equilibrium with $\tau = 1$. White (gray) indicates regions of positive (negative) dissipation. Black again indicates unstable regions without gyro-relaxation.
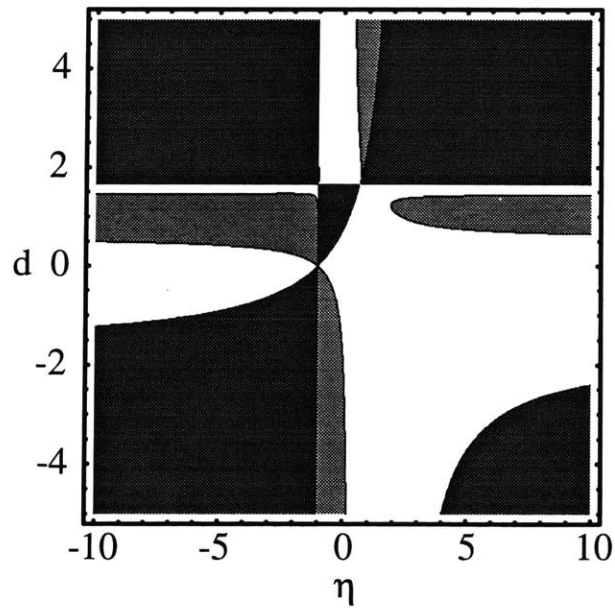

Figure G-4: Same as in Figure G-3, but for the λ_- branch of the entropy mode.

propagating toroidally in the direction of the electron magnetic drift becomes unstable and not the λ_+ branch (Fig. G-3) propagating in the ion magnetic drift direction.

Appendix H

Flute Character of the Entropy Mode and MHD Mode Near Marginal Stability Boundary

This appendix gives a proof that the only solution of Eq. (5.45) with the order b_i terms neglected (the entropy mode case) or the leading order solution with the order b_i terms assumed small (the MHD mode case and the coupled mode case with d near 5/3) is a flute except perhaps on some special flux surfaces.

We begin by writing Eq. (5.45) with the $O(b_i)$ terms neglected in the form

$$
\frac{\rho_i^2 V_A^2}{2} \boldsymbol{B} \cdot \boldsymbol{\nabla} \left(\frac{\ell^2}{R^2 B^2} \boldsymbol{B} \cdot \boldsymbol{\nabla} \tilde{\Psi}_i \right) = \omega_{*i} \left(1 + \eta \right) C \left(\frac{\left\langle C \tilde{\Psi}_i \right\rangle_\theta}{\left\langle C \right\rangle_\theta} - \tilde{\Psi}_i \right), \qquad \text{(H.1)}
$$

where we take into account the fact that $\Gamma = d$ for the entropy mode and $\Gamma \approx 5/3 \approx d$ for the MHD and "coupled" modes with d near 5/3 (for these modes $\lambda \gg 1$ and $\lim_{\lambda \to \infty} \Gamma = 5/3$). In Eq. (H.1), C is defined as

$$
C \equiv \omega_{*i} \left(1 + \eta \right) \beta + 2 \omega_{di} = \frac{c \ell T_i}{Z_i e R^2 B^2} \left(\boldsymbol{\kappa} \cdot \boldsymbol{\nabla} \psi \right) > 0,
$$

where we use Eqs. (5.29) and (5.34) to obtain the last equality, assume the toroidal

mode number $\ell > 0$ (since the right hand side of Eq. (H.1) is independent of the sign of ℓ) and take into account that $(\boldsymbol{\kappa} \cdot \boldsymbol{\nabla} \psi) > 0$ for a dipolar magnetic field.

First, we notice that a flute is a solution of Eq. (H.1). Next, we show that it is *the only* solution by multiplying Eq. (H.1) by $\tilde{\Psi}_i$, averaging along a magnetic field line, and integrating the term on the left hand side by parts to obtain the following equation:

$$\frac{\rho_i^2 V_A^2}{2} \left\langle \frac{\ell}{R^2 B^2} \left(\boldsymbol{B} \cdot \boldsymbol{\nabla} \tilde{\Psi}_i \right)^2 \right\rangle_\theta + \omega_{*i} \left(1 + \eta \right) \left(\frac{\left\langle C \tilde{\Psi}_i \right\rangle_\theta^2}{\langle C \rangle_\theta} - \left\langle C \tilde{\Psi}_i^2 \right\rangle_\theta \right) = 0. \quad \text{(H.3)}$$

The expression in the parenthesis can be shown to be non-positive by a Schwartz inequality and the sign of $\omega_{*i} \left(1 + \eta \right)$ coincides with the sign of $dp/d\psi$. Consequently, in regions with $dp/d\psi < 0$ (for example, in the region near the levitated ring in LDX) both terms are non-negative and the equality can be satisfied only if $\tilde{\Psi}_i = \left\langle \tilde{\Psi}_i \right\rangle_\theta$.

In regions with $dp/d\psi > 0$ (for example, in the outer region of the LDX), on the other hand, the second term in Eq. (H.3) is negative and so we cannot easily conclude from this equation that the mode is a flute. In order to see that the flute is still the only solution of Eq. (H.1) in such regions we introduce the new function

$$\Xi \equiv \frac{\left\langle C \tilde{\Psi}_i \right\rangle_\theta}{\langle C \rangle_\theta} - \tilde{\Psi}_i, \quad \text{(H.4)}$$

so that

$$\langle C \Xi \rangle_\theta = 0, \quad \text{(H.5)}$$

and rewrite Eq. (H.1) in the form

$$\frac{\rho_i^2 V_A^2}{2} \boldsymbol{B} \cdot \boldsymbol{\nabla} \left(\frac{\ell^2}{R^2 B^2} \boldsymbol{B} \cdot \boldsymbol{\nabla} \Xi \right) = \omega_{*i} \left(1 + \eta \right) C \Xi. \quad \text{(H.6)}$$

As $\tilde{\Psi}_i$ is periodic in poloidal angle, Ξ is periodic as well.

The system of equations (H.5) and (H.6) is equivalent to Eq. (H.1) (except that

134

Ξ a constant is not a solution of Eq. (H.6)). Equation (H.6) together with periodic boundary conditions represents a Sturm-Liouville problem with the eigenvalue $\omega_{*i}(1+\eta)$ which depends on ψ. As a result, this problem has a solution only for special values of $\omega_{*i}(1+\eta)$, that is only on special flux surfaces. Equation (H.5) places additional constraint on these solutions so that some or all of them may have to be discarded.

Consequently, the system of equations (H.5) and (H.6) may have solutions only on some special flux surfaces, so that the only solution of Eq. (H.1) is a flute except on these flux surfaces.

Bibliography

[1] S.I. Krasheninnikov, P.J. Catto, and R.D. Hazeltine. *Phys. Rev. Lett.*, 82:2689, 1999.

[2] M. Kallenrode. *Space Physics: An Introduction to Plasmas and Particles in the Heliosphere and Magnetospheres.* Springer-Verlag, Berlin, 1998.

[3] J. Lemaire and M.J. Rycroft. *Advances in Space Research*, volume 2. Pergamon Press, Oxford, 1982.

[4] J.R. Ferron, A.Y. Wong, G. Dimonte, and B.J. Leikind. *Phys. Fluids*, 26:2227, 1983.

[5] H.P. Warren and M.E. Mauel. *Phys. Plasmas*, 2:4185, 1995.

[6] M.N. Rosenbluth and C.L. Longmire. *Ann. Phys.*, 1:120, 1957.

[7] M. Schulz and L.J. Lanzerotti. *Particle Diffusion in the Radiation Belts, Physics and Chemistry in Space*, volume 7. Springer-Verlag, Berlin, 1974.

[8] A. Hasegawa. *Comments Plasma Phys. Control. Fusion*, 1:147, 1987.

[9] J. Kesner, L. Bromberg, M.E. Mauel, and D. Garnier. In *17th IAEA Fusion Energy Conference*, number IAEA-F1-CN-69/ICP/09, Yokahama, Japan, 1999. International Atomic Energy Agency, Vienna.

[10] B. Coppi. *Phys. Rev. Lett.*, 22:50, 1969.

[11] B. Coppi, G. Laval, R. Pellat, and M.N. Rosenbluth. *Plasma Phys.*, 10:1, 1968.

[12] B. Coppi. *Ann. Phys.*, 30:178, 1964.

[13] B. Coppi, J.M. Green, and J.L. Johnson. *Nucl. Fusion*, 6:101, 1966.

[14] R.L. McNutt Jr., P.S. Coppi, R.S. Selesnick, and B. Coppi. *J. Geophys. Res.*, 92:4377, 1987.

[15] S.I. Krasheninnikov and P.J. Catto. *Phys. Plasmas*, 7:626, 2000.

[16] C. Mercier and M. Cotsaftis. *Nucl. Fusion*, 1:121, 1961.

[17] J. B. Taylor and R. J. Hastie. *Phys. Fluids*, 8:323, 1965.

[18] I. B. Bernstein, E. A. Frieman, M. D. Kruskal, and R. M. Kulsrud. *Proc. R. Soc. London*, 244:17, 1958.

[19] D.T. Garnier, J. Kesner, and M.E. Mauel. *Phys. Plasmas*, 6:3431, 1999.

[20] A.N. Simakov, P.J. Catto, S.I. Krasheninnikov, and J.J. Ramos. *Phys. Plasmas*, 7:2526, 2000.

[21] J. Kesner, A.N. Simakov, D.T. Garnier, P.J. Catto, R.J. Hastie, S.I. Krasheninnikov, M.E. Mauel, T. Sunn Pedersen, and J.J. Ramos. *Nucl. Fusion*, 41:301, 2001.

[22] M. Velli and A.W. Hood. *Solar Phys.*, 106:353, 1986.

[23] M. Velli and A.W. Hood. *Solar Phys.*, 109:351, 1987.

[24] B.B. Kadomtsev. *Reviews of Plasma Physics edited by M.A. Leontovich*, volume 2, page 170. Consultants Bureau, New York, 1965.

[25] L. Chen and A. Hasegawa. *J. Geophys. Res.*, 96:1503, 1991.

[26] A.A. Chan, M. Xia, and L. Chen. *J. Geophys. Res.*, 99:17351, 1994.

[27] A.N. Simakov, R.J. Hastie, and P.J. Catto. *Phys. Plasmas*, 7:3309, 2000.

[28] M.D. Kruskal and C.R. Oberman. *Phys. Fluids*, 1:275, 1958.

[29] G.F. Chew, M.L. Goldberger, and F.E. Low. *Proc. R. Soc. London*, 236:112, 1956.

[30] A.W. Hood. *Solar Phys.*, 103:329, 1986.

[31] J. Kesner. *Phys. Plasmas*, 5:3675, 1998.

[32] W. Horton, H.V. Wong, and J.W. Van Dam. *J. Geophys. Res.*, 104:22745, 1999.

[33] J. Kesner. *Phys. Plasmas*, 7:3837, 2000.

[34] B. Coppi. *Princeton Plasma Physics Laboratory Report No. MATT-649 (unpublished)*, 1968.

[35] A.N. Simakov, P.J. Catto, and R.J. Hastie. Kinetic stability of electrostatic plasma modes in a dipolar magnetic field. *submitted to Phys. Plasmas*.

[36] A.B. Mikhailovskii. *Electromagnetic Instabilities in an Inhomogeneous Plasma.* IOP Publishing, Bristol, Philadelphia and New York, 1992.

[37] H.P. Furth, J. Killeen, and M.N. Rosenbluth. *Phys. Fluids*, 6:459, 1963.

[38] H.P. Furth, J. Killeen, M.N. Rosenbluth, and B. Coppi. In *IAEA Fusion Energy Conference*, number CN-21/106, page 103, Culham, Great Britain, 1966.

[39] B.B. Kadomtsev. *Sov. Phys. - JETP*, 10:780, 1960.

[40] W.M. Tang, R.L. Dewar, and J. Manickam. *Nucl. Fusion*, 22:1079, 1982.

[41] K.V. Roberts and J.B. Taylor. *Phys. Rev. Lett*, 8:197, 1962.

[42] G. Ara, B. Basu, B. Coppi, G. Laval, M.N. Rosenbluth, and B.V. Waddell. *Ann. Phys.*, 112:443, 1978.

[43] J. P. Friedberg. *Ideal Magnetohydrodynamics*, pages 262–263. Plenum Press, New York, 1987.

[44] P. J. Catto, S. I. Krasheninnikov, and R. D. Hazeltine. In R. M. Pick, editor, *6th EPS Conference on Controlled Fusion and Plasma Physics, Europhysics Conference Abstracts*, volume 23J, Yokahama, Japan, 1999. European Physical Society,Paris.

[45] J. W. Connor and R. J. Hastie. *Phys. Fluids*, 19:1727, 1976.

[46] W. A. Newcomb. *Ann. Phys.*, 10:232, 1960.

[47] E. Hameiri, P. Laurence, and M. Mond. *J. Geophys. Res.*, 96:1513, 1991.

[48] J. Kesner. *private communication.*

[49] W.M. Tang, J.W. Connor, and R.J. Hastie. *Nucl. Fusion*, 20:1439, 1980.

[50] J.W. Connor and L. Chen. *Phys. Fluids*, 28:2201, 1985.

[51] S. Chapman and T.G. Cowling. *The Mathematical Theory of Non-Uniform Gases.* Cambridge University Press, Cambridge, England, 3rd edition, 1970.

[52] J. H. Ferziger and H. G. Kaper. *Mathematical Theory of Transport Processes in Gases*, pages 262–263. North-Holland Publishing Company, Amsterdam, Netherlands, 1972.

[53] S. I. Braginskii. *Reviews of Plasma Physics edited by M. A. Leontovich*, volume 1, page 205. Consultants Bureau, New York, 1965.

[54] A.A. Ware. *Nucl. Fusion, Supplement*, 3:869, 1962.

[55] L.V. Mikhailovskaya. *Sov. Phys. - Tech. Phys.*, 12:1451, 1968.

[56] A.B. Mikhailovskii and V.S. Tsypin. *Sov. Phys. - JETP*, 32:287, 1971.

[57] G.I. Budker. *Reviews of Plasma Physics and Problems of the Controlled Thermonuclear Reactions edited by M. A. Leontovich*, pages 145–152. Pergamon Press, Oxford, 1961.

[58] A. Schluter. *Z. Naturf.*, page 822, 1957.

[59] A. Bers and S. Gruber. *Appl. Phys. Lett.*, 6:27, 1965.

[60] B.B. Kadomstev, A.B. Mikhailovskii, and A.V. Timofeev. *Sov. Phys. - JETP*, 20:1517, 1965.

[61] A. Bers. In C. DeWitt and J. Peyraud, editors, *Plasma Physics*, Les Houches, 1975. Gordon and Breach Science Publishers, New York.

[62] P.J. Catto, W.M. Tang, and D.E. Baldwin. *Plasma Phys.*, 23:639, 1981.

[63] P.S. Carter, D.N. Edwards, P.R. Mossack, M.G. Rusbridge, and R.J. Hastie. *Plasma Phys.*, 23:819, 1981.

[64] D. B. Nelson. *Phys. Fluids*, 23:1850, 1980.

[65] J.W. Van Dam and Y.C. Lee. In *Proceedings of the Workshop on EBT Ring Physics*, page 471, Oak Ridge National Laboratory, Oak Ridge TN, 1979.

[66] M.N. Rosenbluth. *Phys. Rev. Lett.*, 46:1525, 1981.

[67] L. Chen, R.B. White, and M.N. Rosenbluth. *Phys. Rev. Lett.*, 52:1122, 1984.

[68] C. Huang, J. Tonge, J.N. Leboeuf, and J.M. Dawson. In *2001 International Fusion Theory Conference*, number 1C46, Santa Fe NM, 2001.

[69] S.I. Braginskii. *Sov. Phys. - JETP*, 6:358, 1958.

[70] M. Taguchi. *J. Phys. Soc. Jap.*, 52:2035, 1983.